Seasonal trends of rainfall intensity, ground cover and sediment dynamics in the Little Pot River and Gqukunqa River catchments, South Africa

A thesis submitted in fulfilment of the requirements for the degree of

MASTER OF SCIENCE

of

RHODES UNIVERSITY

By

SEAN HERD-HOARE

NOVEMBER 2019

Supervisor: Dr Bennie van der Waal

Co-supervisors:

Dr Kaera Coetzer-Hanack and Professor Ian Meiklejohn

Seasonal trends of rainfall intensity, ground cover and sediment dynamics in the Little Pot River and Gqukunqa River catchments, South Africa

"I have read and adhered to the Rhodes University plagiarism policy. All of the work presented in this thesis is my own. I have not included ideas, phrases, passages or illustrations from another person's work without acknowledging their authorship."

Name: Sean Herd-Hoare

Student Number: g14h0325

Signed: 

Date: 28/11/2019

Disclaimer

The capacity building, implementation and research has been funded by the Department of Environment, Forestry and Fisheries (DEFF), Chief Directorate: Natural Resource Management Programmes (NRM), Directorate: Operational Support and Planning

The content of this thesis does not necessarily reflect the view and policies of the DEFF, Chief Directorate: NRM, nor does the mention of trade names or commercial products constitute endorsement or recommendation for use.

Abstract

Natural rangelands provide a variety of ecosystem services including livestock production which occurs on land under freehold land tenure and on land under communal tenure. There is an ongoing debate around the extent to which land degradation is occurring on these rangelands under different land management and land tenure systems and what the main degradation drivers are. Over-grazing, rainfall and soil type are key drivers of rangeland dynamics and the resultant sediment yield in the river systems, however, over-grazing is an outcome of land management while rainfall and soil type are natural drivers. This study explores the relationship between rainfall and daily sediment flux as well as the seasonal trends of vegetation cover and the study is part of a greater research effort called the Tsitsa Project which is based in the Tsitsa River catchment (near Maclear, Eastern Cape, South Africa). The Tsitsa Project aims at developing and managing both land and water in a sustainable way by improving the land, water and lives of people living in the Tsitsa River catchment. The restoration efforts of the Tstisa Project will aid in extending the lifespan of both the proposed dams on the Tsitsa River. The Tsitsa River catchment is characterised by grasslands, steep topography, highly erodible soils with many large gullies present and a very high sediment yield in the Tsitsa River which allowed for the exploration of some of the system drivers of sediment yield in this catchment.

The study involved two sub-catchments of the Upper Tsitsa River catchment of different land management strategies: one dominated by commercial livestock farms (*Little Pot River catchment*) and one dominated by communal rangelands (*Gqukunqa River catchment*). The aim of this study was to determine the seasonal trends of rainfall intensity, ground cover and sediment dynamics in the Little Pot River and Gqukunqa River catchments. The purpose of the findings was to improve management strategies in degraded areas and catchments. In order to achieve this aim a variety of field and desktop methods were used. Field methods involved measuring variables including: vegetation biomass, vegetation cover, soil surface hardness, biocrust cover and slope angle for a range of Normalized Difference Vegetation Index (NDVI) values from the Sentinel-2A sensor. The study assessed the system response of the field variables in both catchments over one rainfall season (2018-2019). Desktop methods included various NDVI analyses as well as analyses of trends and relationships between vegetation dynamics, rainfall and sediment. The relationship between erosive rainfall events, daily rainfall, antecedent rainfall and daily sediment flux was explored over the time period of January 2016 to January 2019 and October 2015 to January 2019 for the Little Pot River catchment and the Gqukunqa River catchment respectively. NDVI was explored as a proxy for vegetation cover to extrapolate across the catchments and monitoring period.

NDVI was found to have a weak positive relationship with vegetation cover and biomass (R^2 values ranged from 0,04 to 0,525). Mean monthly catchment NDVI values, biomass and vegetation cover increased throughout the wet season of 2018-2019 in both catchments. Mean monthly NDVI values increased from 0,26 to 0,55 in the Little Pot River catchment and from 0,29 to 0,53 in the Gqukunqa River catchment over the course of the 2018-2019 wet season. NDVI, biomass and vegetation cover was found to be higher on south-facing slopes than north-facing slopes in both catchments for the majority of the wet season. The Gqukunqa River has significantly higher daily sediment fluxes than the Little Pot River despite similar NDVI and rainfall intensities which is owed to the dispersive soils in the Gqukunqa River catchment. Soil surface hardness results were inconclusive due to rainfall before or during every field trip which changed the properties of the soil.

The largest erosive rainfall, daily rainfall and daily sediment events occurred from January to March each wet season in both catchments. Rainfall intensity and sediment fluxes were found to have a weak relationship, however, there was a stronger relationship found between antecedent rainfall and sediment flux. The larger daily sediment fluxes in each catchment often did not result from an erosive rainfall event on the same day but rather from multiple days of rainfall which can result in saturated soils and runoff leading to surface and sub-surface erosion. The possibility of sub-surface erosion via chemical processes contributing to the larger sediment events was also explored to explain the stronger relationship between antecedent rainfall and daily sediment flux.

Keywords:

Rainfall; NDVI; high-intensity rainfall; sediment; sediment dynamics; ground cover; Tsitsa River; Little Pot River catchment; Gqukunqa River catchment; Maclear; Eastern Cape; South Africa

Acknowledgements

The completion of this thesis would not be possible without the invaluable support from many individuals, groups and institutions, to whom I would like to express my utmost gratitude.

The financial support for this research, in the form of a bursary and fieldwork costs, from the Department of Environmental Science – Natural Resource Management Operational Support and Planning, is gratefully acknowledged.

To my supervisor, Dr Bennie van der Waal, thank you for your constant support, guidance and encouragement throughout my Master's degree. In particular, I am grateful to you for highlighting from which direction to tackle difficult tasks and for your never-ending patience and guidance. To my co-supervisor, Dr Kaera Coetzer-Hanack, thank you for sharing your time so willingly by providing such detailed feedback and for your incredible support, particularly with GIS and remote sensing. To my second co-supervisor, Professor Ian Meiklejohn, thank you for sharing your wisdom which only comes with many years of experience in this field.

The support and assistance with fieldwork from my colleague, Gareth Snyman, and mom, Terry Herd, is also gratefully acknowledged. Thank you for assisting with the countless quadrat field measurements and food preparation, come rain or shine! Many thanks to Carole and Dallas Sephton for having us at Cornlands Farm in the Little Pot River catchment and for sharing your local knowledge about the landscape. It was a priceless contribution to my understanding of the catchment.

To Laura Bannatyne, Nic Huchzermeyer and Pippa Shlegel, thank you for mentoring me these past two years and for the sediment and rainfall data used in this study. Thank you to Margaret Wolff, Karen Milne, Cindy Kepe and Tracy van Aarde for the admin work related to my field trips, you made my field trip organisation a breeze. To Kathleen Smart, I am grateful for your expert insight and guidance with statistical analyses. Thank you for your patience!

Lastly, thank you to my family and friends for your constant emotional support. The biggest thanks, however, is to my Lord and Saviour for your beautiful creation that I have got to explore in an intimate way.

Contents

List of figures

List of tables

List of abbreviations

ASL – Above sea level

DF – Degrees of freedom

DWS – Department of Water and Sanitation

DPM – Disk pasture meter

EI – Ecological infrastructure

ET – Evapotranspiration

GRC – Gqukunqa River catchment

GLM – Grazing land management

LPRC – Little Pot River Catchment

MTF - Modulation transfer function

NDVI – Normalised Difference Vegetation Index

NIR – Near infrared

NPP – Net primary production

PCA – Principal components analysis

SS – Suspended sediment

SSC – Suspended sediment concentration

SIC – Satellite Imaging Corporation

TRC – Tsitsa River Catchment

USGS – United States Geological Survey

UTRC – Upper Tsitsa River catchment

UWP – Mzimvubu Water Project

VI – Vegetation Index

WUE – Water use efficiency

Chapter 1: Introduction

1.1 Background

Natural rangelands comprise most of the uncultivated semi-arid to arid landscapes around the world and support livelihoods by providing a variety of goods and services (Reid *et al.,* 2008). One of these services is livestock production which occurs as extensive ranching under freehold tenure and as collective ranching on land under communal tenure (Reid *et al.,* 2008; Sayre *et al*., 2017). The productivity of rangeland systems is under threat by land degradation at an annual global cost of US$40 billion to the ranching industry (Palmer and Bennett, 2013). However, there still remains a debate around the extent to which land degradation is occurring under different land management and land tenure systems and what the main degradation drivers are in each system (Rowntree *et al*., 2004). The debate is focused around overgrazing and land management as well as erosion on land under communal tenure (Rowntree *et al*., 2004).

Vetter (2013) quantifies land degradation as per vegetation productivity and community structure, but more recently, considerations of land degradation have progressed beyond only biophysical measures of soil loss and vegetation change. Instead, definitions of land degradation emphasise multifunctionality (Palmer and Bennett, 2013) and the reductions in the capacity of the land to carry out ecosystem services that are able to assist society (FAO, 2010). In this regard, land degradation is considered to have occurred when the functionality of the landscape has declined to a point where water and nutrients have ceased to be effectively controlled by the landscape and are lost to rivers (Palmer and Bennett, 2013).

Many ecosystems around the world have undergone significant land degradation caused by human activities (Ratsele, 2013), of which poor fire management and overgrazing have had considerable impact (Anderson *et al*., 1970; Palmer and Bennett, 2013). Fire can have harmful effects on ecosystems that are fire-prone which can result in physical, chemical, biological and hydrologic degradation and as a result reduces agricultural production and makes restoration of the land more difficult (Hurni, 1990; Pereira *et al.,* 2016). Overgrazing can have multiple negative effects on vegetation including altering the rates of nutrient cycling, reduction in grass cover and the resultant enhancement of soil erosion (Ratsele, 2013). Independently, the effects of poor fire and grazing management can have considerable negative repercussions on vegetation, but the *combination* of grazing and burning can have synergistic effects on rangelands (Zaady *et al*., 2001; Vetter, 2013). It is believed that when overgrazing is coupled with a high frequency of burning, it can result in negative

changes in herbaceous vegetation as well as a reduction in livestock wellbeing (Anderson *et al.*, 1970). However, the effects of fire and grazing are not always destructive as when grazing and fire are well managed independently and together they have the potential to promote productivity and vegetation growth (Ratsele, 2013), both of which grasslands are dependent on (Mucina and Rutherford, 2006).

Although fire and grazing outcomes are a result of land use management decisions, rainfall is a key driver of rangeland dynamics overall. Often rainfall determines the system's resilience to poor grazing and fire practices, specifically sensitivity to erosion (Palmer and Bennett, 2013). It is a key abiotic driver of rangeland vegetation dynamics that plays a role in soil moisture content and vegetation growth (Palmer and Bennett, 2013), increasing with decreased vegetation cover (Bai *et al.*, 2008; van Tol *et al.*, 2016). In this regard overgrazing can result in the compaction of soil, causing a lower infiltration rate, and the removal of biomass which disrupts the soil structure, making it more prone to erosion (van Tol *et al.*, 2016).

Although fire and grazing outcomes are a result of land use management decisions, rainfall is a key driver of rangeland dynamics overall. Often rainfall determines the system's resilience to poor grazing and fire practices, specifically sensitivity to erosion (Palmer and Bennett, 2013). It is a key abiotic driver of rangeland vegetation dynamics that plays a role in soil moisture content and vegetation growth (Palmer and Bennett, 2013), increasing with decreased vegetation cover (Bai *et al.*, 2008; van Tol *et al.*, 2016). In this regard overgrazing can result in the compaction of soil, causing a lower infiltration rate, and the removal of biomass which disrupts the soil structure, making it more prone to erosion (van Tol *et al.*, 2016). As a result, there is a need to understand the interaction between ground cover, rainfall and different grazing patterns that lead to soil erosion, which is where this study fits in.

This study is part of a broader research effort known as the Tsitsa Project which is set in the Mzimvubu River catchment. The Mzimvubu River catchment is a primary catchment in the Eastern Cape of South Africa, and the Tsitsa River catchment is a tertiary catchment falling within Mzimvubu River catchment. There is an ongoing project based in the Mzimvubu River catchment called the Mzimvubu Water Project (UWP) (led by the Department of Water and Sanitation (DWS)) which aims to develop and sustainably manage both land and water to improve the service deficits caused by historical legacies in South Africa (Fabricius *et al*., 2016). One of these interventions is through the construction of two dams: the proposed Ntabalenga and Lalini Dams, both of which are to be built on the Tsitsa River (Fabricius *et al*., 2016). The aim of the UWP is to supply potable water to 730 000 people by 2050 and to irrigate 2900 ha of agricultural land (Fabricius *et al*., 2016) by producing two

dams with good quality water with as little sedimentation as possible – as this reduces the life span of the dams. In order to achieve this, it is important that the upstream ecological infrastructure (EI) is healthy, hence the importance of The Tsitsa Project (Fabricius *et al*., 2016). The Tsitsa Project aims at developing and managing both land and water in a sustainable way by improving the land, water and lives of people living in the Tsitsa River catchment. The restoration efforts of the Tstisa Project will aid in extending the lifespan of both the proposed dams on the Tsitsa River (Fabricius *et al*., 2016).

Gully erosion in the Mzimvubu River catchment is one of the major contributors to the sediment levels in the Mzimvubu River (Le Roux and Van Den Berg, 2015). At current erosion rates in the Tstitsa River catchment, the life expectancy of the proposed Ntabalenga Dam, which is based on sediment yield results and digital elevation data, is estimated to be between 34 and 49 years without any siltation prevention or design measures (Le Roux and Van Den Berg, 2015).

The research project undertaken below involves individual case studies of two different catchments within the spatial extent of the Tsitsa Project: one of which is dominated by extensive commercial livestock farms and Southern Drakensberg Highland Grasslands (the Little Pot River catchment) and the other, which is dominated by communal rangelands and Drakensberg Foothill Moist Grasslands (the Gqukunqa River catchment) (Le Roux *et al*., 2007). Land use legacy as dictated by past management practices will shape the evolution of landscape processes and erosional processes (Meadows and Hoffman, 2002), with implications for soil erodibility and thus sedimentation in these catchments (Le Roux *et al*., 2015).

1.2 Academic Problem

Little research has been undertaken in the Mzimvubu River catchment on how the relationship between vegetation cover and rainfall intensity influences sediment dynamics. There are rainfall and sediment flux data available for the two study catchments and surrounds of this research project but there is a lack of vegetation cover data available. The two sub-catchments studied in this research are different in terms of various physical factors including: shape, elevation, vegetation type, geology, soils and land use. Anecdotal evidence from the Gqukunqa River catchment (Bannatyne, 2018, *pers. comm.*) has found that the sediment yield is significantly higher than that in the Little Pot River catchment. Given that authors suggest that land use/cover is one of the main causes for high levels of erosion and sediment yields in the Tsitsa River catchment (Fabricius *et al*., 2016), the dynamics between vegetation cover, rainfall intensity and sediment dynamics are likely an important, as yet unstudied element in the system. At present, empirical evidence to support these

observations is lacking. This study will thus further investigate the cause for sediment yield levels in each sub-catchment. Literature on vegetation cover, rainfall and sediment flux and their interaction exists for other parts of the world, however, what is unique about this study is that it will be assessing the changes of the relationship between ground cover, rainfall intensity, daily rainfall and the resultant daily sediment flux throughout a wet season in the Tsitsa River catchment.

1.3 Motivation

The vegetation in communal rangelands in South Africa undergoes heavy ongoing pressure from livestock grazers and a high frequency of fires due to heavy and non-rotational grazing and locally inappropriate management practices (Vetter, 2013). High stocking densities and a lack of rest periods, coupled with frequent fires in communal rangelands are destructive to the vegetation and make it difficult for growth and production (Ratsele, 2013).

The biomass within the two study catchments fluctuates spatially and temporally due to the seasonal rainfall and pressure from grazers and fire (Pretorius, 2016). The Gqukunqa and Little Pot River catchments receive summer rainfall with consequences for available grazing in the winter months (Moore, 2016; Pretorius, 2016). During the winter months the grasslands are heavily grazed and subject to frost (which prevents plant growth) and burning with little or no rainfall to promote compensatory vegetation growth (Pretorius, 2016). Many areas will be left bare and exposed to high-intensity rainfall with the return of the rainy season, leading to a greater likelihood of soil erosion (Le Roux *et al*., 2015). Soil erosion can lead to gullies in dispersive soils, which are found in both catchments but the numbers of gullies in the Gqukunqa River catchment are much higher than the Little Pot River catchment (Moore, 2016). Therefore, it is argued that sediment flux in rivers will increase as a result of high-intensity rainfall that falls on bare ground early in the growing season.

In recent years, Geographic Information Systems (GIS) and Remote Sensing technology have advanced, allowing for easy and accepted measurements of biomass using remotely sensed images (Ali *et al*., 2016). This study will contribute to addressing the greater research need of sustainable land management in the Tsitsa Project, providing insight on the drivers of sediment erosion of two representative sub-catchments under different management regimes. The sediment fluxes in both catchments have the potential to be influenced by rainfall intensity and ground cover, as indicated by amount of vegetation cover. This will be explored within a catchment dominated by commercial agriculture, the Little Pot River catchment, and within a catchment dominated by communal rangelands, the Gqukunqa River catchment.

1.4 Aim, research question and objectives

1.4.1 Aim

The aim of this study is to determine the rainfall intensity, ground cover and sediment dynamics in the Little Pot River and Gqukunqa River catchments, South Africa, for a single wet season through the use of two case studies of two different sub-catchments of contrasting grazing management systems.

1.4.2 Research Question

What are the seasonal trends of rainfall intensity, ground cover and sediment dynamics in the Little Pot River and Gqukunqa River catchments, South Africa?

1.4.3 Objectives

In order to achieve this aim there are four objectives that need to be met:

1) Determine the spatial and temporal fluctuation of vegetation cover in the Little Pot and Gqukunqa River catchments.
2) Determine the periods of high-intensity rainfall in both catchments.
3) Determine daily sediment flux for each catchment.
4) Determine how the relationship between vegetation cover and rainfall intensity affects daily sediment flux.

1.4 Study area

1.4.1 Introduction and location

The Mzimvubu River catchment is a primary catchment located mainly in the north-east of the Eastern Cape Province and partially in the south-west of KwaZulu-Natal, South Africa, and extends from 29° 54’ 51” S to 31° 38’ 35” S and from 27° 55’ 56” E to 29° 39’ 14” E (Figure 1.1) (Le Roux *et al.*, 2015). The source of the Mzimvubu River is found in the Drakensberg Mountains and has five tertiary rivers/catchments that feed it, namely from west to east the Tsitsa, Thina, Kinira, Mzimvubu and Mzintlava (Le Roux *et al.*, 2015). After a course of approximately 200 km, the Tsitsa River flows into the Thina River which then flows into the Mzimvubu River about 5km downstream from the Tsitsa-Tina confluence (Le Roux *et al.*, 2015). Both the Little Pot and Gqukunqa Rivers and their respective quaternary catchments, are located in the Upper Tsitsa River catchment (UTRC) (Figure 1.1). Both rivers are tributaries of the Tsitsa River. The Tsitsa River catchment is made up of 13 quaternary catchments, namely T35A-M, but the UTRC (T35A-E) is the focus of this study. Maclear is

the major town found within the UTRC and the main rivers in T35A-E are the Tsitsa River, Little Pot, Pot, Tsitsana, Gqukunqa, Hlankomo, Klein-Mooi and Mooi (which runs through Maclear) (Bannatyne *et al.*, 2017).

The Tsitsa River catchment (TRC) has an abundance of rolling grasslands, scenic mountainous areas and significant environmental assets. The ecosystems within the TRC are, however, under pressures that have arisen from historical forces caused by colonial and apartheid policies. Owing to forced resettlement and betterment policies, large numbers/high densities of African people live in this area and engage in migrant labour elsewhere (Andrew and Fox, 2004). This was alongside a withdrawal of financial investment from the area (Coastal & Environmental Services, 2009). As a result of this, the study area is characterised by high rates of poverty and unemployment as well as many severely degraded areas (van Tol *et al*., 2014).

Current land use practices including non-rotational grazing have made an impact on the river system (Coastal & Environmental Services, 2009). This improper management practice has caused siltation and erosion within the system through over-grazing that has contributed to a reduction of grassland vegetation cover, increased patches of bare soil and gullying which results in high sediment fluxes downstream (Coastal & Environmental Services, 2009; Le Roux *et al*., 2015).

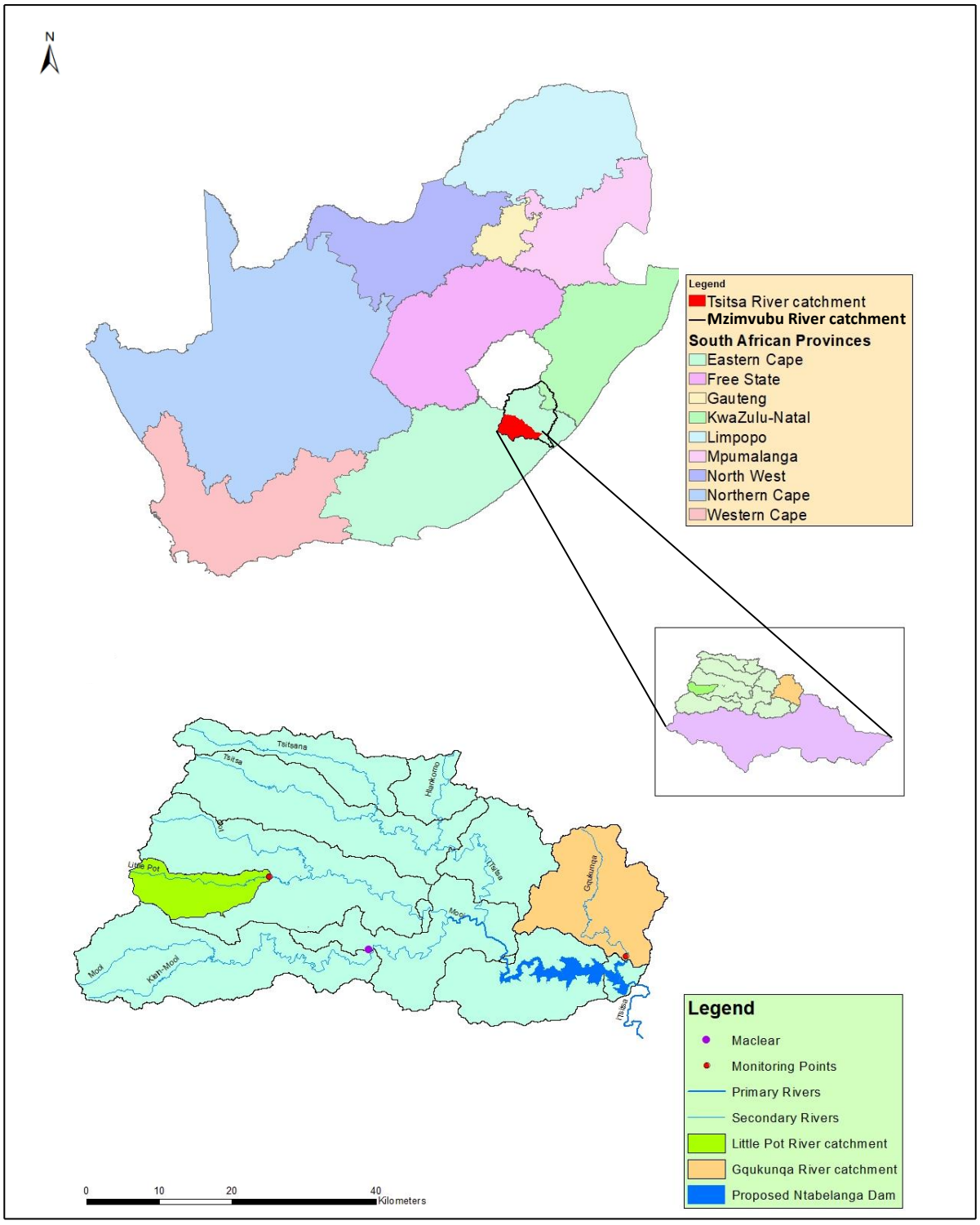

Figure 1.1: Location of the Upper Tsitsa River catchment within the Tsitsa River catchment and South Africa (From: Bannatyne *et al.*, 2017).

1.4.2 Climate

The TRC has a temperate subtropical climate and receives summer rainfall (Bäse *et al.*, 2006). The mean annual rainfall in the TRC ranges from 1327 mm in the high mountainous regions to 672 mm in the lower plains of the catchment (Le Roux *et al.*, 2015). Maclear is the main town found within the TRC (which lies between the LPRC and GRC) and has a mean annual rainfall of 823,87 mm (Moore, 2016). The lowest mean monthly rainfall in Maclear is 14,5 mm in July and the highest is 132,9 mm in January (Moore, 2016) (Figure 1.2). The greater area of the UTRC has been in a prolonged drought and the past four rainfall years have been below the average (Sephton, 2019, *pers. Com.*) (Figure 1.3). The Eastern Cape Province as a whole has also been in a prolonged drought and has recently become a disaster zone. The rainy season normally starts in October and ends in April, however, 75% of the mean annual rainfall occurs between the months of November and March and most of the rainfall comes in the form of high-intensity thunderstorms (Bäse *et al.*, 2006; Moore, 2016). Maclear has a mean midday temperature of 26° C in January (summer) and 17° C in June (winter) (Moore, 2016). This means that the TRC area is strongly seasonal and has a warm, wet summer and cooler, dry winter. The mean annual potential evaporation in the Mzimvubu catchment is 1573 mm and the climate is classified as sub-humid (Le Roux *et al.*, 2015).

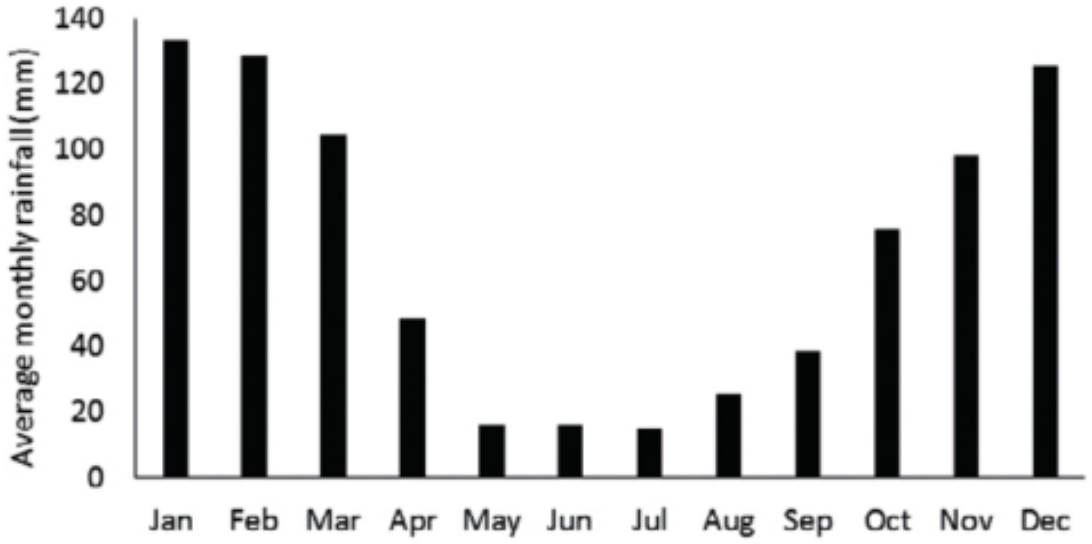

Figure 1.2: Average monthly rainfall (1978–2012) measured in Maclear (From: Moore, 2016).

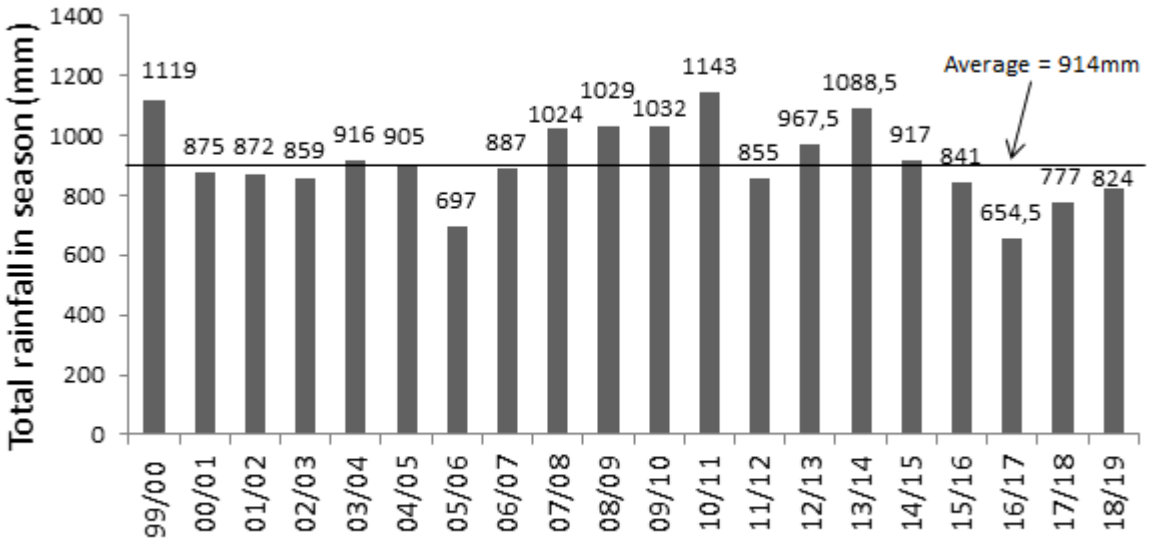

Figure 1.3: Annual rainfall from August to July of each rainfall season at Cornlands Farm in the Little Pot River catchment from 2000-2019 (From: Sephton, 2019, *pers. comm*.).

1.4.3 Vegetation

Vegetation type in the UTRC, which is mainly influenced by altitude and geology (Moore, 2016), is classified as sub-escarpment grasslands and sub-escarpment savanna bioregions (Pretorius, 2016). The area is dominated by various grassland types but includes patches of Montane Forest and Mistbelt Forest on south-facing slopes in protected valleys as well as timber plantations (pine trees) in isolated areas (Mucina and Rutherford, 2006). There are several grassland types that are found within the UTRC, however, the Little Pot River catchment is dominated by Southern Drakensberg Highland Grassland (77%) with a small portion of Lesotho Highland Basalt Grassland (10,3%) in the west and East Griqualand Grassland (12,6%) in the east (Figure 1.4). Common species that are found in the Southern Drakensberg Highland Grassland are *Alloteropsis semialata, Aristida junciformis and Eragrostis caesia*. The Gqukunqa River catchment is dominated by Drakensberg Foothill Moist Grassland (76%) with large areas of East Griqualand Grassland (22,9%) and small portions of Southern Mistbelt Forest (1%) (Mucina and Rutherford, 2006). Common species that are found in the Drakensberg Foothill Moist Grassland are *Diheteropogon filifolius*, *Elionurus muticus* and *Eragrostis capensis*. Natural vegetation comprises 72% of the land cover in the catchment which is made up of: 90% grassland, 6.9% thicket, 3% forest and 0.1% shrubland (Mucina and Rutherford, 2006).

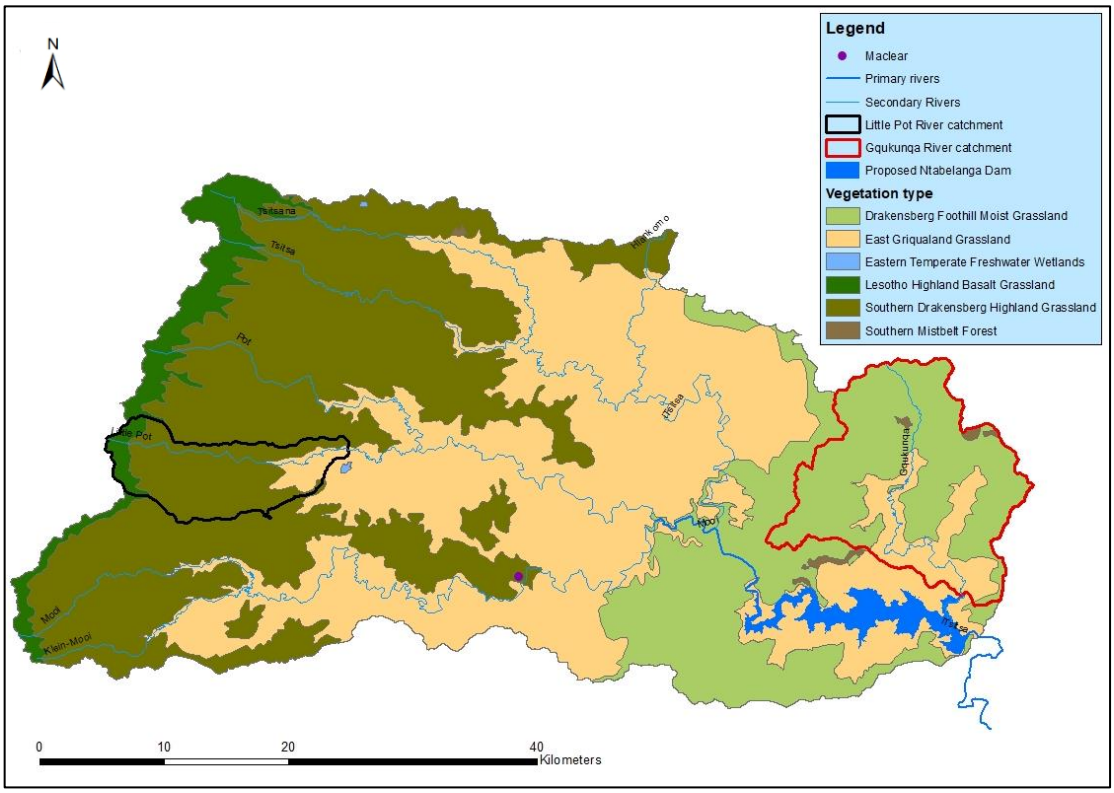

Figure 1.4: Vegetation types in the Upper Tsitsa River catchment (SANBI, 2012).

1.4.4 Topography

The TRC is approximately 4000 km^2 in extent and elevations range from 2730 m above sea level (asl) in the north-eastern headwaters of the Drakensberg Mountains down to about 600 m asl (Figure 1.5) where the Tsitsa River flows into the Mzimvubu River (Le Roux *et al.*, 2015). The UTRC is characterised by rolling grasslands which are separated by steep hills and mountains (Bäse *et al.*, 2006). The Little Pot River catchment is higher in elevation and is 84 km^2 whereas the Gqukunqa River catchment is lower in elevation and is 203 km^2.

There are multiple doleritic dykes and sills of Jurassic age that cut through the Karoo sequence of the middle and lower TRC which structurally control the tributary system in the catchment and results in deeply incised river valleys (Pretorius, 2016). The Molteno Formation that underlies the catchment results in a terraced hillslope topography which consists of outcrops of large, flat slabs of coarsely grained sandstone which are scattered around the lower slopes of the catchment (Pretorius, 2016).

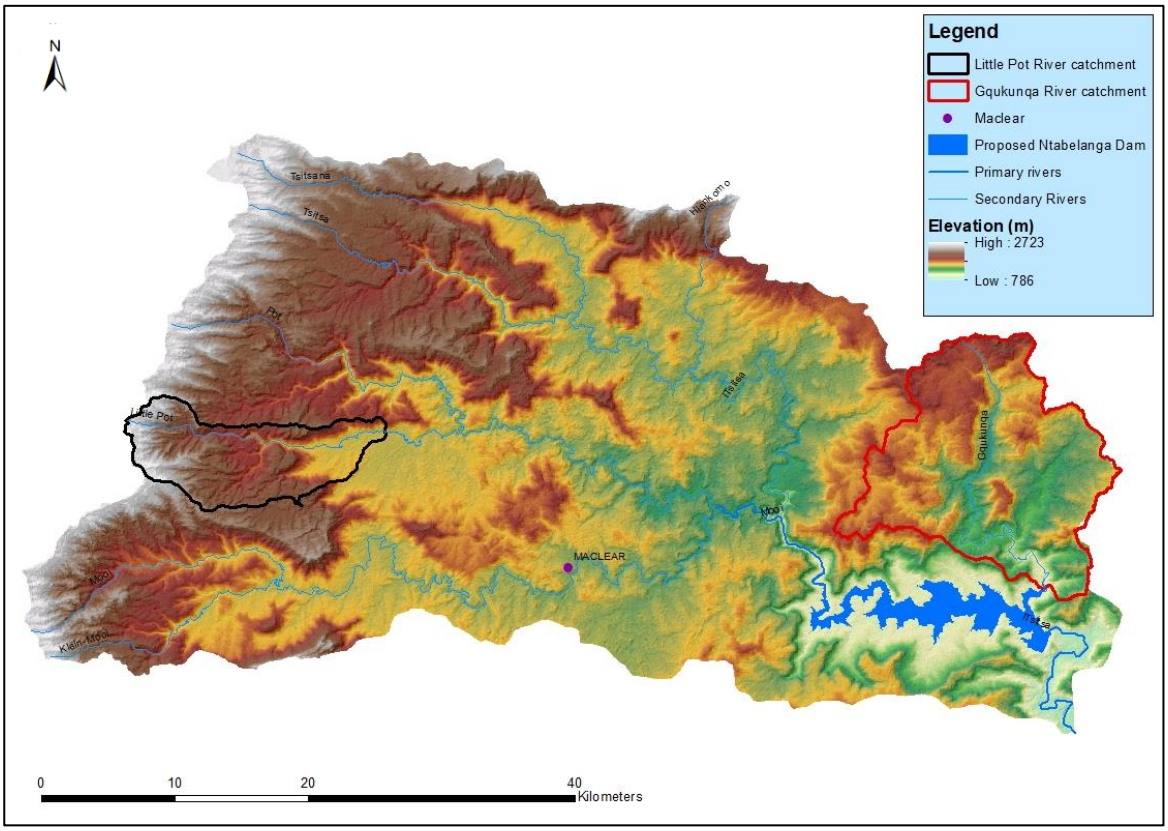

Figure 1.5: Elevation map of the Upper Tsitsa River catchment (National Geospatial Information, 2017).

1.4.5 Soils and Geology

The geology of the UTRC is varied (Figure 1.6) (Pretorius, 2016). Sedimentary rocks dominate the catchment with intrusions of igneous dykes and sills from the Jurassic (Pretorius, 2016). The upper regions of the catchment comprise extrusive basalts of the Drakensberg Formation, which is between 1300 m and 1800 m thick (Pretorius, 2016). The Little Pot River catchment is dominated by Elliot and Clarens Formations with the minority (Table 1.1) of the sub-catchment being underlain by the Drakensberg Formation which consists of basalt. Soil that is underlain by basalt is less likely to contribute much sediment to the Little Pot River because it has been found that streams that drain basalt in the Drakensberg Mountains are clear and produce negligible sediment (Compton and Maake, 2007). Sediment tracing studies in the surrounding study area have confirmed that the sedimentary geologies within a catchment, like sandstones and mudstones, contribute to most of the suspended sediment in rivers draining the Drakensberg Escarpment (van der Waal, 2015).

In contrast to the surface geologies of the LPRC, the surface geology of the GRC comprises mainly sedimentary Molteno and Tarkastad Formations with a small part of the sub-catchment underlain by Karoo dolerites (Table 1.1).

The UTRC has many areas that are characterised by duplex soils which are highly erodible in nature and widespread within the catchment (Le Roux *et al*., 2015). These duplex soils often lead to dense, deep gully networks which vary in shape (either V or U shaped) and size; from 0,5 m to 30 m deep and from 0,5 to 300 m wide (Le Roux *et al.*, 2015). The majority of the soils are dominated by poorly drained and shallow (30-50 cm) to moderately deep loams (50-70 cm), which usually show little development on hard or weathered rock (Le Roux *et al.*, 2015). The shallow soils (<30 cm) are most often found on the rocky and steeply sloped areas whereas the deeper soils (<50 cm) are most often found on gentler gradients, flatter terrain and valley bottoms (Pretorius, 2016).

The soils derived from Tarkastad, Molteno and Elliot Formations are associated with duplex soils with a non-reddish colour and are highly erodible that result in gully erosion throughout the area (Le Roux *et al.*, 2015). Duplex soils are those which have a distinctive difference between the topsoil and sub-soil layers as a result of the high clay content in the sub-soil which is caused by leaching (Fey, 2010).

The characteristics and properties of the soils in the UTRC catchment are highly variable throughout the catchment which are derived from the local geology and the varied rainfall and temperatures in the catchment (Pretorius, 2016). The majority of the soils are acidic because of the siliceous nature of the underlying lithology which the soils are derived from and because of the high level of rainfall the upper catchment receives. The average pH of the soils is below 5.5 while soils with a pH between 5.5 and 6 are found mainly near the outlet of the catchment (Pretorius, 2016).

Table 1.1: The area and proportion of each geology of each study catchment (From: Council for Geoscience, 2008).

Catchment name	Geology type	Area covered in catchment (Km^2)	Proportion of catchment (%)
Little Pot	Elliot	26	31,3
Little Pot	Clarens	45	54,2
Little Pot	Drakensberg	12	14,5
Gqukunqa	Molteno	71	35,1
Gqukunqa	Tarkastad	129	63,9
Gqukunqa	Karoo Dolerite	2	1

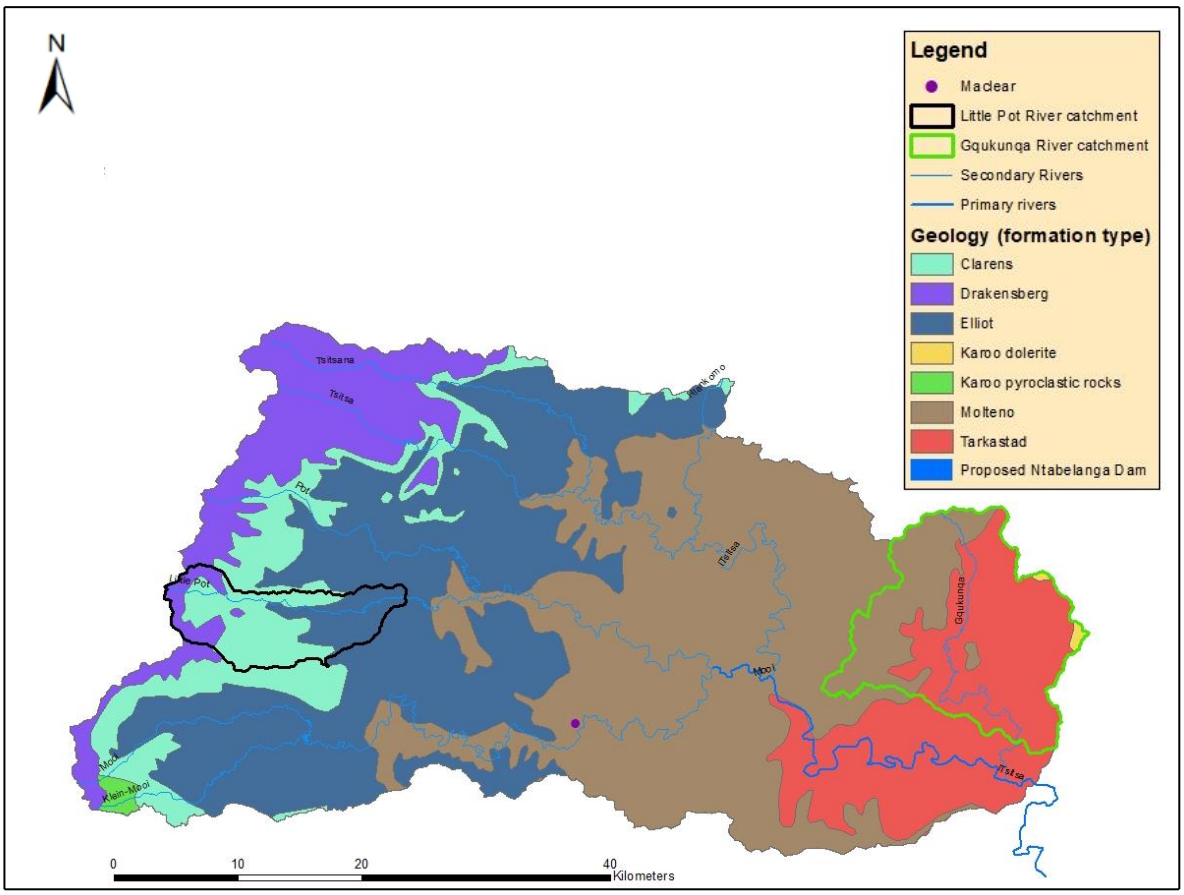

Figure 1.6: The Geology of the Upper Tsitsa River catchment (From: Council for Geoscience, 2008).

1.4.6 Land use and land cover

The land use in the UTRC consists of: commercial timber forests, indigenous/alien invasive woody vegetation, crop production and livestock farming that is either on land under private ownership or under communal land tenure (Bannatyne *et al.*, 2017).

Commercial and subsistence agriculture and livestock grazing comprises 15% of the land cover in the catchment, however, it is important to note that all the grassland regions in the UTRC are used for livestock production (Figure 1.7) (Pretorius, 2016). The commercial farms in the catchment are predominantly sheep and cattle farms for meat and dairy (Pretorius, 2016). Plantations, towns, forests and waterbodies comprise 13% of the land cover in the catchment (Pretorius, 2016). The timber forest plantations (*Pinus*) are mainly part of the PG Bison Forestry Group higher up in the catchment above Maclear and between Maclear and the towns of Ugie and Elliot (Figure 1.7) (Pretorius, 2016). The lower regions of the UTRC are comprised of the former Transkei homelands and even though the policy was removed in 1994 the region still remains an extremely impoverished and a poorly developed region of South Africa which has a high density of gullies (Figure 1.8) (Pretorius, 2016).

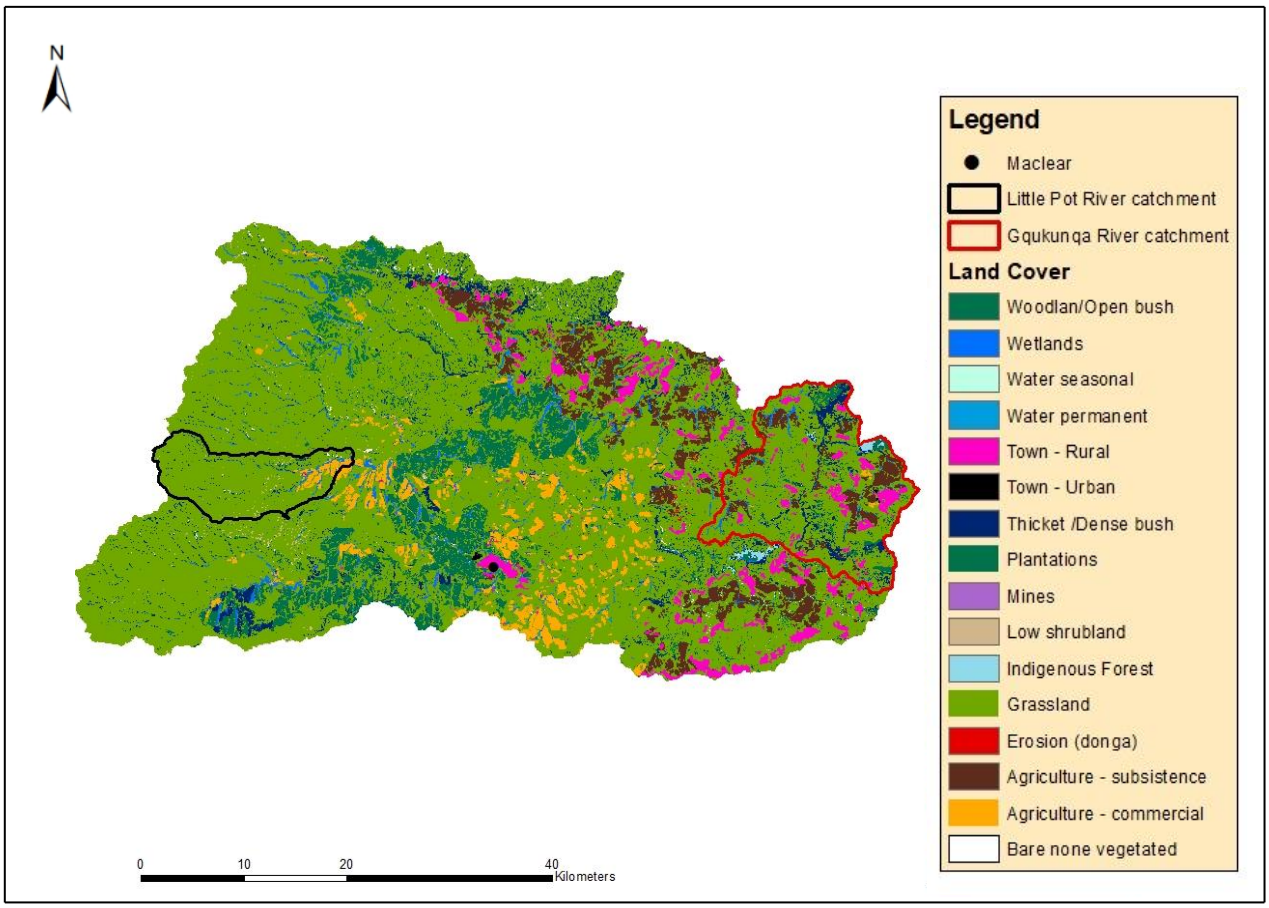

Figure 1.7: Land Cover map of the Upper Tsitsa River catchment (SANBI, 2009).

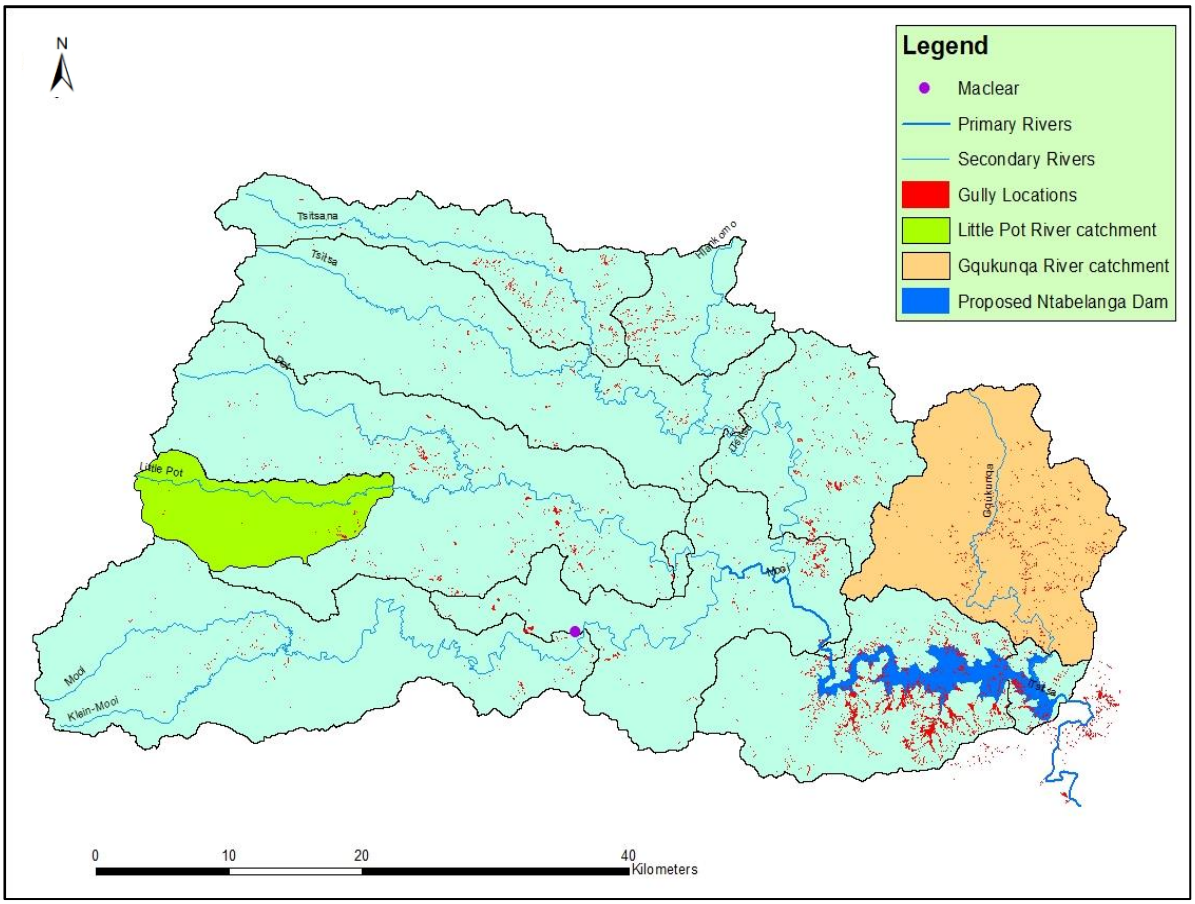

Figure 1.8: Location of the gullies in the Upper Tsitsa River catchment (Gully layer from: Le Roux, 2017).

1.5 Thesis outline

This thesis is composed of six chapters divided into two parts. In part one, the scene and context for the research is provided and in part two, the empirical results relating ground cover, rainfall intensity and sediment flux are presented. Part two concludes by bringing out the implications and making recommendations for future research on unpacking the relationship between ground cover, rainfall intensity and sediment flux. Part one of my thesis begins with Chapter One, where I present a chapter overview of the overall research, discuss the possible research gaps and rationale for this research, as well at provide the geographical context for the study. In Chapter Two, I discuss existing literature body and provide the status quo of this research from the existing scholarship. In Chapter Three I discuss the methodology used by other researchers as well as what field and desktop/analytical methods I used to conduct this study. Part 2 of my thesis begins with Chapter Four, where I display the results of the field variables from the field work as well as the results from the desktop/analytical methods. In Chapter Five I discuss the meaning of the results with reference to pre-existing literature and in Chapter 6 I discuss the limitations and recommendations as well as the future research agendas.

Chapter 2: Literature Review

2.1 Introduction

Soil erosion is a natural process that is active in all landscapes, however, various factors can increase the erosion in landscapes (Le Roux *et al*., 2008). Within the Tsitsa River catchment the following factors are thought to drive sediment erosion: vegetation cover and type, rainfall intensity, management practices/land use, high slope angle and soil type (Le Roux, 2011).

Hillslopes that have low vegetation cover are exposed to erosive raindrops and high-energy runoff (Francis and Thornes, 1990). Poor vegetation cover results in higher erosion and can often be seen in areas where land use change has degraded vegetation cover (Bai *et al*., 2008). High-intensity rainfall on bare ground will remove soil particles which will run down the slope and into the rivers thus increasing sediment transport and loss (Vacca *et al*., 2000). The Tsitsa River catchment, particularly the communal areas, has dispersive soils which are more prone to water-induced erosion thus results in high sediment yields (Le Roux *et al*., 2008). There are many negative effects that too much sediment in a river system can cause which will be discussed further on in this literature review.

In order to understand the seasonal fluctuation of the sediment concentration in the Tsitsa River, the seasonal fluctuation of vegetation cover and/or biomass as well as the seasonal fluctuation of the erosive storm events needs to be examined and reviewed. This chapter will discuss and expand on the drivers of soil erosion mentioned above in more detail as well as: ground cover, land degradation and erosion phenomena and sediment effects on hydrological systems.

2.2 Biomass

Above-ground biomass/standing biomass of grasses is the term given to all living plant matter in an area that is located above the surface of the soil and includes the stem, foliage and seeds (Coe *et al*., 1976). Above-ground biomass in grasslands has been found to reduce the erosion potential of the soil (Kort *et al*., 1998). Grasses provide year-round soil cover and limit erosion by improving water infiltration and by reducing raindrop impact on the soil (Kort *et al*., 1998). There are various methods to measure biomass, including ground measurements and using remotely sensed data. Remote sensing has multiple platforms for monitoring grasslands (Ali *et al.*, 2016) including sensors on satellites. This section will discuss the various ground methods, the satellite considerations required to measure biomass and the ground-truthing of remotely sensed data.

2.2.1 The effect of rainfall and grazing on biomass

Many researchers have found that there is a positive relationship between annual rainfall and above-ground biomass (Coe *et al*., 1976; Fynn and Connor, 2000; Pandey and Singh, 2007). Pandey and Singh (2007) found, in tropical Savannas in India, that biomass was related to rainfall that fell later in the rainy season rather than early on, which is evidence of a lag effect between the timing and amount of rain falling, vegetation response and grassland productivity. Rainfall and the status of soil nutrients are the key factors that affect the pattern of net primary production (NPP) (i.e. active plant growth; hereafter referred to as such) (Burke *et al*., 1990) and quality (i.e. palatability) of the plant and thus influence the type and level of herbivory (Huntley and Walker, 1982; Pandey and Singh, 2007; Huston and Wolverton, 2009).

Precipitation, in the form of rain, affects water and nutrient availability in the soil for plants and hence influences active plant growth (Pandey and Singh, 2007; Deshmukh, 2008). This means that "green" biomass, which is a function of soil moisture, will be greater in a year with greater rainfall (Pandey and Singh, 2007; Deshmukh, 2008).

A study by Robertson (1998) in New South Wales, Australia, found that during quarterly periods (of a year), when the biomass of pasture was protected from grazing, rainfall explained 93% of the variance in biomass change. When considered across the full temporal extent of the study (independent of whether biomass increased or decreased) the rainfall resulted in 72% of the variance of biomass change and the initial biomass present accounted for a further 14%. This suggests that the initial biomass levels are not as important as the amount of rainfall received because the amount of rainfall received determines the growth rate of biomass (Robertson, 1998).

Rainfall variability and grazing intensity are two independent variables that control active plant growth and biomass removal through herbivory in an interactive manner in savannas and grasslands (Pandey and Singh, 2007). Pandey and Singh (2007) found that grazing stimulated a 4-45% greater increase in plant growth at sites that were grazed lightly to moderately. Similarly, a study done by Fynn and Connor (2000) in a municipal district in north-eastern KwaZulu-Natal, South Africa, revealed that high rainfall and light grazing promoted tufted perennial grasses (which are high in biomass and important for grazing) whereas heavy grazing and low rainfall promoted the predominance of annuals and weakly tufted perennial grasses. The authors found that rainfall positively influenced the above-ground active plant growth of herbaceous plants in a semi-arid savanna. They also found that heavy stocking rates of cattle had a deleterious effect on active plant growth which left the land vulnerable to erosion. Both of these effects are in agreement with global patterns.

2.2.2 Measuring biomass on the ground

The disk pasture meter (DPM) was initially developed in New Zealand by Phillips and Clarke (1971) but has since been widely used in South Africa as a fast and simple tool to measure compressed grass height, i.e. above-ground standing biomass. The instrument is made entirely of aluminium and consists of: 1) a rod of ± 170 cm, 2) a tube that slides over the rod, and 3) a thin base plate (disk) that is attached to the base of the tube. The DPM is often used in veld management, for example in calculating the biomass prior to burning and determining the stocking rate of the area (Bransby and Tainton, 1977; Trollope, 1990). The DPM is considered more efficient than the clipping and drying method, and it is, hence, often used for rangeland research. However, the DPM usually requires calibration to the specific area in order to increase accuracy owing to the variability of grassland types the DPM is used in.

2.2.3 Measuring biomass remotely

In recent years Remote Sensing technologies have advanced majorly and have enabled cost-effective, statistically reliable, and consistent remote monitoring of grassland sites around the world, as well as acquiring data about their behaviour (Jin *et al.*, 2014; Ali *et al.*, 2016). Optical sensors mounted on towers, aerial vehicles, aircraft and spaceborne platforms can collect and produce data at a spatial resolution of 25 cm to 1 km. The data and/or derived products from Landsat OLI/ETM+/TM/MSS, SPOT, AVHRR, MODIS and RapidEye sensors have been used frequently to classify and map land cover and land cover change, including rangelands, pastures and meadows (Ali *et al.*, 2016). Remote Sensing technologies have become effective tools to estimate biomass which enables its quantification over large spatial extents (Jin *et al.*, 2014). Remotely sensed vegetation indices (VIs) capture the amount of photosynthetic activity of the vegetation and as a result this method is increasingly used to calculate biomass in grasslands and various other biomes (Jin *et al.*, 2014).

To determine different terrestrial ecosystem types and measuring their active growth or productivity, Remote Sensing techniques rely on vegetation indices that combine spectral reflectance values at two or more wavelengths (Song *et al*., 2013). Certain wavelengths are selected to accentuate particular features such as greenness, water content or light use efficiency (Song *et al*., 2013).

Grassland biomass has been measured successfully using the Normalized Difference Vegetation Index (NDVI) (e.g. Jianlong *et al.*, 1998; Silleos *et al.*, 2006; Butterfield and Malmström, 2009; Guay *et al.*, 2014). NDVI is the normalised ratio of red and near-infrared (NIR) reflectance (Guay *et al.*, 2014).

The amount of reflectance is determined by the chemical and structural component of leaves (i.e. chlorophyll and mesophyll) and is generally an acceptable proxy that indicates photosynthetic activity (Guay *et al.*, 2014). Vegetation that is healthy/growing, and thus green due to the presence of chlorophyll, reflects more NIR and absorbs more red light in comparison to other wavelengths (Guay *et al.*, 2014). In order to calculate the NDVI the following formula is used:

NDVI = $\frac{(NIR-Red)}{(NIR+Red)}$ (Equation 1)(Butterfield and Malmström, 2009).

Low vegetation cover with low plant activity is associated with low NDVI values (<0.2) and high vegetation cover with active plant growth is associated with high NDVI values (0.6) (Gao, 2006). NDVI values are increased by daylight hours and higher temperatures (Adole *et al*., 2019).

It is beneficial to have a time series of images that are acquired through the growing season so as to provide more information on yields and management (Clevers *et al*., 2007). This enables the rate of growth and productivity to be determined, as well as capturing phenological responses to seasonal cues and changes therein (Ali *et al.*, 2016). During the growing season, the phenological stages of grasslands develop due to a variety of factors including weather, germination, management strategies, nutrient input and grazing pressures (Ali *et al.*, 2016). Butterfield and Malmström (2009) found that the understanding of grassland dynamics could be improved by observing the relationship between NDVI and biomass at different phenological stages because capturing all the stages of grassland growth throughout the course of the wet season ensures all active vegetation is captured.

2.2.4 Satellite imagery for vegetation analysis

When measurements are compared from similar sensor types that have different spatial resolutions it emphasises the 'scale effects' in measuring biodiversity pattern and/or quantifying a system response (Anderson, 2018). An example of this can be seen in a study done by Brown *et al* (2006) who compared NDVI measurements from four different satellite sensors and found that the image pixel size is a main driver for up to 20% of the variance of NDVI measurements from different sensors. This suggests that NDVI measurements are sensor specific and it emphasises that sensors need to be carefully selected for the phenomenon under investigation. Small variations in NDVI have been observed between sensor systems that are very similar which can be attributed to modulation transfer function (MTF) which includes sun elevation, atmospheric conditions and earth-sun distance (Abuzar *et al*., 2014).

NDVI is, in general, calculated using data sets that are calibrated through appropriate preprocessing (Abuzar *et al*., 2014). Calibration will result in the data having precision from a particular sensor meaning that the rest of the data sets from the same sensor can be compared (Abuzar *et al*., 2014). The USGS Earth Explorer website offers freely available multispectral imagery from various sensors including: MODIS, IKONOS-2, Landsat, Aster and Sentinel-2A (USGS EE, 2019). The spatial and temporal resolutions of these sensors, as well as a brief review of each sensor and its limitations/advantages, are portrayed in Table 2.1. Landsat 5 was explored in Table 2.1, however, there are more recent Landsat missions like Landsat 7 (which was the scan line error mission) which was then replaced by Landsat 8 which is also used in vegetation studies. Sentinel-2A has the highest spatial and temporal resolutions (of the red and near-infrared band for NDVI) for the satellite images that are freely available on the USGS Earth Explorer website that have data available for the required dates of this study period (SIC, 2019; USGS EE, 2019). Figure 2.1 indicates that the Sentinel-2A sensor is considered appropriately sensitive for quantifying ecosystem functioning, owing to its midrange spatial and temporal resolution compared to all the sensors displayed in Figure 2.1.

Table 2.1: A variety of satellite sensors and their spectral and temporal resolutions; uses for vegetation analysis and advantages/limitations

Satellite sensor	Spatial resolution (m)	Temporal Resolution (days)	Uses to quantify vegetation parameters	Advantages/ limitations	Reference
MODIS	250	1	Used to assess drought in grasslands via NDVI	Limitation - Spatial resolution is too coarse for NDVI for this study	(SIC, 2019; Gu *et al.*, 2007)
IKONOS-2	4	3	Used to quantify the biomass of an African savanna area using NDVI	Limitation - Mission ended March 2015 (before start of this study)	(SIC, 2019; Thenkabail, 2004)
LANDSAT 5	30	16	Used to quantify grassland cover density using NDVI. A strong linear regression (R^2 = 0,745) was found between NDVI and grassland cover density	Limitation – Mission ended June 2013 (before start of this study)	(SIC, 2019; Yan-Sui *et al.*, 2005)
Aster	15	16	Used for inter-sensor comparison to MODIS using NDVI	Limitation – Atmospheric aerosols are not corrected for in the ASTER algorithm which result in variable reflectance values.	(SIC, 2019; Miura *et al.*, 2008)
Sentinel-2A	10	5	The Sentinel-2A sensor was used to analyse the change in land use and land cover as well as vegetation cover using NDVI	Advantage – freely available, fairly high spatial and temporal resolution. Limitation – only a short mission so far.	(SIC, 2019; Dumitrascu, 2016)

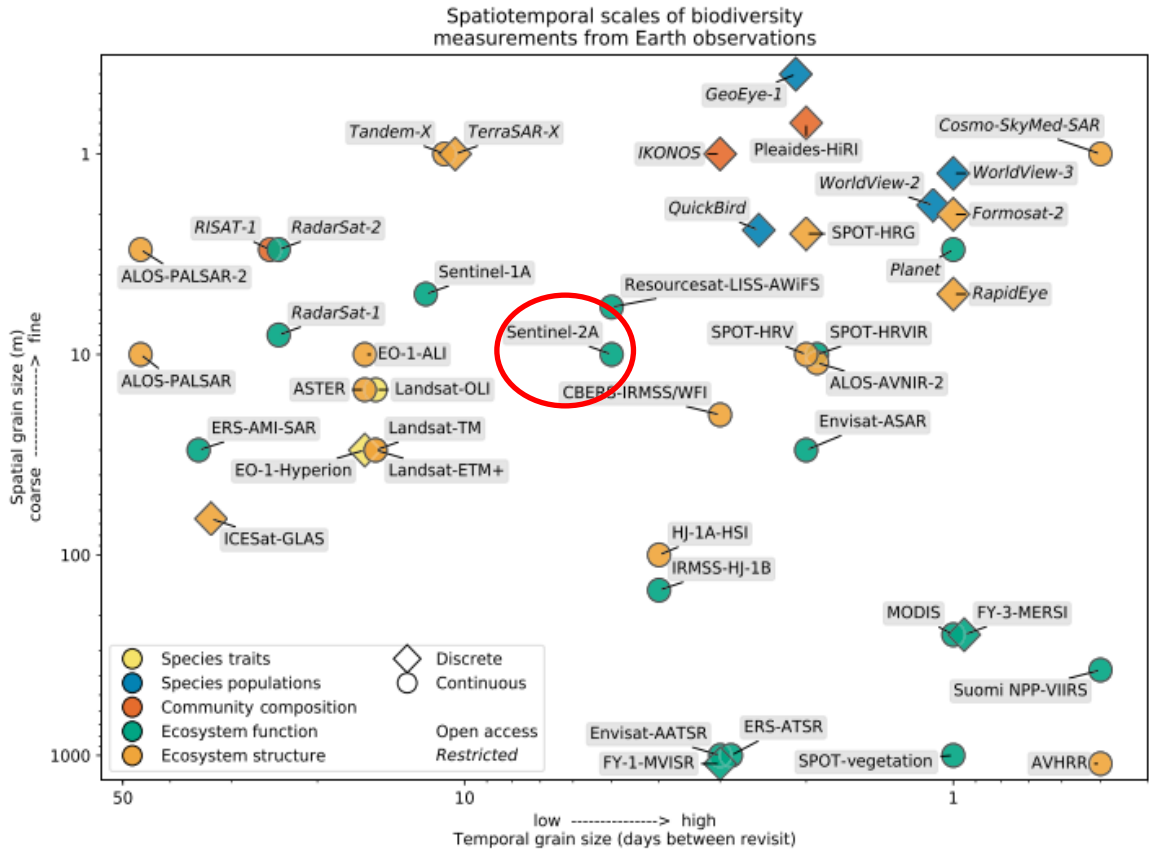

Figure 2.1: Log–log plot of spatial and temporal and grain sizes for 44 current and historic satellite Earth observation (EO) sensors, coloured by biodiversity pattern type. Sentinel-2A is circled to indicate the chosen sensor for NDVI analyses (From: Anderson, 2018).

2.2.5 Ground truthing methods of remotely sensed data for biomass and vegetation cover

Due to sensor specificity and variance among sensors there may be a slight difference in the NDVI's calculated via different sensors (Washington-Allen *et al*., 2008). This variance means that the NDVI layer created using a specific sensor will need to be ground-truthed to calibrate the sensor with the specific area and vegetation type (Washington-Allen *et al*., 2008).

There are various ground-based methods used for the retrieval of grassland biophysical parameters and other management-related information (Ali *et al.*, 2016). These methods include: visual assessments, cut and dry (clipping), rising plate meter (disk pasture meter – DPM) and field spectrometry (Ali *et al.*, 2016). Visual assessments are done using the human eye for grassland cover, for example in quadrats (Ali *et al.*, 2016). The cut and dry (clipping method) requires grass to be harvested from the field and dried and weighed in order to determine the dry matter yield but it is time-intensive (Xie *et al*., 2009).

Field spectrometry is conducted using a spectrometer held at waist height and calibrated to the in situ species. The reflectance at red and near-infrared wavelengths is able to retrieve data about biomass and leaf area index (Flynn *et al*., 2008). Table 2.2 presents the advantages and limitations of each method.

Table 2.2: Comparison among ground-based methods (From: Ali *et al*., 2016: 652).

Methods	Scale	Benefits	Limitations	Category
Visual	Field/paddock	Quick and cheap	Expertise needed, vague estimation	Non-destructive
Clipping		More accurate than visual assessment	It can be time consuming if a large number of samples are needed	Destructive
DPM		Easy and cheap to operate	Time consuming	Non-destructive
Field Spectrometry		Information on various biophysical parameters can be retrieved	Requires a trained operator, postprocessing is required	Non-destructive

2.3 Land degradation

The drivers and forms of land degradation in South Africa are diverse with some of the causes including population growth and land tenure patterns (Hoffman *et al*., 1999). This section details these drivers on a global scale as well as at a local scale and outlines the inherent characteristics thereof including soil erosion.

2.3.1 Global land degradation drivers

Between the years of 1982 and 2006 land degradation has occurred on approximately 30% of the total land surface area around the world which in turn results in negative impacts on national economies and agricultural livelihoods (Mirzabaev *et al*., 2016). It has become an urgent priority to combat land degradation and to restore degraded land in order to protect the biodiversity and ecosystem services which are important to all forms of life on Earth (Scholes *et al.*, 2018). Without urgent action land degradation will become increasingly worse with factors like population growth and climate change (Scholes *et al.*, 2018).

There are a number of drivers of land degradation and many of them are complex and interrelated, which means that it is important to be able to identify its key drivers so that international efforts can be made to prevent any negative effects thereof (Mirzabaev *et al*., 2016).

Degradation drivers can be divided into two categories: proximate and underlying drivers (Belay *et al*., 2014). Proximate drivers of land degradation include those that directly affect the terrestrial environment, including topography, climate, soil characteristics, unsuitable land uses, poor land

management practices and uncontrolled fires. Compared to underlying drivers, there is a general consensus about the causal mechanisms of proximate drivers (Mirzabaev *et al*., 2016). One example of this is that soils that have a higher silt content will erode naturally which leads to land degradation (Bonilla and Johnson, 2012) (Table 2.3). Underlying drivers of land degradation include poverty, land tenure, population density and poor policy implementation (Mirzabaev *et al*., 2016) and are more difficult to determine and quantify the direct effects of the mechanisms.

Table 2.3: Global proximate and underlying land degradation drivers and their causality (Adapted from: Mirzabaev *et al*., 2016)

Drivers	Type	Example of causality
Topography	Proximate	Steep slopes can cause water-induced soil erosion
Land cover change	Proximate	Deforestation; rangeland conversion to irrigated agricultural land
Climate	Proximate	Dry areas being prone to wild fires which lead to soil erosion. Heavy rainfall events can cause flooding and erosion.
Soil erodibility	Proximate	Soils with high silt content are more prone to natural soil erosion, however, only when the clays are dispersive.
Population density	Underlying	Population density may lead to land degradation
Land tenure	Underlying	Insecure land tenure may lead to improper land management
Poverty and unemployment	Underlying	Poverty and unemployment have the ability to lead to land degradation and vice versa

Regardless of the lack of a single definition of degradation, Palmer and Bennett (2013: 58) define degradation as 'a deleterious change in the rangeland for livestock production, encompassing a range of changes, including a shift in species composition from desirable (to livestock) to unpalatable or toxic species, a decline in basal cover of perennial grasses, an increase in the density of woody shrubs and dwarf shrubs, a decline in water use efficiency (WUE), a decline in net primary production, and an increase in soil erosion'. The following review of land degradation will be separated into proximate and underlying drivers with soil erosion being a main component of land degradation (Palmer and Bennett, 2013).

2.3.2 Proximate drivers of land degradation

2.3.2.1 Soil erosion

Soil erosion occurs when the soil surface loosens due to physical processes like rain, flowing water, ice, wind, temperature change, gravity as well as any other natural or anthropogenic factors that

detach and transport soil/geological material and deposit it away from its point of origin (Pretorius, 2016). A general pattern found is that soil loss increases with increasing slope angle (Laker, 2004). Runoff usually increases with increasing slope angle however this is not true for every soil type or situation (Laker, 2004). The kinetic energy of the runoff water is found to increase steadily as the angle of the slope increase thus it is the kinetic energy of the water that causes the detachment and transport of soil particles (Laker, 2004). Sediment can be deposited locally or downstream within the catchment meaning that not all the sediment generated in the catchment will be transported to the outlet of the catchment (Pretorius, 2016). Below are the main erosional processes:

Rain splash dislodges individual particles or soil whereas sheet wash is more extensive and is caused by a layer of water flowing over the surface (Nearing *et al*., 1994). The detached soil particles are then transported downslope by overland flow in the form of a sheet (Nearing *et al*., 1994). This causes loss of fertile top soil, occurring commonly in ploughed fields or areas that have little vegetation cover. Where sheet flow is concentrated it forms rills through increased vertical erosion, thus know as rill erosion (Pretorius, 2016). When rills erode vertically and become larger they turn into gullies.

Gullies are erosional land-forms that occur in various shapes, sizes and complexities (d'Oleire-Oltmanns *et al.*, 2014). Gullies range from basic longitudinal and linear cuts in the land to complex deeply incised networks that can be V-shaped, U-shaped or overhanging (d'Oleire-Oltmanns *et al.*, 2014). The length of a gully can range from a couple of meters to several hundred metres and the width of a gully can range from 0,5 m to tens of metres (d'Oleire-Oltmanns *et al.*, 2014). Gully depth can range from 30 cm to 30 m deep (Mararakanye and Nethengwe, 2012). Gullies are often found in drainage ways and on lower slope positions, forming when runoff is channelled into narrow rills and over time these grooves will deepen and create a gully which has steep sides that may collapse due to water seepage or undermining of water in the gully (Mararakanye and Nethengwe, 2012). They can be classified as either continuous or discrete/discontinuous. Continuous gullies have a dendritic pattern with many branches while discrete/discontinuous gullies are independent and have no direct connection with the main gully or stream (Mararakanye and Nethengwe, 2012).

2.3.2.2 Assessment of soil erosion in South Africa

Over 70% of South Africa's land has been affected by different forms and degrees of soil erosion (Le Roux *et al*., 2007). National assessments of the type and extent of soil erosion have suggested the widespread occurrence of rill and gully erosion. Wind erosion of soil is only a problem in coastal regions and areas with sandy loam topsoils (Hoffman and Todd, 2000).

The degree and extent of soil erosion due to water has been based on approximations from mean annual sediment data which has the potential to be inappropriate or even inaccurate (Meadows and Hoffman, 2002). Certain regions in South Africa are subject to higher levels of soil loss in the form of sheet, rill and gully erosion caused by either environmental factors and/or land use management issues (Meadows and Hoffman, 2002). This can be seen in either socio-economic or environmental problems in a variety of ways. The effects of soil erosion do not only affect onsite land resources, such as fertile top soil, but also offsite water resources due to the eroded soil ending up in streams, rivers and dams (Le Roux *et al*., 2007). Excessive volumes of sediment that run into a watercourse cause a loss of water quality and reduction in biodiversity (Flugel *et al*., 2003). When the dominant land use form is grazing the severity of soil degradation is greatest in communal rangelands compared to commercial livestock farms, due to the concentration of livestock around homesteads and poor livestock rotation (Meadows and Hoffman, 2002). The provinces that are most severely affected by over grazing of lands, and thus soil degradation, are KwaZulu-Natal, Limpopo, Northern Cape and Eastern Cape (Meadows and Hoffman, 2002; Le Roux *et al*., 2007).

Beckedahl *et al* (1988) estimated that in 1988 South Africa lost 360 million tons of soil annually. However, it is contended that this figure has increased since then (Le Roux *et al*., 2015). The main reasons cited for the extreme soil loss in South Africa are the poor farming methods implemented coupled with the erodible nature of South African soils (Le Roux *et al*., 2007).

2.3.2.3 Rainfall intensity, vegetation and soil cover and erosion

Rainfall erosivity is one of the main causes of sheet and rill erosion (Le Roux, 2011). Le Roux (2011: 7) defines erosivity as “the ability of rainfall and runoff to cause soil detachment and transport”. Rain is able to detach and transport soil particles through hortonian overland flow (which occurs when the rainfall exceeds the rate of infiltration (Huggett, 2007)) due to a combination of raindrop impact and runoff that is created by rainfall and the subsequent movement of water under the influence of gravity (Le Roux, 2011). Rainfall erosivity is a measure of the kinetic energy that the rain possesses. The kinetic energy of rain is determined by the intensity and duration of the rainfall as well as the mass, diameter and velocity of the actual raindrops (Morgan, 2005). There are certain areas in South Africa that are subjected to occasional high-intensity storms, like the northern and eastern parts of the country, where erosivity values are four to eight times higher than other parts of the country (Smithen and Schulze, 1982). Storms that are short and intense produce overland flow which causes the majority of the seasonal soil loss in an area (Le Roux, 2011).

High rainfall volumes and intensities cause the pores between soil particles to become saturated which results in increased runoff and runoff energy and therefore higher levels of erosion (Vacca *et*

al., 2000). Francis and Thornes (1990) determined that there is an intensity-dependent relationship between vegetation, runoff and erosion. When a rainfall event has a high intensity the time that water has to infiltrate the soil is shorter and causes the amount of runoff to increase. Similarly, Chirino *et al* (2006) found that there is also a clear link between rainfall intensity and erosion as well as the rainfall volume also being involved in erosion with sediment yields highly variable from year to year, and, the majority of sediment exports are created during high-intensity rainfall events (Gallart *et al.,* 2002).

To study rainfall erosivity, one needs to analyse erosive storm events that relate to high kinetic energy (Nel and Sumner, 2007). For a rainfall event to be classified as an erosive storm event, the rainfall must be more than 12.5 mm and the maximum five-minute (5-min) intensity of the rainfall event must be more than 25 $mm.hr^{-1}$, as well as the rainfall event being isolated by a minimum rain-free period of two hours (Stocking and Elwell, 1976). The classification requirements for an erosive rainfall event have been used by various researchers in their South African studies including Nel and Sumner (2007).

Vegetation cover plays role in the production of overland flow and soil erosion and Gallart *et al* (2002) found that unvegetated sites do result in runoff during average rainfall events, compared to vegetated sites which only produce runoff during high-intensity storms. Gallart *et al* (2002) support the findings of Francis and Thornes (1990) who found that erosion rates from low-intensity rainfall were low in all vegetation cover types, including degraded sites. Only high intensity rainfall events had a major effect on erosion on bare slopes, with erosion decreasing exponentially while cover increased (Francis and Thornes, 1990).

Vegetation cover is not the only mechanism that protects soil from rainfall as biocrusts play a role similar to plants, just at a smaller scale. Biocrust is made up of cyanobacteria, mosses, lichens and various microorganisms that form a thin layer on top of the soil surface on bare ground between the surrounding vegetation (Chamizo *et al*., 2017). The thickness of a biocrust ranges from a few millimetres to a few centimetres and forms a layer on the soil surface which results in a resistant layer to water and wind erosion (Zhang *et al.,* 2006; Bowker *et al.,* 2008). The biocrust acts as a binding agent and binds soil particles together which increases soil stability and reduces soil erosion (Gao *et al*., 2017). Chamizo *et al* (2017) found in the south-east of Spain that removing biocrust from the soil resulted in losses that were 20 times higher (particularly after the first rainfall event) than in soils that were covered by well-established lichen biocrusts.

2.3.2.4 Soil erosion in the upper Tsitsa River catchment

Within the upper Tsitsa River catchment the level of soil erosion is high, especially in the inter-fluvial regions that are adjacent to the stream channels (Pretorius, 2016). Le Roux *et al* (2015) states that in the Tsitsa River catchment high rainfall intensities, steep slopes, the easily erodible character of the soils and land use are the main drivers for soil erosion. Although sheet and rill erosion are present in the catchment, gully erosion is thought to be the most prominent erosion phenomenon (Le Roux *et al*., 2015) and between 2007 and 2012 there was an overall increase in gully erosion in the UTRC by 28% (Pretorius, 2016). The majority of gully erosion occurs in the deeper soils on gentle slopes in the catchment (Le Roux *et al*., 2015) and the sediment yield caused by gully erosion is estimated to be between 7 and 14 $t.ha^{-1}.yr^{-1}$ (Pretorius, 2016), in comparison to the South African average predicted soil loss rate of 12,6 $t.ha^{-1}.yr^{-1}$ (Le Roux, 2014). The majority of sediment yield in the catchment is found to originate from gully erosion, which accounts for 70 times more sediment yield per year than sheet and rill erosion (Pretorius, 2016).

The hydromorphic soils along drainage lines are prone to erosion due to surface flow concentration. Over-grazing and cultivation on steep, terraced slopes are two of the main causes of vegetation cover reduction and the loss of root stability, as well as the intensification of rill and sheet erosion (van Veelen *et* al., 2014). Pretorius (2016) found that on average 0,18 $t.ha^{-1}.yr^{-1}$ of sediment is generated in the UTRC from sheet and rill erosion. Pretorius (2016) found that current land use in the UTRC is optimal for the least amount of rill and sheet erosion and that if the land use was converted to maize crops then this will have a major impact on the sediment yield.

Another important factor in determining soil erodibility is the parent material of an area (Laker, 2004; Le Roux and Sumner, 2011). An example of this is shown by the Tarkastad and Molteno Formations, which underlie approximately half of the UTRC (below the Escarpment), but more specifically the lower half of the catchment where the communal areas are found. These Formations are associated with duplex soils that are highly dispersive and erodible, which are closely linked to widespread gully erosion in the UTRC, especially in the lower parts (Le Roux, 2011; Le Roux *et al*., 2015). Duplex soils are those that have a clearly defined change in texture between horizons in the soil profile (van Zijl, 2010). The texture of duplex soils varies from lightly textured topsoil to a heavier, finer textured soil like clay. Duplex soils are susceptible to tunnelling and gully erosion as result of the lateral sub-surface flows between the two different horizons which is enhanced in highly dispersive sub-soils (Beckedahl, 1996).

The duplex soils found lower down in the catchment are in contrast to areas higher up in the catchment (the Drakensberg Escarpment), where there are fewer gullies. Buhmann *et al* (1996) showed that the dominant soil constituents of silty soils, like chemically inert quartz and feldspars,

for example, increase their susceptibility to erosion and dispersion. This means that other factors can override the effects of sodium on dispersion and erosion (Buhmann *et al*., 1996). The soils higher up in the catchment are derived from Drakensberg basalts and dolerite which have much higher iron content meaning they are not as dependent on organic matter to promote the aggregation of soil particles to create structure in the soil (Laker, 2004).

The physical and chemical properties of a soil control its ability to resist erosion, which is determined by its resistance to disaggregation and/or dispersion (Laker, 2004). Soils derived from the Beaufort Formations (silts and mudstones) in the UTRC have high dispersion rates caused by the erodible nature of these soils (Garland *et al*., 2000). Laker (2004) indicates that silt particles and some members of the clay fraction that are most inert are the most actively involved in disaggregation. Two important factors in soil stability are soil organic matter content and the presence of iron and aluminium oxides (Laker, 2004). In soils that are derived from Beaufort Formations, like those found in the Tsitsa catchment, the presence of organic matter is the primary retainer of soil structure which means that when organic matter is removed via overgrazing and improper farming practices this will result in increased soil erodibility (Laker, 2004).

2.3.2.5 Land degradation variation with lithology and land-use history

Neighbouring communal rangelands with comparable climate and grazing regimes can sometimes have different vegetation trajectories and can display different vegetation end-points (Vetter, 2013). In the former Transkei where continuous grazing on acidic soils (formed from dolerites and sandstones) led to rangelands becoming dominated by high-biomass, less-palatable grasses like *Eragrostis plana* (Finca, 2012). This state of rangeland can still be useful to grazers with the higher grass biomass, basal cover and active plant growth than a neighbouring catchment that is on Karoo Supergroup Formation (mudstones) (Finca, 2012). A catchment underlain by mudstones will have lower standing biomass, leaf area index, basal cover and mean MODIS NPP (Finca, 2012). This emphasises how different vegetation conditions can be achieved under the same topographic, climatic and management conditions. The catchment underlain by mudstone is perceived as more degraded than the catchment underlain by dolerites and sandstones (Finca, 2012).

Degradation is not only driven by continuous or excessive herbivory but also by various other co-occurring processes that occur under continuous herbivory that contribute to vegetation changes (Finca, 2012). Some of these processes include the concentration of nutrients caused by livestock near homesteads due to kraaling, as well as along drainage lines and around livestock drinking points. The combination of livestock behaviour and high livestock numbers will often result in localised effects like soil compaction on livestock paths and around water points (Finca, 2012). This

effect of grazing around water points is known as the piosphere effect (Lange, 1969). The result of concentrated nutrients, especially nitrogen, around homesteads and water points is short, perennial grazing lawns that are dominated by *Cynodon dactylon.* This grass species is not leafy but provides high-productivity grazing for sheep during the wet season. During the dry season these grazing lawns are depleted and, as a result, this reduces the amount of available forage for livestock and also reduces the amount of soil protection by vegetation (Finca, 2012).

2.3.2.6 Vegetation degradation in South Africa

There are various types of veld degradation in South Africa which include: loss of cover and change in species composition, bush encroachment, alien plant infestation and deforestation (O'Connor *et al.,* 2014). Reduced vegetation cover and species composition change is often likely to be the first indication of degradation. It is, however, difficult to determine the difference in changes in veld conditions due to either environmental factors (e.g. changes in rainfall) or mismanagement. The term 'change' does not, however, always equate with 'degradation' because changes can occur due to natural variability, in climate for example (Meadows and Hoffman, 2002).

Reduced veld condition caused by wood-cutting, fire, drought and overgrazing is a significant problem in the higher rainfall grassland biome in South Africa, particularly in KwaZulu-Natal, Gauteng and the Eastern Cape (Meadows and Hoffman, 2002). Communal rangelands, especially those susceptible to heavy grazing, are particularly susceptible to reduced veld condition.

When vegetation degradation is taken as a whole, the degree, extent and rate of veld deterioration in South Africa is significantly higher in communal rangelands compared to land under commercial tenure (Hoffman *et al*., 1999). When a veld degradation index was combined with a soil degradation index, the Eastern Cape was revealed as one of the top provinces with a highly impacted ecosystem (Meadows and Hoffman (2002). Novel ecosystems views widely held in South Africa is that vegetation degradation is irreversible meaning that the vegetation needs to be preserved and protected in its current form (Hoffman *et al*., 1999).

2.3.3 Underlying drivers of land degradation

2.3.3.1 Factors causing land degradation in South Africa

In the past, in South Africa it was viewed that human influences were the only cause of land degradation but further studies showed that long term climate change, resulting in changing precipitation patterns, coupled with temperature increases are also influential causes of land degradation (Hoffman *et al*., 1999). Humans in South Africa often depend on agricultural land and

when this dependency is combined unsustainable practices and increased intensification of agricultural practices, it often leads to land degradation in South Africa (Hoffman *et al*., 1999). Regardless of long term climate change and over intensification of agriculture, two key issues in the process of land degradation in South Africa are population growth and land tenure patterns.

It has been found that the increase in population size does not always lead to more erosion as would be expected (Mason and Jury, 1997). This suggests that the relationship between land degradation and population size and growth rate is more complex than originally thought (Mason and Jury, 1997). Due to the lack of intensification of agriculture in communal rangelands and increased stocking rates, the land use practice in these areas led to degradation (Hoffman and Todd, 2000).

In the communal rangelands of South Africa, growing human populations have resulted in greater erosion due to the communal land tenure system. This means that on South African communal rangelands the combined effects of population growth and communal land tenure are some of the key underlying factors of land degradation (Hoffman *et al*., 1999).

Communal land tenure has been found to be the most significant factor that controls the severity, rate and extent of degradation (Meadows and Hoffman, 2002). The type of tenure, either land under commercial or communal tenure is, thus, the primary determinant of the amount of land degradation that will occur (Hoffman and Todd, 2000). There are districts in the Eastern Cape that are among the most severely degraded landscapes in South Africa due to possessing the combination of physical and socio-economic factors that have led to both severe and sometimes irreversible levels of land degradation in communal landscapes (Meadows and Hoffman, 2002).

2.3.3.2 Land degradation in South Africa and its former homelands

The first official reports of land degradation in South Africa in terms of overgrazing and soil erosion were recorded during the 1880s in the Herschel district of the Ciskei (Beinart, 2003). By the 1920s there were reports of widespread land degradation in both the Ciskei and Transkei, both of which comprise significant areas under communal tenure (Beinart, 2003). Owing to the drivers of land degradation in South Africa, areas under communal tenure are subject to reduced productivity (Wessels *et al*., 2004), increased soil erosion (Kakembo and Rowntree, 2003), change in vegetation composition and the amount of basal cover (Vetter *et al.*, 2006) and increases in the number of woody shrubs (Shackleton and Gambiza, 2008). These driving factors are largely linked to the social and political history of the country (Beinart, 2003).

2.3.3.3 Social and political factors of land degradation in South Africa

South Africa's unique land tenure pattern, consisting of a distinct divide between commercial and communal farms, has had a direct effect on land degradation in the country (Hoffman and Todd, 2000). This divide is deeply rooted in its colonial and apartheid past (Hoffman *et al*., 1999). During this era, significant numbers of the black population were relocated and the majority were forced onto 14% of South Africa's land, formally classified as homelands (Hoffman *et al*., 1999). Managed under communal tenure, these areas were and continue to be significantly under-resourced in comparison to the agricultural land under the commercial farm system in the country (Meadows and Hoffman, 2002). Communal land is under the management of traditional leadership, which gives individuals few rights to own and sell land. The respect for traditional authorities in communal areas is declining which will have knock-on effects for unsustainable resource management and degradation trajectories in communal rangeland systems (Kirkland *et al*., 2007). Historically the commercial agricultural land, where individuals have property rights enabling them to sell land for profit, was owned by the previously politically dominant white minority. As a result of the differences between the two land tenure systems, it can thus be argued that there are large differences in the degradation status of the two land tenures caused by skewed access to political and socio-economic power (Hoffman *et al*., 1999).

The South African landscape had, and perhaps continues to have, polarised biophysical and socio-economic conditions under different land tenures (Meadows and Hoffman, 2002). Favourable land was parcelled out to the 'privileged elite'. Furthermore, preferential appropriation of productive land meant that commercial areas generally have shallower slopes and a lower rainfall runoff ratio (Meadows and Hoffman, 2002). A prominent sign of the stark contrast in land tenure is the stocking rate which is twice as high in the communal rangelands, with associated high population densities and rural settlement living, compared to commercial agricultural areas (Hoffman and Todd, 2000).

Therefore, South Africa's unique land tenure has shaped much of the current day rangeland management systems and associated degradation (Meadows and Hoffman, 2002). Due to the distinct differences between communal and commercial rangeland systems, it is instructive to explore their inherent characteristics further.

2.3.3.4 Communal rangelands

Communal rangelands are open fields or areas that are used for grazing and are divided into three categories (Palmer and Bennett, 2013). The first is designated rangelands in communal areas that were established before the Land Act of 1913 as native reserves. The second is the rangelands that have been transformed from previously commercial farms to rangelands as part of post-1994 land redistribution. The third is arable lands that have either been abandoned or are still under

cultivation but become a common grazing resource after the harvest has taken place (i.e. the residue of the crops provide grazing for livestock during the dry season) (Palmer and Bennett, 2013). The latter is a common practice in areas under communal tenure where there are no fences or poorly maintained fences, like Lesotho or the former Transkei and Ciskei (Palmer and Bennett, 2013). There is a long history of communal grazing in many of these cultivated croplands with a large proportion associated with claims of land degradation.

Perceptions of soil erosion in rural communal rangelands are significant because they determine the attitudes of people towards rehabilitation and soil resource conservation (Van Tol *et al.*, 2016). This means that if the soil erosion problem and its implications are well understood then the positive involvement in the solution (rehabilitation) and positive support of soil conservation practices will increase by those living in the communal rangelands (Van Tol *et al.*, 2016). On the other hand, in these areas there is a lack of ownership of the erosion issue which has made many people unaware of the soil erosion problem undermining the long-term incentive for soil rehabilitation and conservation (Van Tol *et al.*, 2016).

Degradation in communal rangeland systems has been associated with lack of ownership amongst communal land users. This principle is widely known as the Tragedy of the Commons (Hardin, 1968), a situation believed to arise in a shared-resource or common property resource system. Hardin (1968) proposed that individuals which share common property, such as communal rangeland, act independently according to their own self-interest and behave against the common good of all resource users by depleting a resource for their own gain, resulting in the overall degradation of the common property resource. This is believed to occur unless common property is converted to private property or regulation of the uses and users is instituted by the state (Feeny *et al.*, 1990).

2.3.3.5 Commercial rangelands

Veld management is essential for commercial farmers to maintain rangelands to enable optimum animal production (Camp, 1995). These management practices are grounded on the concept of equilibrium, meaning that rangelands have a carrying capacity and once the capacity has been exceeded the productivity of the rangeland will be reduced (Duma, 2000). This is rooted in the theory of plant succession which highlights that the pressure from the livestock grazing is balanced against the natural ability of plants to regenerate themselves in order to maintain stable rangelands (Duma, 2000). The frequency and intensity of the grazing must be controlled in order to maintain healthy rangelands for the grazing demands of the livestock. According to O'Reagan and Turner (1992) there are six principles on which veld management is based: 1) separation of veld types, 2) determining the best stocking rate, 3) periodic resting of rangelands for re-establishment of

seedlings, 4) animal type, 5) stocking ratios and 6) grazing systems. Failure to conduct veld management properly based on these six principles may result in various forms of land degradation including rangeland degradation caused by woody encroachment (O'Reagan and Turner, 1992; O'Connor *et al.,* 2014).

2.4 Sediment in river systems

Fine-grained sediment is a natural and vital element of river systems as it contributes towards the hydrological, morphological and ecological functioning of the river system (Owens *et al*., 2005). There are many places around the world where the amount of anthropogenic activity has altered the fine-grained sediment yields at a rate which has caused significant changes in the functioning of a river system (Owens *et al*., 2005).

Material that is transported via river systems is found in two forms: solid material and material that is in solution (<0.45 µm) and these two forms can be further divided into organic and inorganic sediments (Wood and Armitage, 1997). Solid load is separated into bedload and suspended load, both of which are often determined by establishing the relationship between the flow of the river, structure, density as well as size of the material system (Owens *et al*., 2005). Suspended sediment is composed of material that is finer and/or less dense than bedload (Wood and Armitage, 1997). Most of the suspended sediment particles in many river systems is less than 2 mm (e.g. sand grains) in diameter, however, a large proportion of the suspended sediment is less than 63 µm (e.g. silt and clay) (Walling *et al*., 2000). The particles of suspended load that are less than 63 µm in diameter have an important role in biogeochemical fluxes in river systems due to the chemically active element of solid loads. These loads contain contaminants and nutrients (e.g. dioxins, heavy metals and phosphorous), which are transported and stored along with the particles that are less than 63 µm (Foster and Charlesworth, 1996; Owens et al., 2001). These particles travel in the river systems as flocculated material/flocs which will have concomitant effects on the river system as a whole (Droppo, 2001). Flocs are able to regulate their own characteristics but can also regulate the surrounding water quality via physical, chemical and biological activity (Droppo, 2001).

2.4.1 The effects of altered sediment yield on hydrological systems

Fine-grained sediment plays a vital role in controlling the hydrological and geomorphological functioning of a river, and these sediments also add to the biological functioning by influencing habitat quality and quantity (e.g. creating mudflats) (Owens *et al*., 2005). Extreme changes in the amount of fine-grained sediment that is put into river systems can have multiple detrimental effects. These effects are separated into two main types: quantity and quality. Extreme amounts of sediment

that are transported into river systems that are derived from increased erosion (e.g. due to agriculture or deforestation) or land surface disturbances (e.g. mining and construction) have the ability to cause multiple physical detriments (Owens *et al*., 2005). These include discoloured water and sedimentation of reservoirs, channels, harbours and estuaries. As a result of these detriments, the sedimentation can change the channel morphology and behaviour as well as navigation. With regards to sediment quantity, it must be noted that too little sediment (coarse and fine) can also be harmful to the geomorphological and ecological functioning of river system just like too much sediment (Kondolf, 1997). If there is too little sediment in a river system it may cause: 'hungry water' (which is where rivers with too little sediment may undergo channel incision), erosion of banks, change in riverine habitats and undermining of bridges (Kondolf, 1997).

With an outlook of global sediment quality, the fine-grained sediments (<63 µm) that are transported in river systems are showing evidence of rising concentrations of nutrients and contaminants that are often near or above the sediment quality guidelines (Blake *et al*., 2003). As a result of this, there are implications for river ecology (e.g. eutrophication) as well as human health (e.g. high levels of pathogens) (Owens *et al*., 2005).

Fine-grained sediment in the water column will increase turbidity, decrease light penetration and potentially decrease the amount of primary productivity which will have knock-on effects for the food chain (Davies-Colley *et al*., 1992). Sedimentation in river channels also changes the channel substrate by modifying the surface conditions as well as the volume of fine-grained sediment in the hyporheic zone (beneath the stream bed) (Graham, 1990; Richards and Bacon, 1994). In cases where there is an extreme amount of sediment in the river, the fine-grained sediments have the potential to smother the whole riverbed which has multiple knock-on effects for habitat availability (Wood and Armitage, 1997).

Various types of pollutants can become adsorbed to sediments that have accumulated at the bottom of rivers and dams (Kim *et al*., 2003). These sediments are accumulated over many years and have the potential to become new pollutant sources to the water column after many years when the water quality has improved (Abrams and Jarrell, 1995). The pollutants that are adsorbed onto the sediments can also be released back from the sediment into the water column if the water quality changes (Furumai *et al*., 1989). The two factors that affect the rate of release are sediment characteristics and the overlying water quality (Kim *et al*., 2003).

Research that is based on long-term monitoring (i.e. multiple decades) of suspended sediment fluxes, sediment budgets and reconstructed sediment yields from dams and reservoirs indicates a

rise in the amount of global fine-grained sediment. There has also been a rise in the transport of fine-grained sediment in rivers within catchments that have been influenced by anthropogenic activity like deforestation and agriculture (Trimble, 1983; Walling and Fang, 2003; Owens *et al*., 2005). Human activities have been directly and indirectly linked to 80-90% of the fluvial sediment that is transported via rivers to the coastal oceans (Farnsworth and Milliman, 2003).

2.4.2 Sediment yield and land use

It is estimated that one-sixth of the global land surface area has been affected by water erosion (Shroter *et al*., 2005). Besides the in-situ problems that relate to the loss of fertile soil, the sediments that travel into the rivers from the eroded landscape pose problems downstream for hydraulic infrastructures like dams, and for fluvial systems (Alatorre *et al*., 2012). Garcia-Ruiz (2010) found that the change in land use/land cover (LULC) is one of the main factors that can be attributed for the intensity of soil erosion and deemed even more important than high-intensity rain and slope angle in certain instances. Multiple studies and researchers have found that LULC change has influenced the amount of sediment yield in many catchments globally (e.g. Dearing, 1992; Piegay *et al*., 2004; Cosandey *et al*., 2005; Gyozo *et al*., 2005). Mountainous areas, where the steeper slopes cause a higher amount of soil erosion, as well as sediment redistribution rates, are the areas that are at greater risk (Alatorre *et al*., 2012).

Suspended sediment that is delivered to oceans around the world has been estimated to be 15-20 x 10^9 tons per year; a disproportional amount of this sediment is discharged by rivers that are in mountainous areas (Farnsworth and Milliman, 2003; Syvitski, 2003). Many mountainous regions around the world are affected by land use change with consequences for vegetative cover, soil conservation, runoff and sediment yield (Garcia-Ruiz *et al*., 1995). Changes in land use results in a change in plant cover density or type (Garcia-Ruiz *et al*., 1995). This, in turn, has direct effects on the rate of soil erosion, infiltration, overland flow, erosion as well as sediment yield. The change of land use within a catchment can affect the buffering functioning of the catchment resulting in different time lags, peak flows and sediment budgets (Garcia-Ruiz *et al*., 1995). The change in these factors will have multiple effects as mentioned above (Alatorre *et al*., 2012).

2.4.2.1 Case studies of the sediment yield in different cultivation

Garcia-Ruiz *et al* (1995) conducted a study in the Spanish Pyrenees Mountains on the sediment yield under different land uses. They found that the greatest soil losses occurred with shifting agriculture. Shifting agriculture is a type of agriculture where vegetation is cleared and the ground is cultivated for a few years and then left to lie for a few years until the fertility of the soil has recovered naturally

(Garcia-Ruiz *et al*., 1995). Under periods of intense rainfall on steep and sunny slopes with low vegetation cover the hydrological response is rapid and the suspended sediment concentration also increases rapidly. Abandoned fields that were once cereal crops lose more soil in their first few years of abandonment caused by sheet erosion and low vegetation cover (Garcia-Ruiz *et al*., 1995). Pristine grasslands with a high percentage of vegetation cover will allow water to pass through them but will yield a low amount of sediment due to its buffering function. These grasslands will act as sediment (dis)connectivity buffers through various functions like increased roughness, sediment trapping and causing a lower flow velocity which increases infiltration (Garcia-Ruiz *et al*., 1995).

In South Africa, soil erosion is highly variable and has a strong link to past land use change (Garland *et al*., 1999; Kakembo and Rowntree, 2003). Erosion that occurred in South Africa during the Holocene epoch (which began 11 700 years ago) took place mainly in areas of high elevation and high rainfall along the Drakensberg Escarpment (Compton *et al*., 2010). The source of erosion has shifted more recently to intensely cultivated agricultural land that is in areas of lower elevation and has only moderate to high rainfall (Compton *et al*., 2010). During the Holocene period, the main source of sediment in the Orange River was the Elliot Formation however in recent years the mud flux in the Orange River has increased ten-fold which is due to catchment-wide soil erosion and not because of irregular flood events (Compton *et al*., 2010). Areas that have high levels of soil erosion often correspond with high levels of vegetation denudation which is indicated by the infilling of dams with sediment (Le Roux, 1990). High-intensity rainfall events are those which cause the most soil erosion (Stocking and Elwell, 1976; Smithen and Schulze, 1982; Le Roux 2011) and as a result of this, it can be deduced that land that is heavily cultivated and receives rainfall as intense summer storms, will have the greatest soil erosion (Le Roux, 1990).

2.4.3 Effects of grazing on sediment yield

In many agricultural areas around the world investments are made to restore catchments and improve land management systems to reduce the amount of sediment leading into river systems (Bartley *et al*., 2010b). Bartley *et al* (2010a) and Bartley *et al* (2010b) state that sediments can be delivered to rivers via three main sources: 1) hillslopes, 2) gullies and 3) bank erosion.

Trimble and Mendel (1995) conducted a study on the impacts that the grazing of cattle can have on various catchment processes such as soil hydrology, runoff, bank erosion and stream channels. They found that when cows heavily graze an area it can result in increased soil compaction, reduction in the amount of infiltration, increase in runoff as well as an increase in sediment yield. The effects of light to moderate grazing are much less significant (Trimble and Mendel, 1995). The results from

Bartley *et al* (2010a), however, show that as the vegetation cover increases the annual average total suspended sediment concentration (mg/l) decreases (Figure 2.2).

Grazing land management (GLM) in rangelands aims to manage vegetation as its primary focus (Noble *et al*., 1984). According to Noble *et al* (1984) there are four methods that can be used to rehabilitate or promote recovery in the vegetation of rangelands: 1) reduce the density of livestock (with or without seasonal field resting); 2) prescribed burning; 3) planting introduced plant species and 4) replanting indigenous plant species. If the vegetation has been managed correctly it will ultimately lead to a reduction in sediment yields in the rivers (Bartley *et al*., 2010a).

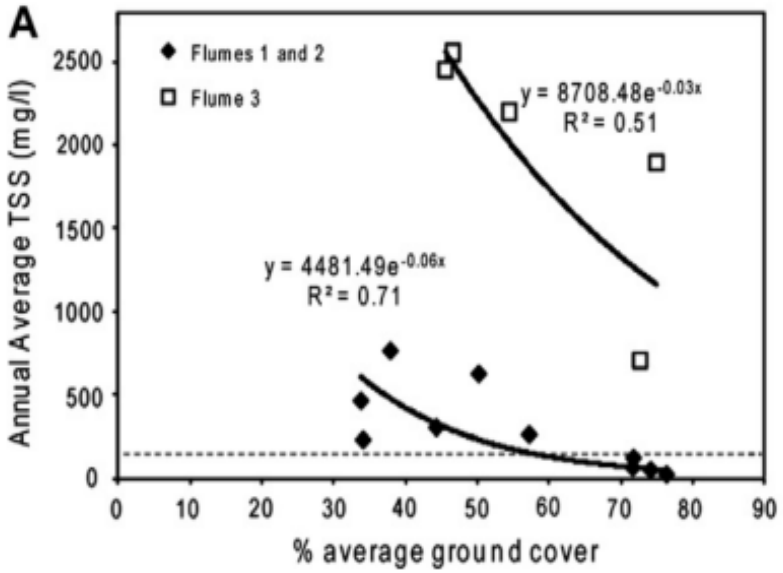

Figure 2.2: The relationship between average annual ground cover (%) and average annual suspended sediment concentration for three hillslope flumes. The dashed line represents the median TSS concentration (122 mg.l^{-1}) from the non-grazed plots at Meadowvale (From: Bartley *et al.,* 2010a: 245).

2.5 Summary

Land degradation has various negative impacts and consequences for terrestrial and aquatic systems that threaten their sustainability. The key drivers of degradation and soil erosion in South Africa have been identified in this research as high livestock populations, erodible parent material, rainfall intensity, absence of conventional grazing management practices (e.g. grazing rotation), poor vegetation cover, poverty and limited access to markets (Laker, 2004; Palmer and Bennett, 2013).

Although NDVI is often used as a proxy for biomass/vegetation cover in grasslands (Jianlong, Tiangang and Quangong, 1998; Silleos *et al.*, 2006; Butterfield and Malmström, 2009; Guay *et al.*,

2014) there is a gap in the literature for the comparison/calibration of satellite data (NDVI) and actual grassland cover, especially in the Tsitsa River catchment.

Certain soils are more erodible than others, namely the soils that are found on the Molteno and Tarkastad Formations which form duplex soils that are most susceptible to gully erosion (Le Roux, 2011; Le Roux *et al*., 2015). South Africa's favourable agricultural and grazing land was unequally distributed due to the political history of the country which means that the biophysical and socio-economic conditions under different land tenures are polarised (Meadows and Hoffman, 2002). The commercial rangelands are in areas of favourable conditions and the communal rangelands are in areas of less favourable conditions and are more susceptible to land degradation due to factors like high stocking rates and overgrazing coupled with erodible duplex soils (Hoffman and Todd, 2000; Le Roux, 2011).

Increased sediment yields in rivers can be caused by a change in agricultural types (e.g. grazing field changing to cereal crops), gully erosion and erosive rainfall coupled with low vegetation cover (Stocking and Elwell, 1976; Garcia-Ruiz *et al*., 1995; Vacca *et al*., 2000; Le Roux, 2011). This increase in sediment yield can have multiple effects on the ecological and hydrogeomorphological functioning of a river system and can result in sediment filling of dams downstream (Graham, 1990; Davies-Colley *et al*., 1992; Richards and Bacon, 1994; Kondolf, 1997; Owens *et al*., 2005).

As such, this literature review positions this study against the backdrop of existing literature thus, the results should be able to provide new insight into the effects that erosive rainfall has on sediment fluxes with seasonally varying grassland vegetation cover, whilst accounting for the complexity of land-use legacy and governance history in system response/behaviour. Not only will this study contribute to the calibration of remotely sensed NDVI data (from the Sentinel-2A sensor) to the grassland vegetation cover and above-ground biomass within the Upper Tsitsa River catchment but it will contribute insight to the added complexity of differing soil types, rainfall intensities, land tenure (commercial and communal rangelands) and governing history and how this can influence erosion and sediment yield.

Chapter 3: Methods

3.1 Study design and Introduction

The research presented examines two contrasting catchments which serve as individual case studies, namely the Little Pot River catchment (LPRC) and the Gqukunqa River catchment (GRC). The two catchments differ in geology and land use. The study design was conducted in the following manner in order to cover a range of geomorphological factors/variables: 1) each sub-catchment was sampled to represent the two main geologies (sandstone and mudstone dominated rock types); 2) given that rivers in the study area flow predominantly from west to east, north and south aspects were separated for each of the above geologies; 3) five sites were selected for ground-truthing per aspect covering a range of four NDVI classes and 4) five repetitions of field measurements within each ground-truthing site which consisted of a 5 x 5 m quadrat. These 80 field measurements per catchment included biomass measurements, vegetation cover estimates, soil surface hardness measurements, biocrust cover estimates and slope angle measurements. The primary consideration in this study was to compare vegetation cover, rainfall intensity and the resultant sediment flux for an early, mid and late rainfall season within each catchment but not between them.

A variety of desktop and field methods were used to achieve the objectives of this study. The desktop analyses included: calculating NDVI and creating maps/surfaces from the metric, choosing ground-truthing sites with ArcGIS, creating rainfall graphs and calculating rainfall intensity of each catchment and calculating the sediment fluxes and yields in each catchment. The ground-truthing and fieldwork were conducted during October 2018, January 2019 and April 2019, i.e. the wet season of 2018-2019. Sediment and rainfall data from both catchments were only available for certain periods. The rainfall data available for the GRC is only from January 2018 to January 2019 whereas in the LPRC it is available from August 2015 to January 2019. The missing rainfall data for the GRC is supplemented with rainfall data from the adjacent Lower Sinxaku catchment (LSC). The sediment data for the LPRC is available from January 2016 to August 2016 and for the GRC is available from January 2016 to January 2019.

3.2 Remote sensing, ground truthing and field methods

3.2.1 Sensor and image selection

The Sentinel-2A sensor has 12 spectral bands of varying spatial and spectral resolutions which vary from 10 m to 60 m (SIC, 2019). This sensor was chosen due to its freely available satellite images as well as its quality of temporal resolution (5 day revisit time) and spatial resolution (10 m) for the

near-infrared (band 8) and red (band 4) bands. The satellite image bands support multiple vegetation indices such as leaf chlorophyll content (which is the basis for NDVI measurements), leaf area index and leaf water content (SIC, 2019). Images were acquired from the USGS Earth Explorer website (USGS EE, 2019) with level-1C preprocessing applied which includes radiometric and geometric correction (ESA, 2019).

NDVI was calculated for both catchments using the fourth band (red) and the eighth band (near infrared) from the Sentinel-2A sensor and using the equation: NDVI = $\frac{(NIR-Red)}{(NIR+Red)}$. The NDVI was only calculated for grassland areas of both study catchments and all non-grassland areas were removed from the assessment. In order to calculate an NDVI the infrared (832,8 nm) and red (664,6 nm) spectral bands are required (Washington-Allen *et al*., 2008) and on the Sentinel-2A satellite, these two bands have a spatial resolution of 10 m (SIC, 2019). Sentinel-2A also has the added flexibility of a short wave infrared spectral (SWIR) band (20 m resolution) which allows for the calculation of Normalised Difference Senescent Vegetation Index (NDSVI) (Qi and Wallace, 2002; SIC, 2019), which some authors have experimented with for use during winter months when grassland vegetation is dry and senescent and lacks active chlorophyll, and when NDVI may potentially not display an accurate representation of the biomass present in the landscape (Qi and Wallace, 2002). The use of NDSVI was explored but it could not distinguish between bare soil and senescent vegetation and so NDSVI was not used.

This study was conducted during the wet season when the high-intensity rainfall events occur with maximum impact so the vegetation and sediment yields are most likely to be influenced. The months of October, January and April were chosen in order to represent the whole rainfall season – early, mid and late rainfall season according to Figure 1.2 (Moore, 2016). Having a time series of multiple NDVI scenes meant that spatio-temporal trends could be identified across the landscape (Washington-Allen *et al*., 2004). The field verification spanned one wet season only (October 2018 - April 2019), however, the calibrated data were used to extrapolate NDVI results from previous years to vegetation cover so that it overlapped with sediment flux and rain data.

The wet season of 2018-2019 was chosen to calibrate the satellite data with field variables as this was the only full wet season that overlapped with the time of this study. The satellite images were chosen to include images with the least amount of cloud cover present for the months of October 2018, January 2019 and April 2019. There were a limited number of cloud-free images with only about one or two available per month. However, a cloud-free image was always available for a date that was one week before or after each field trip was conducted, thereby ensuring that field calibration campaigns were matched with image acquisition dates and, thus, the vegetation

characteristics as measured through NDVI. Acquisition dates of the three satellite images used were 10 October 2018, 22 January 2019 and 12 April 2019.

3.2.2 Field calibration and site selection

Due to the different underlying geologies in both the LPRC and GRC the NDVI field points needed to cover the main geologies as well as two main aspects (north and south-facing slopes) which are known to affect vegetation growth/response at local scales, i.e. aspect related micro-climate (Vetter *et al*., 2006). The Drakensberg Group was excluded from the study in the LPRC because they primarily comprise basalt, a highly resistant rock and only denudes at a rate of six metres per million years based on cosmogenic isotope analysis (Fleming *et al*., 1999). The Karoo Dolerite Formations was excluded from the study in the GRC because it makes up a very small portion (2 km^2, equivalent to 1% of catchment) of the geology within the GRC (Table 1.2) and it forms linear dykes and sills crossing the landscape (Coetzee, 2016). It is primarily made up of dolerite which is also a highly resistant rock formation and is less likely to contribute much sediment to the Gqukunqa River (van Zijl, 2010). As a result, only sedimentary rock layers were targeted in this study in both catchments.

Using the methodology of Huchzermeyer *et al* (2018), NDVI values were separated into 4 classes, these classes were initially determined by looking at the whole range of NDVI values for the month of October 2017 (previous year as this predated the field assessment by several months). NDVI classes captured the full extent of the NDVI values across the scene, with class sizes representative of relative/proportional membership (Figure 3.1 and 3.2). The NDVI values were classified as: very low (< 0,2), low (0,2-0,3), moderate (0,3-0,45) and high (>0,45). Low NDVI values equate to poor productivity in the leaves of the grasses or sparse grass cover (Srur *et al*., 2011). October 2017 was used as a reference for the subsequent October 2018 field trip because the desktop analysis was done before the first field trip in both catchments (Figure 3.1 and 3.2). In South Africa, October, although it signifies the start of the rainy season which initiates greening of the grasslands (Archibald and Scholes, 2007), is typically characterised by the presence of senescent grasses which are inactive and lack growth during the winter/dry season (Zhang *et al*., 2005). However, senescent grasses still provide the same amount of soil protection as green grasses do (Le Roux *et al*., 2008). The presence of senescent vegetation amongst the new green shoots at the start of the wet season will cause the NDVI values to be lower than the field biomass readings would predict due to the low reflectance values of senescent grasses compared to green grasses (Qi and Wallace, 2002).

Once the NDVI spatial surface for each appropriate month and catchment was calculated in ArcMap 10.5.1 (ESRI, 2016) the NDVI data layers were joined with the respective aspect and geology layers

and converted into point data. The point data was used for the ground-truthing sites to be chosen and appropriately stratified to ensure representation by geology and aspect across the full extent of the catchment. These points were used for field-based biomass calibration of the NDVI values. Five points were randomly selected for each NDVI category. As such, each catchment had 80 points, stratified initially by the four NDVI classes (each consisting of 20 points) (Figure 3.3).

The field-based calibration points were further utilised for subsequent months throughout the 2018-2019 wet season in order to monitor the temporal and spatial change of the biomass, vegetation cover, soil surface hardness and biocrust cover.

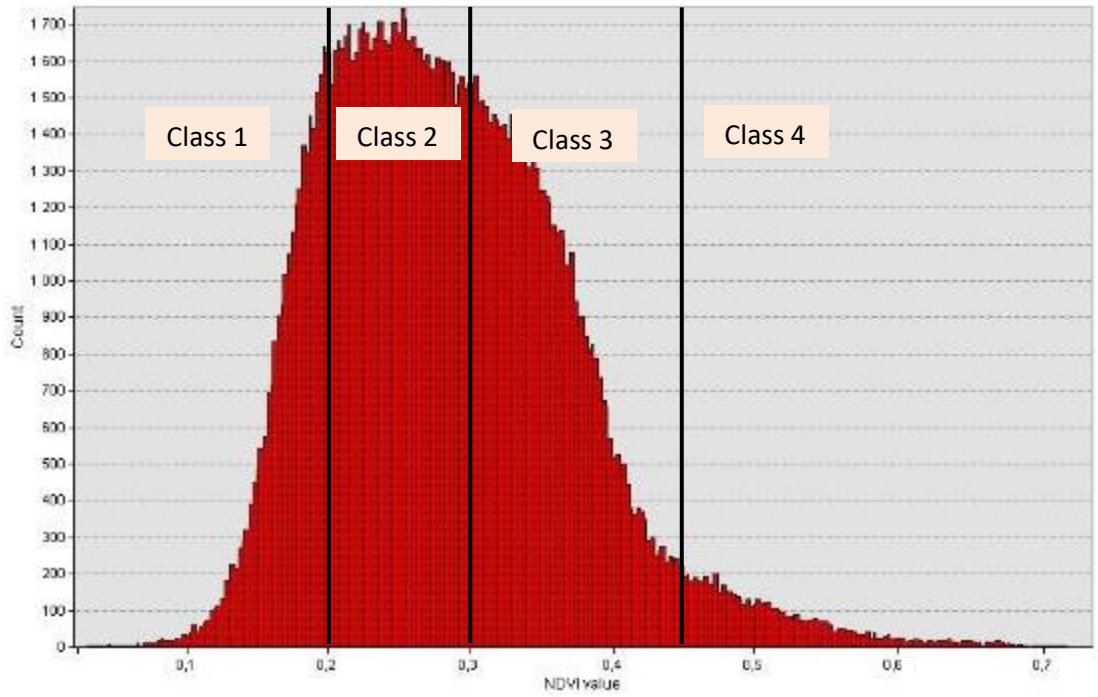

Figure 3.1: Histogram of NDVI values for the month of October 2017 in the Little Pot River catchment. The thick vertical black lines indicate the divide of the four NDVI classes.

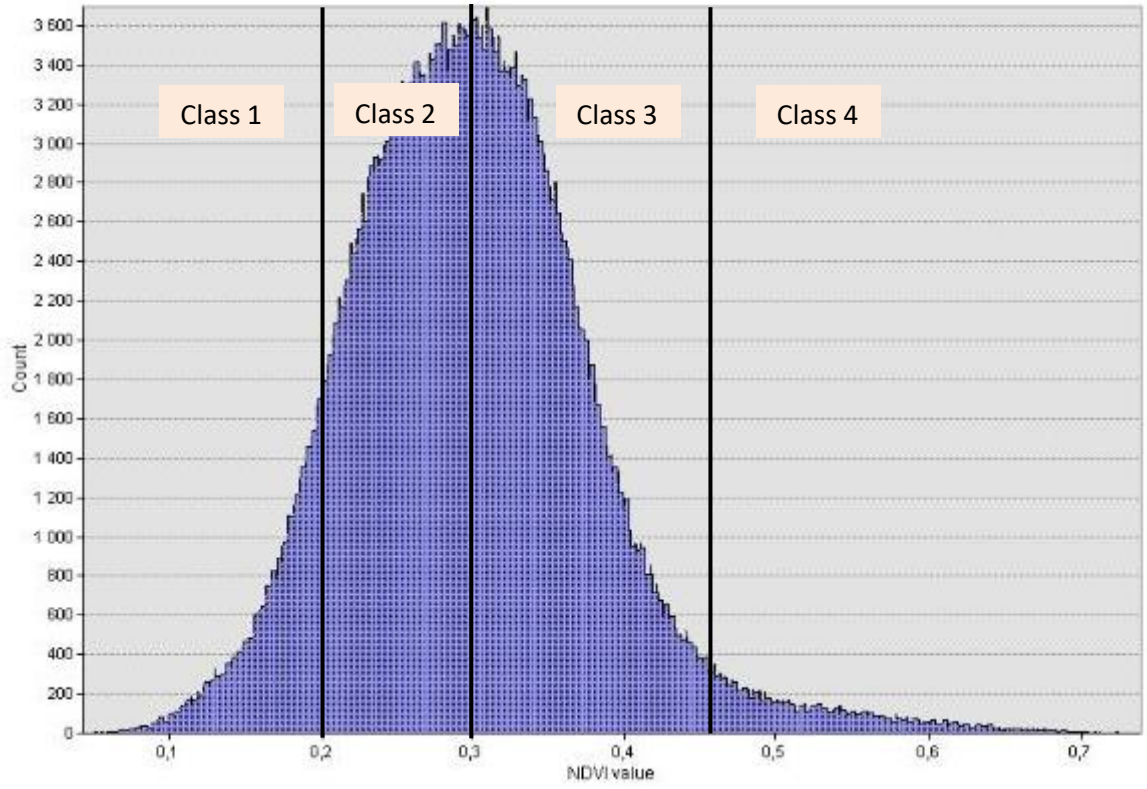

Figure 3.2: Histogram of NDVI values for the month of October 2017 in the Gqukunqa River catchment. The thick vertical black lines indicate the divide of the four NDVI classes.

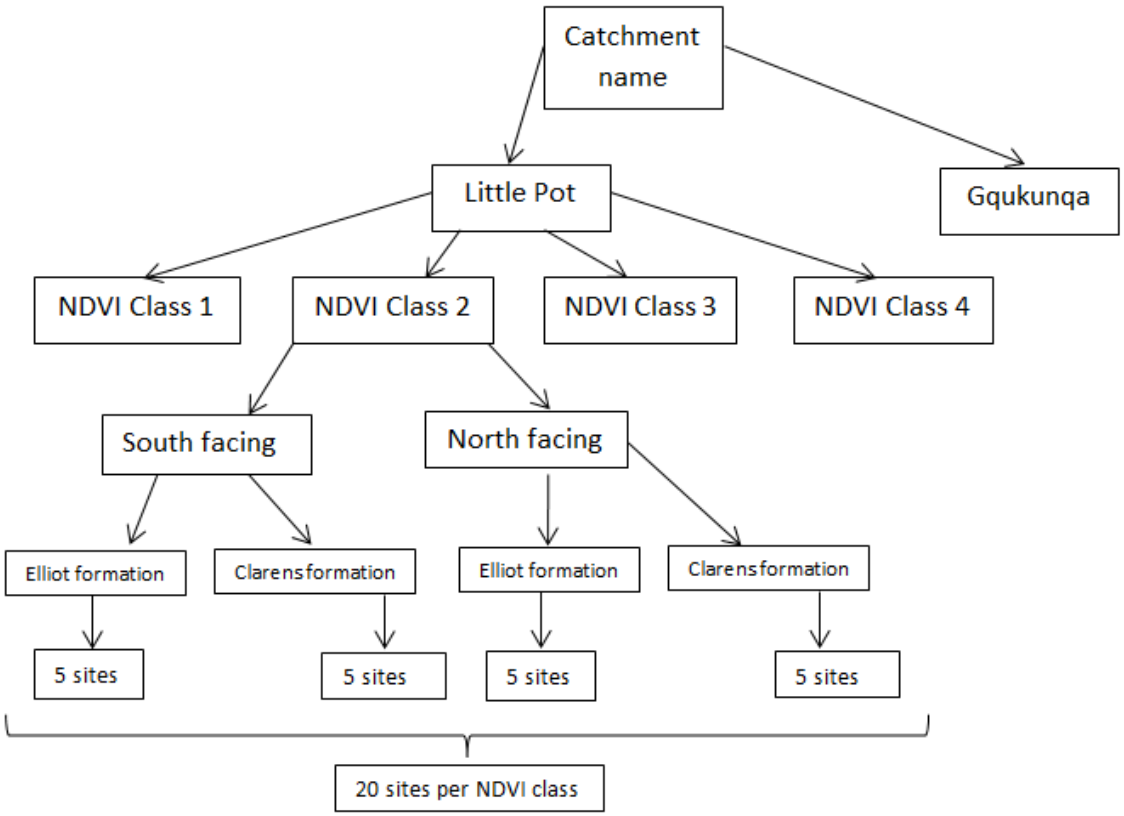

Figure 3.3: Classification framework for study sites, using the Little Pot River catchment as illustrative, resulting in 80 sites per catchment. The point labelling system refers to all aspects of the point: the catchment name, the NDVI class, the geology type, the aspect and the point number.

3.2.3 Field methods and ground-truthing

Three calibration field trips were undertaken to both the Little Pot River catchment and the Gqukunqa River catchment: 11-17 October 2018, 24-30 January 2019 and 5-10 April 2019.

In total there were 160 ground-truthing sites with calibration measurements undertaken in a 5 x 5 m quadrat per field trip. The centre of the 10 x 10 m NDVI pixels were used as the centre of each smaller 5 x 5 m ground-truthing quadrat. The positioning of each 5 x 5 m quadrat at the centre of the 10 x 10 m spatial resolution of the Sentinel-2A satellite images, provided a measurement (in)accuracy buffer ensuring the alignment of field measurements with NDVI pixels. In each quadrat five field variables were measured and recorded: above-ground biomass, vegetation cover, biocrust cover, soil surface hardness and slope angle.

3.2.3.1 Above ground biomass

The above-ground biomass was calculated using a disk pasture meter (DPM) (Figure 3.4). The equation y = 3X - 2.2, from Gwate (2017), was used to calibrate and convert the DPM disk height (cm) to total above-ground dry biomass (g.0,2m^{-2}). Gwate (2017) derived this equation from the local

grasslands in the Tsitsa Catchment (T35B). The biomass was measured in five locations within the 5 x 5 m quadrat, namely in the centre of four smaller 1 x 1 m quadrats in the four corners of the larger 5 x 5 m quadrat and in the very centre of the 5 x 5 m quadrat, and averaged thereafter (Figure 3.5 and 3.6).

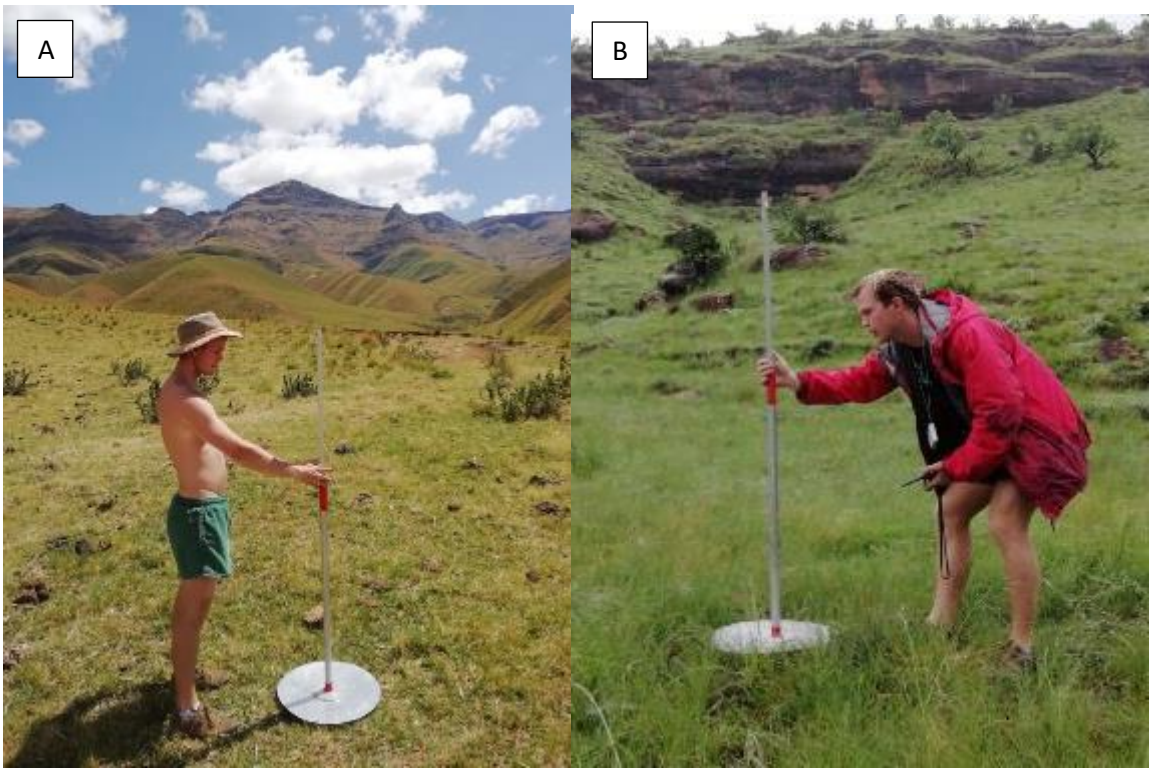

Figure 3.4: Measuring biomass in the Little Pot River catchment with a disk pasture meter. Image A shows low biomass in October 2018 and image B shows higher biomass (in January 2019) than image A (Photo credit: Gareth Snyman (Image A) and Paul Dutton (Image B)).

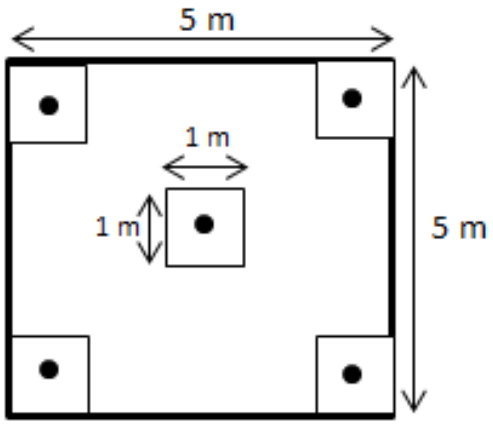

Figure 3.5: The setup of the 5 x 5 m quadrat with the smaller 1 x 1m quadrats within it.

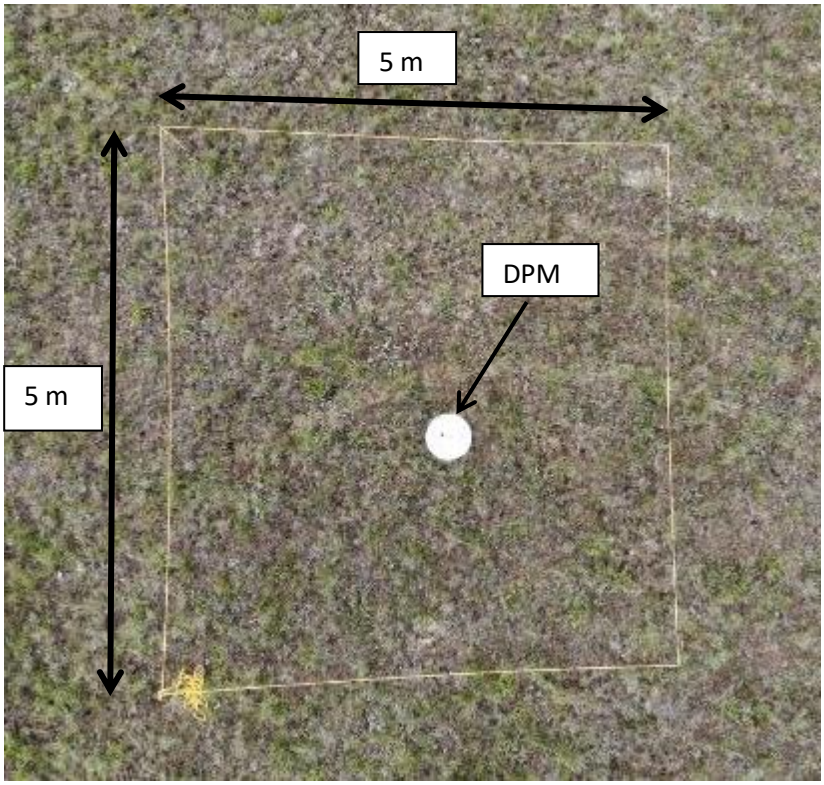

Figure 3.6: Bird's eye view of the 5x5 m quadrat in the Little Pot River catchment.

3.2.3.2 Vegetation cover

The vegetation cover was estimated as a percentage through a visual assessment of each 5 x 5 m quadrat. Figure 3.7 was used as reference in the field for estimations. Vegetation cover for each quadrat was determined by the same person throughout every field trip to reduce inter-observer bias and ensure consistency (Morrison, 2016).

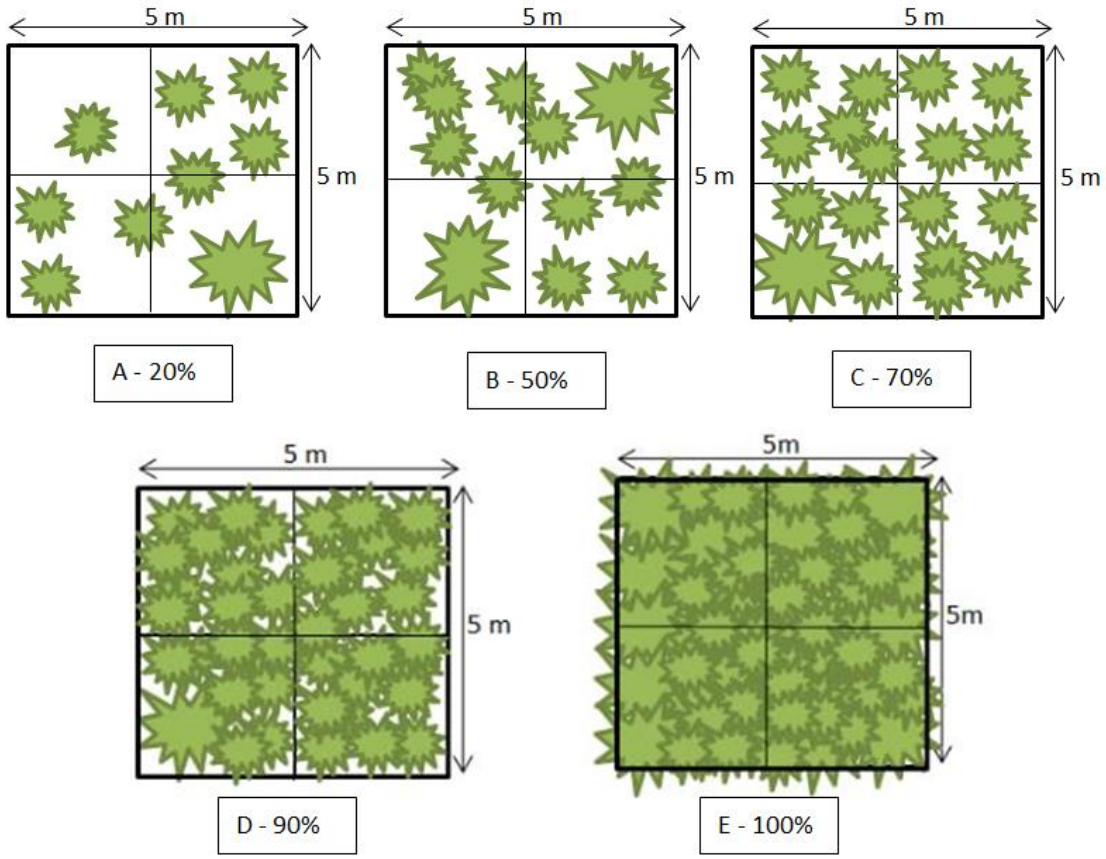

Figure 3.7: Examples of vegetation cover percentages used to determine vegetation cover (Own schematic diagram).

3.2.3.3 Soil surface hardness, biocrust cover and slope angle

The hardness of the soil surface or soil crusting was measured using a soil penetrometer which measures the amount of force required to penetrate the soil crust which ranges from 0 - 5000 KPa (Figure 3.8). Higher penetrometer values reflect greater cohesion of the soil surface. The soil crust penetration was measured in the same five locations within the 5 x 5 m quadrat as the biomass measurements.

Biocrust was also measured in the same five locations within the 5 x 5 m quadrat as the biomass and soil surface hardness measurements, and averaged per ground-truthing site/5 x 5 m quadrat. The biocrust cover (Figure 3.9) was measured by visually observing the amount of biocrust present on the soil surface in each of the five smaller 1 x 1 m quadrats (Figure 3.5) and averaged to obtain a biocrust percentage cover of the whole 5 x 5 m quadrat. The slope angle of each quadrat was measured using a clinometer.

Figure 3.8: Measuring soil surface hardness with a penetrometer in the Gqukunqa River catchment. Image A shows a soil surface hardness of 3000 KPa and image B shows a hardness of 2500 KPa. (Photo credit (image B): Terry Herd).

Figure 3.9: Biocrust present in a ground truthing site.

3.3 Rainfall data

The rainfall data for this study were collected by other parties. A tipping bucket rain gauge (Davis Scientific tipping bucket) was installed in August 2015 in the Little Pot River catchment (Figure 3.10) and the same type of rain gauge was installed in the Gqukunqa River catchment only in January 2018 (Figure 3.11). As a result of this, the rainfall data for the Gqukunqa River catchment was complimented with rainfall data from the Lower Sinxaku rain gauge (installed August 2015) which is the neighbouring sub-catchment, with similar elevation, to the south of the Gqukunqa River catchment. The Davis Scientific tipping bucket rain gauge has a diameter of 165 mm and is calibrated to 0,2 mm. The majority of the rainfall data in the LPRC is from the rain gauge on Woodcliffe Farm, located on the east side of the catchment. The 2015 rainfall data was substituted with rainfall data from Cornlands Farm, in the LPRC, because the rainfall data for the LPRC was not available for all the months of 2015. The Cornlands Farm rain guage is located in the extreme east of the Little Pot River catchment, about 4km east of Woodcliffe Farm.

Rainfall intensity data was calculated using the five-minute rainfall accumulation data from August 2015 to the end of April 2019, and converted thereafter to an hourly rate (five-minute maximum intensity per hour). Only the five-minute maximum intensity rainfall events that were greater than 25 $mm.hr^{-1}$ and isolated by a minimum rain-free period of two hours were classified as erosive rainfall events (Stocking and Elwell, 1976).

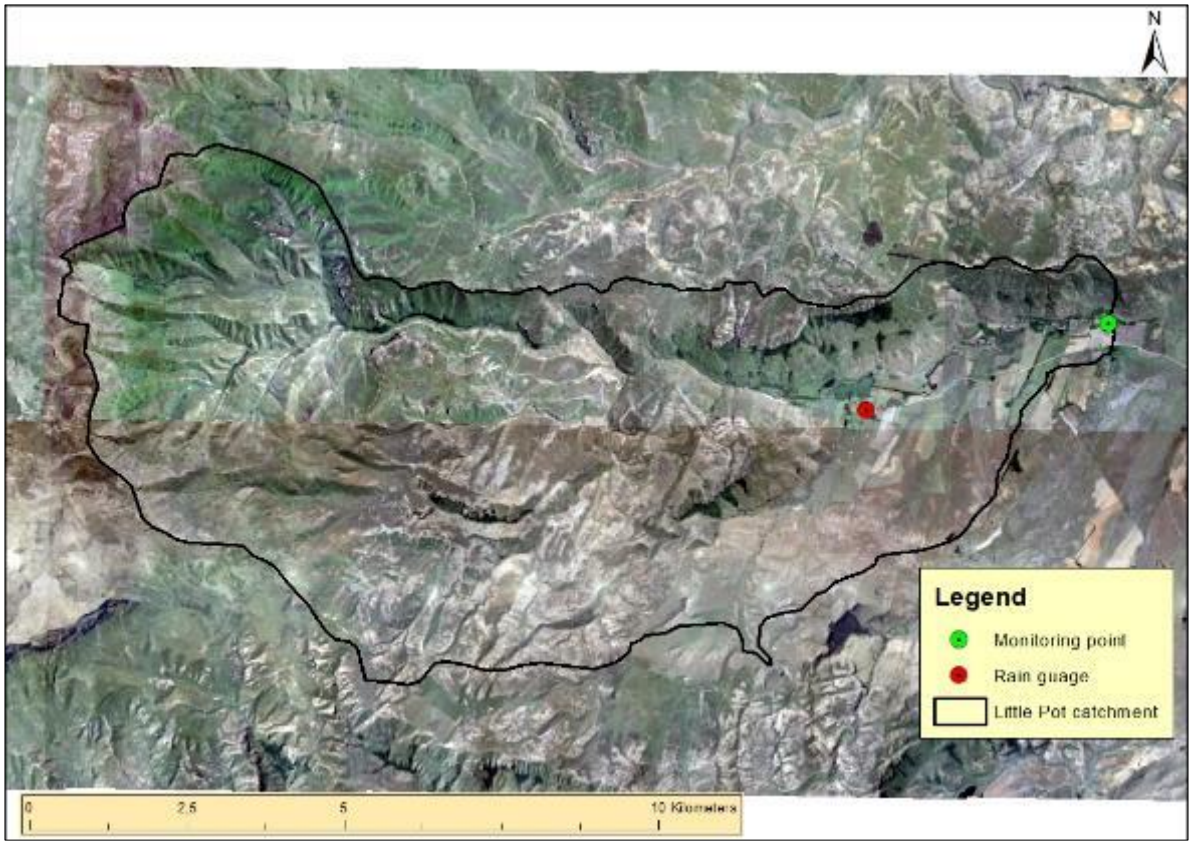

Figure 3.10: The locations of the rain gauge and sediment monitoring point in the Little Pot River catchment.

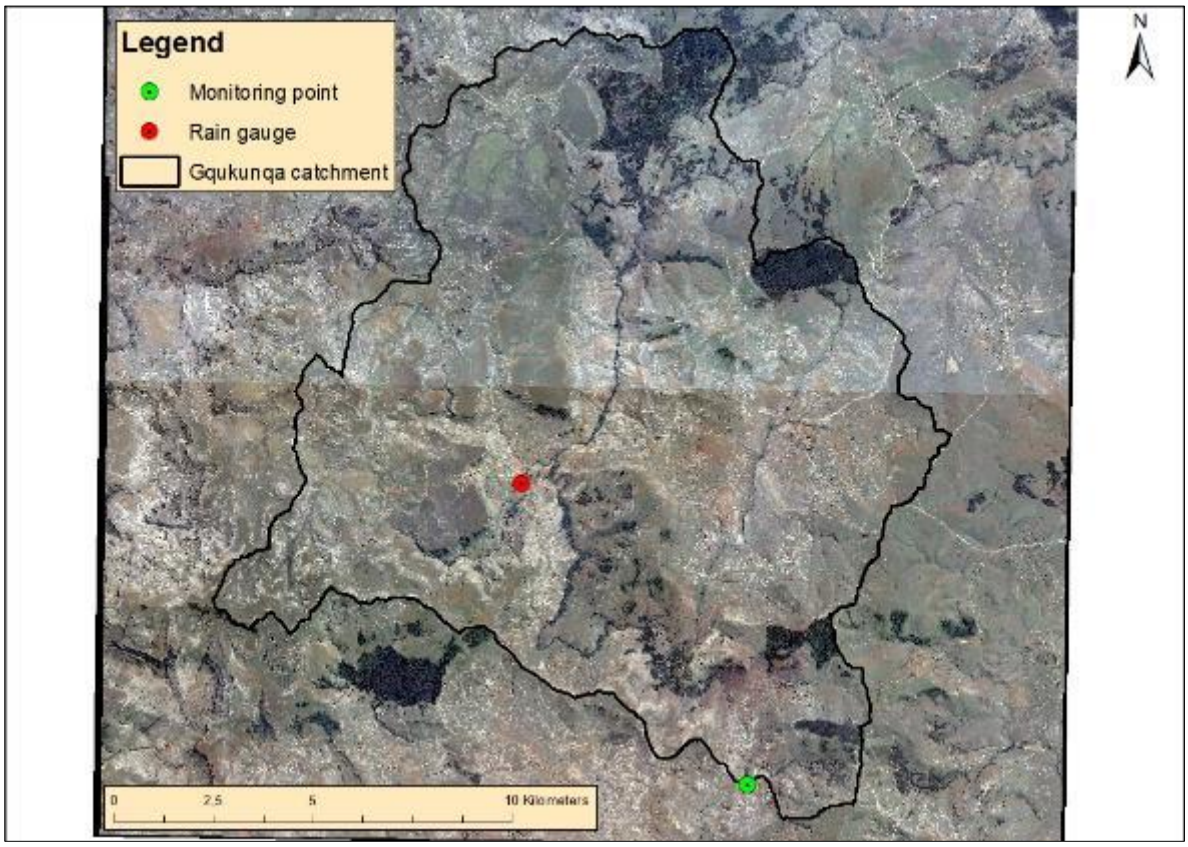

Figure 3.11: The locations of the rain gauge and sediment monitoring point in the Gqukunqa River catchment.

3.4 Sediment yield data

Total sediment yield and sediment flux were calculated from discharge and sediment concentration data. Discharge data were calculated from channel cross-sectional surveys, discharge and depth observations, rating curves and continuous water level monitoring. Sediment concentration data were based on sub-daily sediment samples that were analysed for suspended sediment concentration. Sediment flux is then calculated from the discharge and sediment concentration time series. These data were acquired by the greater project team but applied as necessary hereafter.

3.4.1 Measuring channel slope and channel cross-section

Water slope and a cross-sectional profile were surveyed along a straight reach with a stable bedrock bed. A total station and the water surface were used to measure the slope angle or energy gradient of the channel (Gordon *et al*., 2004). Multiple points along the channel were surveyed in order to include all the main breaks in slope to represent the dimensions of the natural channel.

3.4.2 Flow measurement

At each cross-section a Flow Mate (an electromagnetic flow meter) was used to measure the average velocity and depth at 20 verticals. These data were used to calculate discharge. Simultaneous discharge and stream depth measurements were taken over a range of three varied (low, medium and high) discharges to establish a stage-discharge (depth-discharge) relationship.

3.4.2.1 Discharge calculation

To measure continuous flow-depth in the Little Pot River and Gqukunqa River a Solinst Level Logger Junior Edge (model 3001) was installed in August 2015 and set to record the water level at 20 min intervals. The level logger measures the combined pressure of the water depth above the logger as well as the atmospheric pressure above the water. In order to calculate water depth alone and to compensate for changes in atmospheric pressure, the atmospheric pressure (from a barologger in the Lower Sinxaku catchment) was subtracted from the level logger reading.

Bovee and Milhous (1978) determined that developing a depth-discharge relationship with only three points gives more reliable results than Manning's equation when it is extrapolated within the 40-250% of the calibrated flow. Bovee and Milhous (1978) also showed that adding four points or more did not lead to much improvement. The following rating equation was used to calculate the discharge from the continuous depth record: $Q = a(h)^b$, where Q = discharge ($m^3.s^{-1}$), h = water depth (m) and a and b are coefficients from the rating equation(Gordon *et al.,* 2004).

The calibrated data from the level loggers coupled with the rating equation from the stage-discharge rating curve allowed for the discharge flow series from each river to be produced in Microsoft Excel.

3.4.3 Water sample collection

Local resident citizen technicians who live close to the monitoring sites in the two selected rivers for this study used basic field water sampling equipment and Open Data Kit-enabled smartphones to collect flood-focused suspended sediment (SS) samples (Bannatyne *et al*., 2017). Citizen technicians conducted baseline sampling at the flow monitoring sites (Figure 3.10 and 3.11) during the dry season (morning and afternoon sample daily). Flood sampling was conducted at shorter time intervals which resulted in 20 samples per flood event. Samples were collected using pole-and-jar isokinetic samplers. Sampling began in December 2015 in the Upper Tsitsa River catchment on the Tsitsa River and various tributaries including the Little Pot River and the Gqukunqa River (Bannatyne *et al*., 2017). Sampling is still currently (2019) being carried out in the Gqukunqa River however in October 2016 all sampling of sediment was stopped in the Little Pot River due to the low levels of sediment in the river (even during flood events) (Bannatyne, 2019, *pers. comm*.).

The sampling jars from both rivers were labelled according to number, date and time and brought back to the laboratory in the Geography Department at Rhodes University, Grahamstown, for analysis.

3.4.4 Suspended sediment data analysis

Once in the laboratory, the outside of the sample jars were cleaned and dried. For samples that had visibly high sediment (>200 nephelometric turbidity units) the suspended sediment concentration (SSC) was determined by carrying out the following process in the original jars (Bannatyne *et al*., 2017). Each sample was weighed to two decimal places and left to settle for one month. After one month the clear water was removed from the jars with a pump and J-tube and the remaining water was evaporated by placing the original jars in an oven (Bannatyne *et al*., 2017). The jars and dry sediment were then weighed to four decimal places after which the jars were washed and dried and then weighed again to four decimal places to determine the mass of the sediment (Figure 3.12) (Bannatyne *et al*., 2017).

For samples that had visibly low sediment samples (<200 nephelometric turbidity units) turbidity was measured using a turbidity meter and used as a surrogate to calculate the suspended sediment (Bannatyne *et al*., 2017).

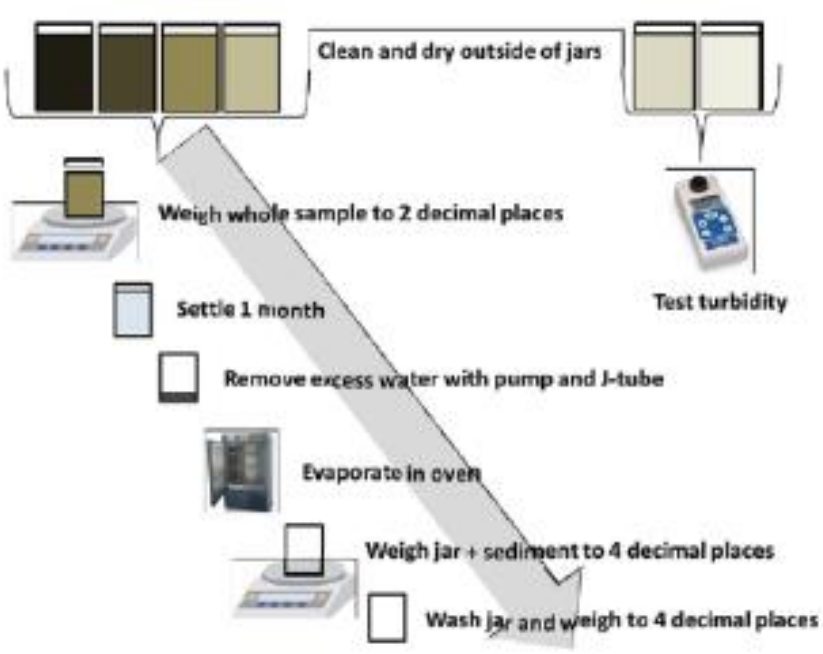

Figure 3.12: The laboratory process followed to determine the suspended sediment concentration of the water samples from the relevant rivers (From: Bannatyne *et al*., 2017).

3.5 Data analysis of NDVI data, field data, rainfall and sediment data

3.5.1 NDVI analysis

NDVI maps were created for the grassland areas in each catchment for October 2018, January 2019 and April 2019 in order to visualise the green-up of the grassland areas over the course of the 2018-2019 wet season. The standard deviation between the three months in each catchment was calculated in order to determine the specific areas where there is greatest variability in the NDVI values over the course of the 2018-2019 wet season in each catchment. An NDVI image differencing was conducted for each of the three months in order to determine the difference between the NDVI value of each pixel and the associated mean monthly NDVI for the grassland areas of the LPRC and GRC throughout the wet season of 2018-2019. This difference indicates the areas which are most productive in each catchment.

NDVI was also separated into north-facing and south-facing aspect for both catchments for October 2018, January 2019 and April 2019, thereafter the NDVI values were extracted per aspect and run through R-Studio to produce a box-and-whisker plot. The NDVI was also separated into four slope classes: gentle (0 – 5°), moderate (5 – 16,5°), steep (16,5 – 24°) and very steep (24 – 68°) for both catchments for each month (Barcelona Field Studies Centre, 2019), thereafter the NDVI values were extracted per slope class and run through R-Studio to produce a box-and-whisker plot.

3.5.2 Field data analysis

The relationship between all the field variables and between all the field variables and NDVI was determined by plotting each variable against each other as scatter plots and determining the correlation coefficient (R^2 value). The relationships between each variable and between each variable and NDVI were used to determine if there were any significant relationships that could be used to explain the findings in the rainfall and sediment data. Appropriate statistical tests (two tailed t-tests in Microsoft Excel) were applied thereafter to determine the change in variables over the course of the 2018-2019 wet season and the effect that aspect and geology had on the field variables.

"There are a number of statistical techniques used as an exploratory approach for data analysis. A principal component analysis (PCA) is one such technique that is often used to emphasize variation within a dataset and has been used successfully in research of this nature to visualise the relationships between all the field variables (e.g. Gordon *et al* 2004). A PCA has the advantage to other similar techniques like an exploratory factor analysis which is a measurement model of a latent variable whereas a PCA combines variables in a linear manner. It is for this reason that a PCA was utilised in this study. As such, the interactions between field variables within their respective catchments were determined by conducting a PCA in Microsoft Excel by using the Analyse-It plugin."

3.5.2 Rainfall analysis

Using the rainfall data from the tipping bucket rain gauges in each catchment, the dates of all the erosive rainfall events in the last four wet seasons (2015-2016; 2016-2017; 2017-2018; 2018-2019) were determined using Microsoft Excel.

3.5.3 Sediment flux and load calculations

The sediment load for both the Little Pot River and the Gqukunqa River was determined using the following equation: Suspended sediment load ($mg.s^{-1}$) = suspended sediment concentration ($mg.L^{-1}$) x instantaneous discharge ($L.s^{-1}$). The daily suspended sediment flux was determined using the following equation: Average daily sediment flux ($t.day^{-1}$) = 24 hour discharge ($m^3.d^{-1}$) x suspended daily average ($g.m^{-3}$) x ($1,1023x10^{-6}$).

3.5.4 The interaction between rainfall intensity, NDVI and sediment flux during the wet season

To address the aim of the study, as well as understand the relationships and interactions between NDVI (vegetation cover/biomass), erosive rainfall events, daily rainfall and daily sediment flux, a

comprehensive graph was constructed showing all four factors over the period of January 2016 to January 2019 for both catchments. The relationships between daily sediment flux and rainfall intensity, daily sediment flux and daily rainfall and daily sediment flux and antecedent rainfall were also established via scatter plots. R^2 values were used to determine the strength of the relationship between variables. R^2 values between 0 and 0,5 indicate a weak relationship between two factors; R^2 values between 0,5 and 0,7 indicate a moderate relationship between two factors and R^2 values between 0,7 and 1 indicate a strong relationship between two factors (Moore, 1996).

Chapter 4: Results

4.1 Introduction

This study explored and interrogated multiple field variables (biomass, vegetation cover, soil surface hardness, biocrust cover and slope), remotely sensed data, daily rainfall, rainfall intensity data and daily sediment flux data. The aim was to determine the seasonal trends of rainfall intensity, ground cover and sediment dynamics in the Little Pot River and Gqukunqa River catchments. This was achieved by analysing the field and remotely sensed data, daily rainfall data and high-intensity rainfall data in relation to the daily sediment flux data for both catchments. Rainfall is one of the main drivers of grassland greening after the dry season (Archibald and Scholes, 2007) which was explored through NDVI image differencing. The relationship between the field variables was also used to help understand the role that the field variables played in the resultant sediment dynamics before, during and after erosive rainfall periods.

4.2 Remotely sensed data

In this section the NDVI data and associated NDVI spatial layers created for both study catchments are presented as well as the variability of the NDVI in each catchment throughout the 2018-2019 wet season. The NDVI data relative to north- and south-facing slopes and slope angle classifications are also presented.

4.2.1 NDVI spatial data and variability

The mean monthly NDVI values for the grassland areas of both the LPRC and GRC increased over the course of the 2018-2019 wet season (Figure 4.1a-f and Table 4.1). The mean NDVI value in the LPRC increased from 0,26 ± 0,066 to 0,50 ± 0,113 to 0,55 ± 0,100 in October 2018, January 2019 and April 2019 respectively (Figure 4.1a-c and Table 4.1). In the GRC the mean NDVI value increased from 0,29 ± 0,065 to 0,42 ± 0,105 to 0,53 ± 0,094 in October 2018, January 2019 and April 2019 (Figure 4.1d-f and Table 4.1). However, the overall NDVI standard deviation does not illustrate the spatial heterogeneity of the growth response across the full extent of each catchment.

Table 4.1: Mean NDVI values for the grassland areas of the LPRC and GRC of the 2018-2019 wet season.

Date	Little Pot River catchment mean NDVI value	Standard deviation (±)	Gqukunqa River catchment mean NDVI value	Standard deviation (±)
October 2018	0,26	0,066	0,29	0,065
January 2019	0,50	0,113	0,42	0,105
April 2019	0,55	0,1	0,53	0,094

Figure 4.2 and 4.3 show the variability of NDVI values over the full wet season of 2018-2019 in the LPRC and GRC respectively. The areas with the greatest seasonal variation in NDVI values in the LPRC (Figure 4.2) are those which have low NDVI values at the start of the growing season (October). The areas with the lowest seasonal variation in NDVI values in the LPRC are found mainly in areas with exposed rock and consistently low vegetation cover or bare ground. Similarly, the areas with the greatest seasonal variation in NDVI values in the GRC (Figure 4.3) are also found where low NDVI values were calculated at the start of the growing season (October 2018). However, in the GRC, in contrast, the lowest variation in NDVI is found in areas that have high NDVI values at the start of the growing season, and remain consistently so.

Figure 4.4a-f shows how much the NDVI pixel values for the grassland areas vary from the monthly catchment mean and which areas deviate above or below the mean in the LPRC and GRC. Spatially, the total area (64% in the LPRC and 55% in the GRC) of grasslands above the catchment NDVI mean increased over the course of the 2018-2019 wet season and the total area (38% in the LPRC and 45% in the GRC) of grasslands below the catchment mean decreased over the course of the wet season. In the LPRC the areas in the west of the catchment have the highest relative elevation and have NDVI values that are greater than the catchment mean throughout the season. In the GRC, the areas in the north of the catchment are the highest in elevation and have NDVI values that are greater than the catchment mean. Throughout the course of the 2018-2019 wet season in both the LPRC and the GRC the variability of NDVI values increased with higher variability at the end of the wet season and lower variability at the start of the wet season. The grassland areas 'greened up' faster from the early to middle period of the 2018-2019 wet season.

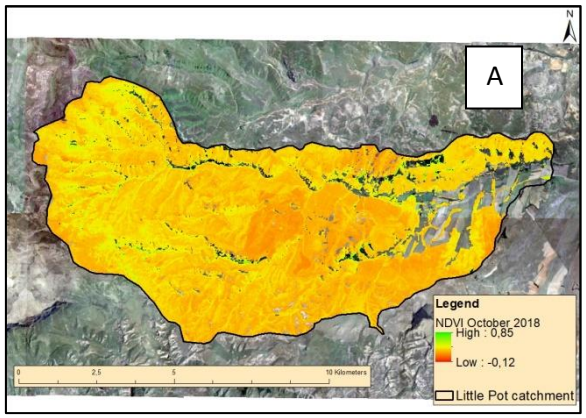

LPRC October 2018

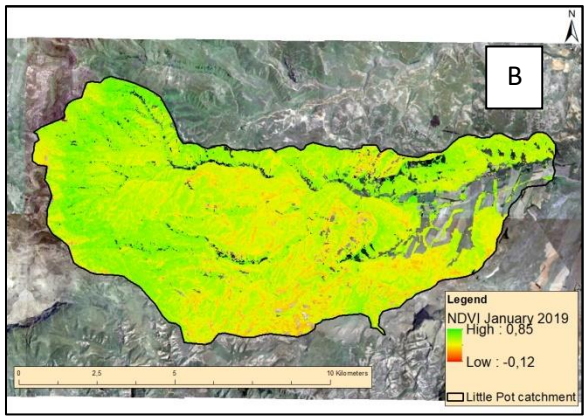

LPRC January 2019

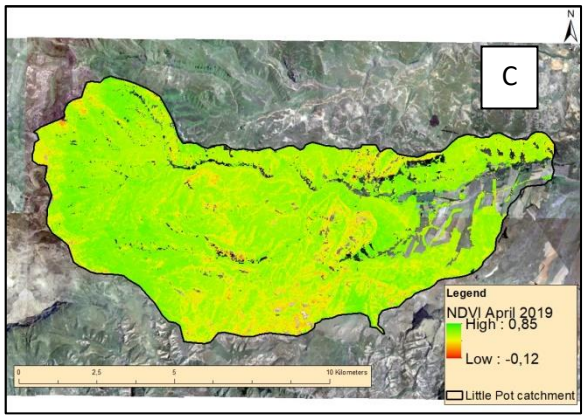

LPRC April 2019

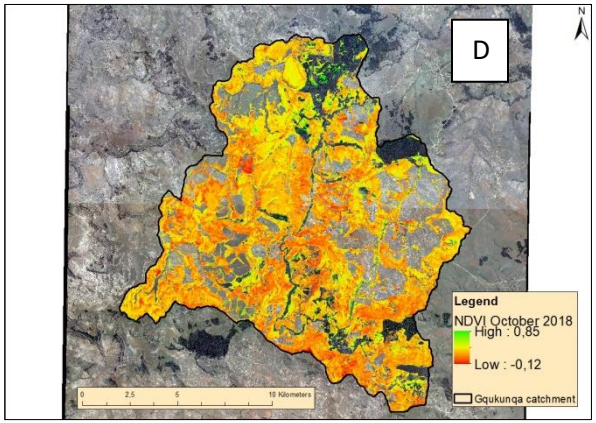

GRC October 2018

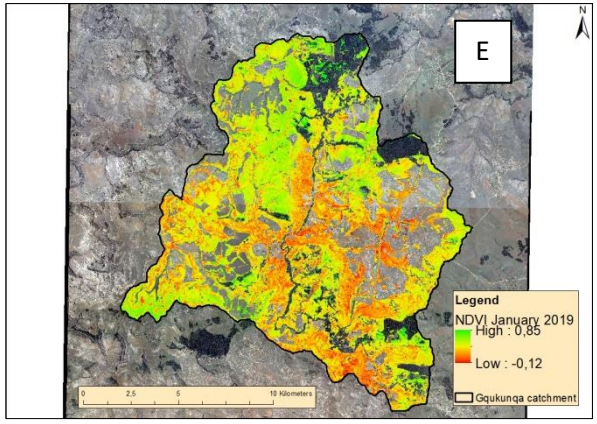

GRC January 2019

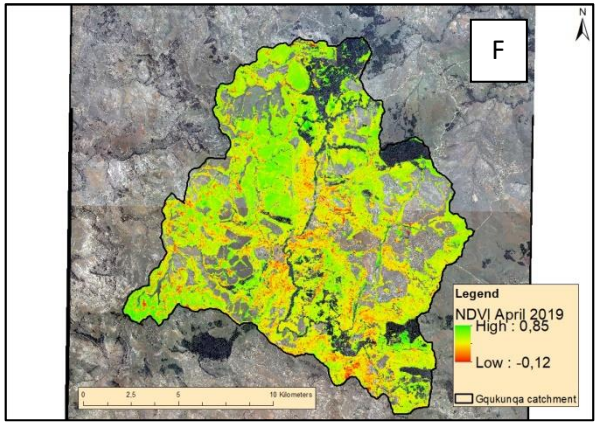

GRC April 2019

Figure 4.1: Maps of the NDVI for grassland areas in the Little Pot River catchment and Gqukunqa River catchment in throughout the wet season of 2018-2019.

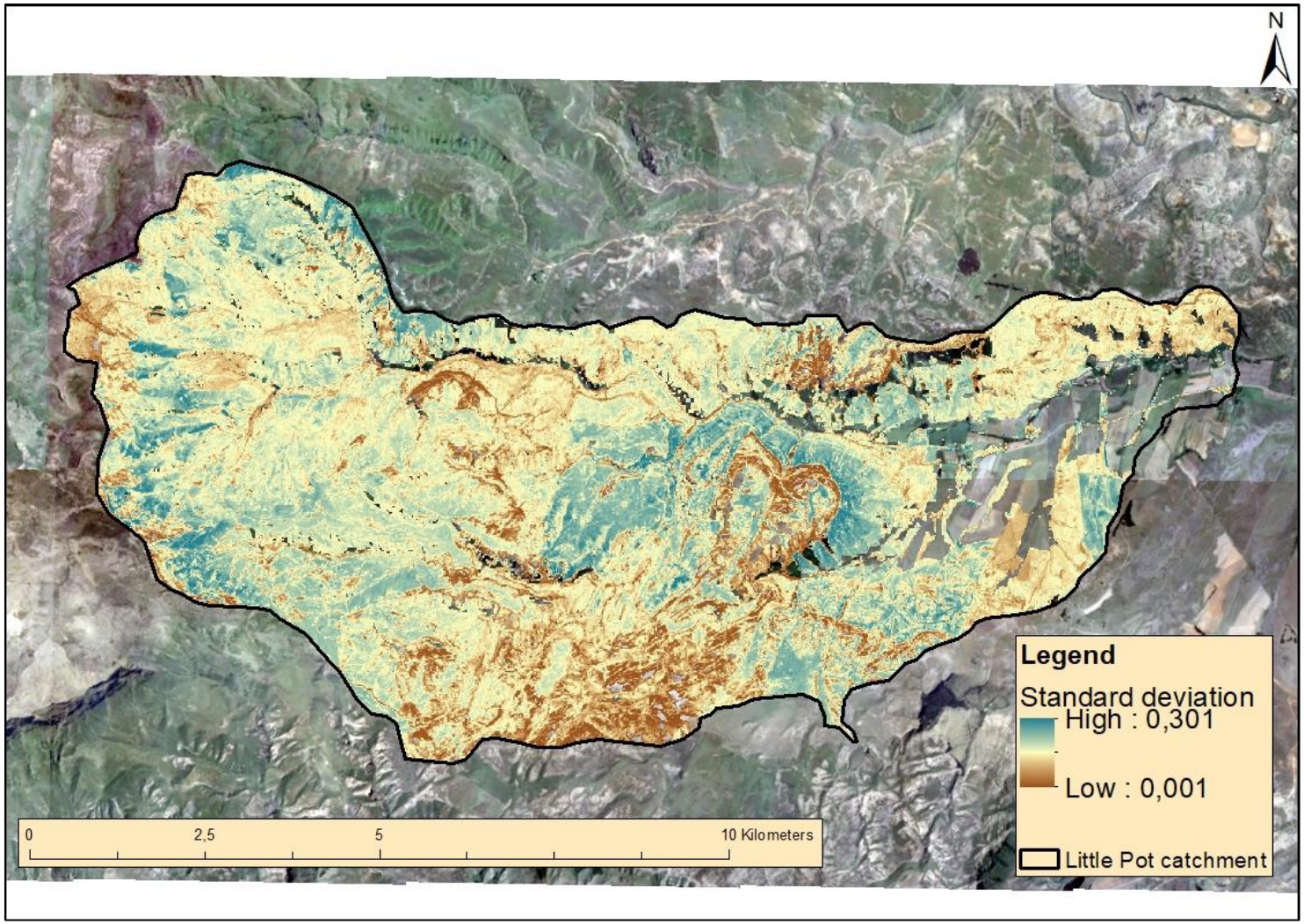

Figure 4.2: The standard deviation of NDVI for grassland across the whole wet season of 2018-2019 in the Little Pot River catchment.

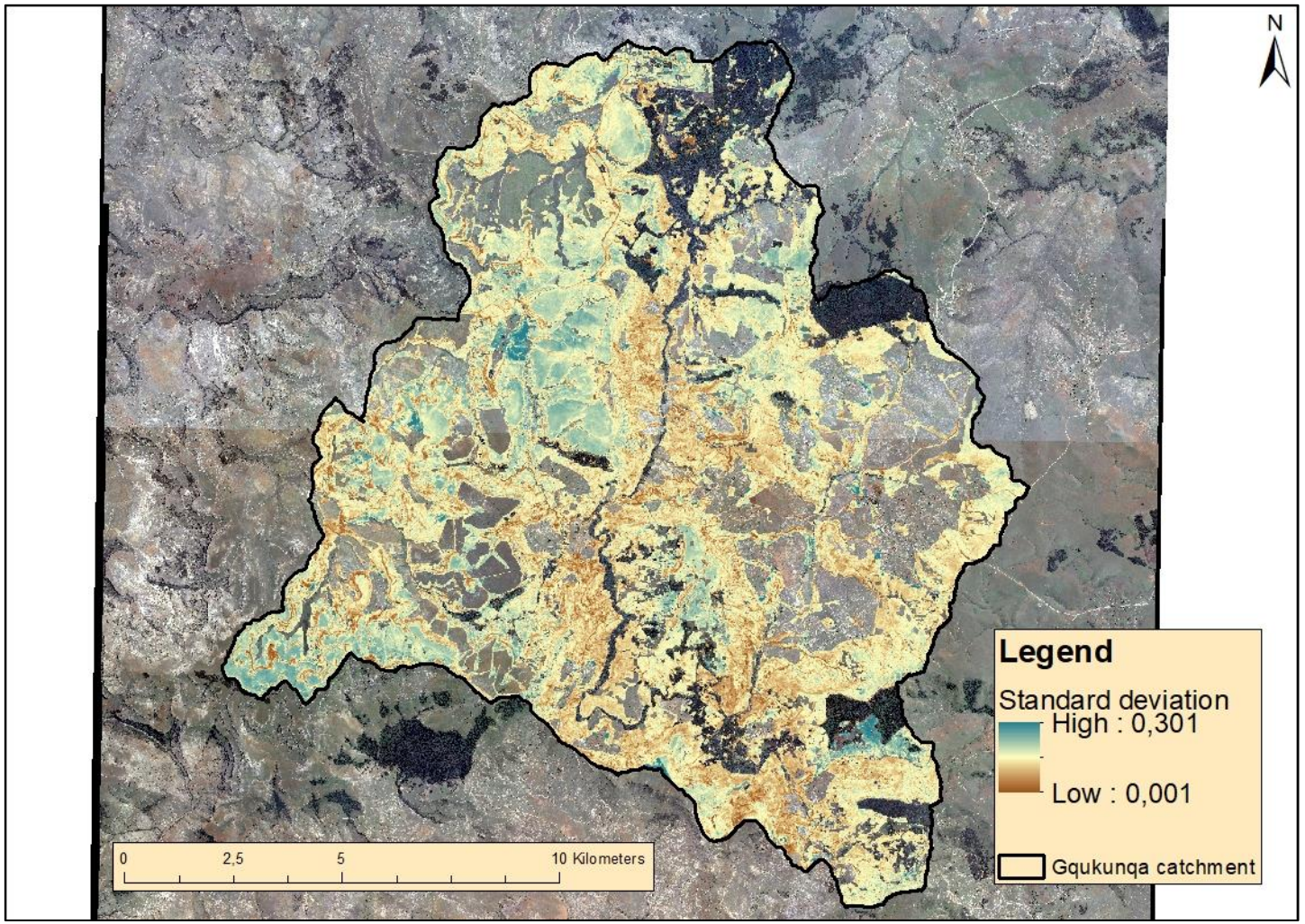

Figure 4.3: The standard deviation of NDVI for grassland areas across the whole wet season of 2018-2019 in the Gqukunqa river catchment.

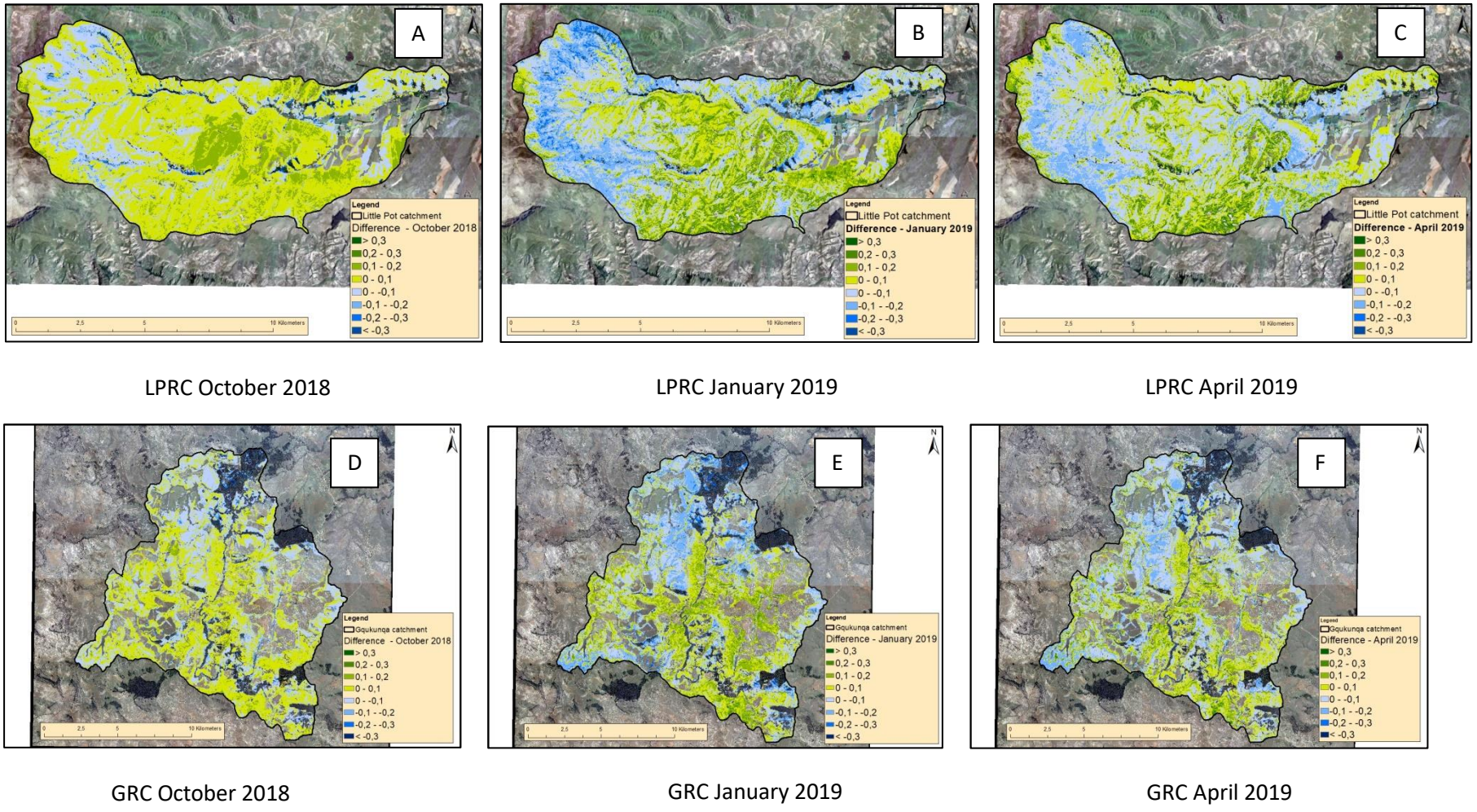

LPRC October 2018 LPRC January 2019 LPRC April 2019

GRC October 2018 GRC January 2019 GRC April 2019

Figure 4.4: The difference between the NDVI value of each pixel and the associated mean monthly catchment NDVI for the grassland areas of the LPRC and GRC throughout the wet season of 2018-2019. Positive difference values are below the catchment mean and negative values are above the catchment mean.

4.2.3 The effect of aspect and slope on NDVI

4.2.3.1 Trends between aspect and NDVI

The mean monthly NDVI values for the grassland areas in the LPRC follow an increasing trend where the values increase from 0,246 to 0,462 to 0,540 in October 2018, January 2019 and April 2019 respectively on north-facing slopes and increase from 0,286 to 0,542 to 0,550 in October 2018, January 2019 and April 2019 respectively on south-facing slopes (Figure 4.5a-c). The mean NDVI value of the south-facing slopes is consistently higher than those of the north-facing slopes during the wet season of 2018-2019 in the LPRC.

The mean monthly NDVI values for the grassland areas in the GRC follow an increasing trend through the wet season, where the values increase from 0,283 to 0,412 to 0,526 in October 2018, January 2019 and April 2019 respectively on north-facing slopes and increase from 0,306 to 0,451 to 0,549 in October 2018, January 2019 and April 2019 respectively on south-facing slopes (Figure 4.5a-c). The mean NDVI value of the south-facing slopes is also consistently higher than those on the north-facing slopes during the wet season of 2018-2019 in the GRC.

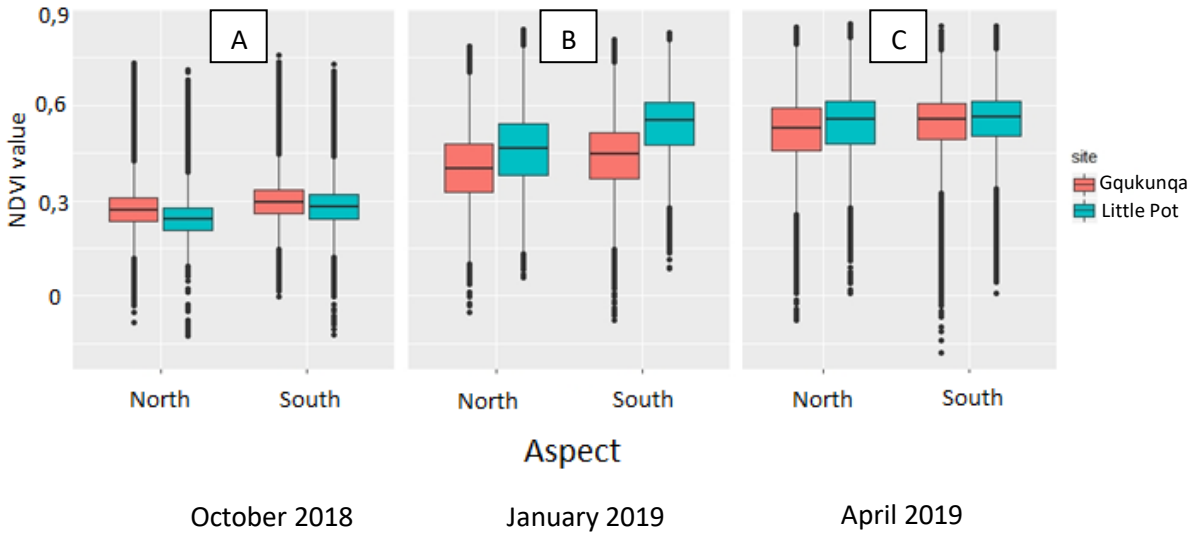

Figure 4.5: Mean NDVI value per month and aspect in the Little Pot River and Gqukunqa River catchments.

4.2.3.2 Trends between slope angle and NDVI

There is a slight increase in the mean monthly NDVI values as slope increases for the grassland areas in the LPRC for October 2018 and January 2019 and a slight decreasing trend in April 2019 (Figure 4.6a). In October 2018 the mean monthly NDVI values were 0,256, 0,258, 0,263 and 0,270 for the

gentle, moderate, steep and very steep slopes respectively. This indicates a slight increasing trend in NDVI with increasing slope angle (Figure 4.6a). In January 2019, there was a slightly larger increasing trend in NDVI with increasing slope angle than in October 2018, where the mean monthly NDVI values were 0,481, 0,482, 0,496 and 0,518 for the gentle, moderate, steep and very steep slopes respectively (Figure 4.6a). However in April 2019, NDVI declined as slope steepness increased: the mean monthly NDVI values were 0,552, 0,546, 0,547 and 0,544 for the gentle, moderate, steep and very steep slopes respectively indicating a very small decrease in NDVI with increasing slope angle (Figure 4.6a).

There is a slight decrease in the mean monthly NDVI values as slope increases for the grassland areas in the GRC for October 2018, January 2019 and April 2019 (Figure 4.6b), i.e. flatter slopes have higher NDVI values irrespective of the month throughout the season, but overall, irrespective of the slope, NDVI increases throughout the season. In October 2018 the mean monthly NDVI values were 0,299, 0,291, 0,282 and 0,280 for the gentle, moderate, steep and very steep slopes respectively indicating a small decreasing trend in NDVI with increasing slope angle. In January 2019 the mean monthly NDVI values were 0,435, 0,423, 0,414 and 0,419 for the gentle, moderate, steep and very steep slopes respectively indicating a slight decreasing trend in NDVI with increasing slope angle. This decreasing trend with increasing slope angle continued in April 2019; the mean monthly NDVI values were 0,548, 0,535, 0,421 and 0,519 for the gentle, moderate, steep and very steep slopes respectively.

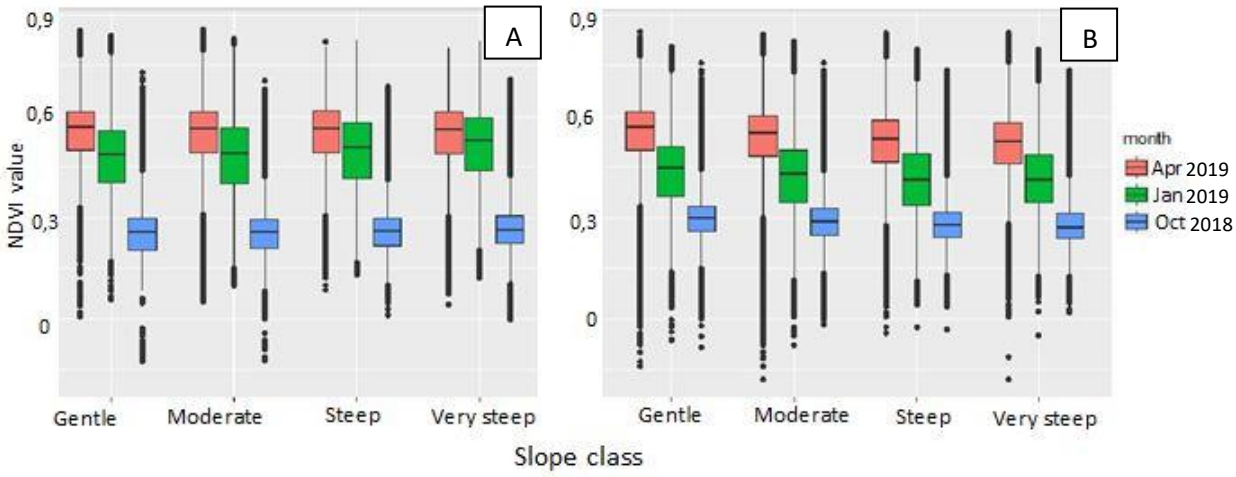

a) Little Pot River catchment b) Gqukunqa River catchment

Figure 4.6: Mean NDVI value per month and slope classification in the Little Pot River catchment and Gqukunqa River catchment. Gentle = 0 – 5 °; Moderate = 5 – 16,5°; Steep = 16,5 – 24°; Very steep = 24 – 68°. The temporal scale moves backwards in time as the graph moves from left to right, i.e. both graphs (A and B) start on the left at the end of the 2018-2019 wet season in April 2019 and move towards October 2018 on the right hand side.

4.3 Field calibrated data

This section compares the field variables to each other in order to find the relationship between them as well as any significant differences between the variables on differing aspects and geologies. Both vegetation cover and biomass data were compared to the NDVI values in order to find a relationship between grassland vegetation cover and NDVI as well as between biomass and NDVI. Scatter-plots were used to explore the relationships between variables and t-tests were used to determine significant differences between the variables on differing aspects and geologies. Slope data were the same in each month in the 2018-2019 wet season in Table 4.2 and 4.3 because slope angle does not generally change significantly over the period of 6 months.

4.3.1 Vegetation cover versus NDVI

Table 4.2 and Figures A1-A4 outline the relationship between grassland vegetation cover and NDVI in the LPRC and the GRC. The R^2 value for each month of the analysis period (October 2018, January 2019 and April 2019) and for the whole wet season is always greater in the GRC than in the LPRC, increasing in both catchments as the wet season progresses. However, these are all weak positive relationships as the LPRC monthly R^2 values range from 0,277, 0,388 to 0,365 in October 2018, January 2019 and April 2019 respectively and in the GRC the monthly R^2 values range from 0,413 to 0,491 to 0,500 in October 2018, January 2019 and April 2019.

Geology and aspect have no significant effect on the relationship between NDVI and grassland vegetation cover. This can be seen by the lack of significant difference ($p<0,05$) between the visual estimates of vegetation cover from the 80 ground-truthing sites and the NDVI values on the Clarens and Elliot Formations nor on the two aspects (north and south) in the LPRC in any of the months that fieldwork was conducted during this study (Table 4.3).

The means of the NDVI values for each of the 80 ground-truthing sites in the LPRC and GRC all increased throughout the wet season (Table 4.3 and 4.4) as discussed in section 4.2. There was no significant difference between the visual estimates of vegetation cover from the 80 ground-truthing sites and the NDVI values on the Molteno and Tarkastad Formations as well as the two aspects (north and south) in the GRC in any of the months that fieldwork was conducted during this study (Table 4.4).

The means of the visual estimates of grassland vegetation cover at each of the 80 ground-truthing sites in the LPRC and GRC also increased throughout the wet season (Table 4.3 and 4.4). The means of the grassland vegetation cover in the LPRC increased from 75% to 85% to 92% in October 2018, January 2019 and April 2019 respectively (Table 4.3). The means of the grassland vegetation cover in

the GRC increased from 72% to 77% to 91% in October 2018, January 2019 and April 2019 respectively (Table 4.4).

The only significant difference ($p<0,05$) found in the grassland vegetation data in the LPRC was between the north and south-facing slopes in October 2018 (Table 4.3). There was also no significant difference ($p<0,05$) between the vegetation cover on the Molteno and Tarkastad Formations as well as the two aspects in the GRC in any of the months that field work was conducted during this study (Table 4.4).

4.3.2 NDVI versus biomass

Table 4.2 and Figures A5-A8 outline the relationship between NDVI and biomass ($g.0,2m^{-2}$) in the LPRC and the GRC. The R^2 values for the LPRC increase from October 2018 (0,049) to peak in January 2019 (0,254) and fall again in April 2019 (0,155), however, all being weak positive relationships. The R^2 values of the GRC follow the same rising and falling trend as the LPRC, however, the R^2 values indicate weak positive relationships and range from 0,024 to 0,042 to 0,040 in October 2018, January 2019 and April 2019 respectively.

The R^2 values representing the whole wet season of 2018-2019 are higher than the individual months represented with the LPRC R^2 value (0,300) being slightly higher than the GRC R^2 value (0,223) however both values indicate weak relationships.

Table 4.2: R^2 values indicating the relationship between various factors measured in the field. W/S is the 2018-2019 wet season. The negative R^2 values indicate negative relationships.

Criteria / relationship	Date	R^2 value LP	R^2 value GQ
Biomass versus NDVI	Oct-18	0,049	0,024
	Jan-19	0,254	0,042
	Apr-19	0,155	0,04
	W/S	0,3	0,22
Vegetation cover versus NDVI	Oct-18	0,277	0,413
	Jan-19	0,388	0,491
	Apr-19	0,365	0,5
	W/S	0,364	0,525
Vegetation cover versus biomass	Oct-18	0,057	0,084
	Jan-19	0,214	0,202
	Apr-19	0,152	0,07
	W/S	0,208	0,149
Soil surface hardness versus NDVI	Oct-18	0,00007	-0,0869
	Jan-19	-0,0173	0,0004
	Apr-19	-0,1627	-0,0462
	W/S	-0,0262	-0,0136
Biocrust versus NDVI	Oct-18	-0,0643	-0,0311
	Jan-19	-0,01168	-0,0893
	Apr-19	-0,0966	-0,1753
	W/S	-0,032	-0,0214
Slope versus NDVI	Oct-18	-0,0405	-0,0465
	Jan-19	-0,0306	-0,103
	Apr-19	-0,0018	-0,0124
	W/S	-0,0054	-0,0032
Soil surface hardness versus biomass	Oct-18	-0,0012	-0,018
	Jan-19	-0,117	-0,0007
	Apr-19	-0,1648	-0,088
	W/S	-0,0554	-0,0278
Soil surface hardness versus vegetation cover	Oct-18	0,0027	-0,0161
	Jan-19	0,0006	-0,0007
	Apr-19	-0,117	-0,155
	W/S	-0,0076	-0,0005
Vegetation cover versus slope	Oct-18	-0,304	-0,087
	Jan-19	-0,157	-0,1017
	Apr-19	-0,1079	-0,1285
	W/S	-0,1555	-0,0456
Vegetation cover versus biocrust	Oct-18	0,144	0,0379
	Jan-19	0,215	0,18
	Apr-19	0,178	0,324
	W/S	0,0549	0,324

Table 4.3: Differences in NDVI, vegetation cover, biomass, soil surface hardness and biocrust throughout the 2018-2019 wet season on the differing geologies and aspects in the Little Pot River catchment. The numbers highlighted indicate the significant differences between Clarens and Elliot formations and north and south facing slopes.

Date	Criteria	Factor	Mean	S.D	P-value	df	Factor	Mean	S.D	P-value	df	Factor	Mean	S.D	P-value	df	Factor	Mean	S.D	P-value	df	Factor	Mean	Standard deviation	P-value	df	Factor	Mean	Standard deviation	P-value	df
Oct-18	Clarens	NDVI	0,27	0,064	0,96	77	Vegetation cover (%)	78,00	17,86	0,30	76	Biomass (g.0,2m^{-2})	9,34	4,58	0,21	70	Soil surface hardness (Kpa)	3235	599,38	**0,04**	78	Biocrust (%)	6,60	17,35	0,40	72	Slope (°)	13,75	8,61	0,375	76
	Elliot		0,27	0,070				73,63	20,13				9,53	6,44				2951	621,53				3,75	12,79				15,60	9,91		
	North		0,26	0,074	0,28	76		80,00	14,77	**0,049**	**76**		10,2	6,39	0,23	70		3158	491,87	0,35	78		1,30	6,56	**0,023**	43		11,85	5,88	**0,006**	59
	South		0,28	0,061				71,63	22,29				8,71	4,58				3029	737,97				9,05	20,36				17,50	11,09		
	All 80 sites		0,27	0,067	N/A	N/A		75,81	19,03	N/A	N/A		9,45	5,56	N/A	N/A		3093	623,28	N/A	N/A		5,18	15,21	N/A	N/A		14,67	9,240	N/A	N/A
Jan-19	Clarens		0,48	0,125	0,207	79		86,63	16,58	0,46	76		15,62	7,40	0,21	71		3028	483,83	0,30	78		7,13	16,51	0,11	59		13,75	8,61	0,375	76
	Elliot		0,52	0,129				83,54	21,10				18,23	10,70				2921	448,00				2,34	8,82				15,60	9,91		
	North		0,50	0,119	0,89	76		80,61	21,86	**0,031**	69		15,54	10,09	0,277	77		2855	529,14	**0,018**	70		8,56	17,67	**0,008**	43		11,85	5,88	**0,006**	59
	South		0,50	0,136				89,63	14,29				18,08	7,43				3096	358,43				0,75	3,50				17,50	11,09		
	All 80 sites		0,50	0,127	N/A	N/A		85,06	18,95	N/A	N/A		16,94	9,26	N/A	N/A		2974	466,26	N/A	N/A		4,70	13,32	N/A	N/A		14,67	9,240	N/A	N/A
Apr-19	Clarens		0,57	0,081	0,62	79		92,38	12,40	1,00	78		20,97	12,53	0,50	79		3187	564,62	**0,02**	77		7,00	16,82	0,09	50		13,75	8,61	0,375	76
	Elliot		0,58	0,081				92,38	14,19				22,87	13,02				2863	678,95				2,13	6,49				15,60	9,91		
	North		0,58	0,075	0,405	78		90,63	15,03	0,23	71		21,03	11,08	0,52	75		2910	755,53	0,1107	69		7,13	17,09	0,0781	47		11,85	5,88	**0,006**	59
	South		0,57	0,087				94,13	11,09				22,86	14,25				3140	485,13				2,00	5,64				17,50	11,09		
	All 80 sites		0,57	0,081	N/A	N/A		92,38	13,24	N/A	N/A		21,93	12,73	N/A	N/A		3025	641,38	N/A	N/A		4,56	12,91	N/A	N/A		14,67	9,240	N/A	N/A

Table 4.4: Differences in NDVI, vegetation cover, biomass, soil surface hardness and biocrust throughout the 2018-2019 wet season on the differing geologies and aspects in the Gqukunqa River catchment. The numbers highlighted indicate the significant differences between two Tarkastad and Molteno Formations.

Date	Criteria	Factor	Mean	S.D	P-value	df	Factor	Mean	S.D	P-value	df	Factor	Mean	S.D	P-value	df	Factor	Mean	S.D	P-value	df	Factor	Mean	Standard deviation	P-value	df	Factor	Mean	Standard deviation	P-value	df
Oct-18	Tarkastad	NDVI	0,311	0,065	0,389	76	Vegetation cover (%)	72	20,11	0,949	72	Biomass (g.0,2m^{-2})	6,55	2,75	0,520	69	Soil surface hardness (Kpa)	2952	478	0,210	78	Biocrust (%)	0,50	3,16	0,780	68	Slope (°)	7,37	3,51	**0,012**	65
	Molteno		0,299	0,055				72	15,05				7,05	3,97				2824	449				0,75	4,74				10,07	5,65		
	North		0,301	0,060	0,550	78		73	19,93	0,489	73		6,64	3,49	0,670	78		2795	419	0,075	76		0,75	4,74	0,782	68		9,35	5,21	0,25	76
	South		0,309	0,059				70	14,98				6,96	3,02				2981	489				0,50	3,12				8,10	4,47		
	All 80 sites		0,305	0,060	N/A	N/A		72	17,65	N/A	N/A		6,80	3,50	N/A	N/A		2888	465	N/A	N/A		0,63	4,01	N/A	N/A		8,72	4,750	N/A	N/A
Jan-19	Tarkastad		0,415	0,072	0,389	78		83	16,00	0,880	75		9,70	2,91	0,408	54		3847	386	0,119	71		1,75	5,43	0,887	68		7,37	3,51	**0,012**	65
	Molteno		0,439	0,075				83	13,35				10,73	6,52				3680	545				2,00	9,66				10,07	5,65		
	North		0,422	0,080	0,530	77		83	13,16	0,880	75		10,23	4,31	0,940	72		3865	439	0,057	77		1,50	5,33	0,670	68		9,35	5,21	0,25	76
	South		0,432	0,070				83	16,36				10,30	6,24				3662	500				2,25	9,74				8,10	4,47		
	All 80 sites		0,359	0,074	N/A	N/A		77	14,75	N/A	N/A		10,26	5,03	N/A	N/A		3277	478	N/A	N/A		0,95	7,81	N/A	N/A		8,72	4,750	N/A	N/A
Apr-19	Tarkastad		0,532	0,075	0,540	66		91	12,95	1,000	78		14,72	5,65	0,440	67		2940	556	**0,0003**	78		1,75	5,94	0,898	77		7,37	3,51	**0,012**	65
	Molteno		0,519	0,118				91	13,34				13,46	8,63				2531	394				1,92	6,03				10,07	5,65		
	North		0,526	0,092	0,950	77		91	11,92	1,000	76		13,97	5,40	0,880	66		2722	509	0,816	70		2,25	6,60	0,532	74		9,35	5,21	0,25	76
	South		0,525	0,105				91	14,27				14,21	8,70				2749	539				1,41	5,25				8,10	4,47		
	All 80 sites		0,526	0,098	N/A	N/A		91	13,07	N/A	N/A		14,09	7,20	N/A	N/A		2735	521	N/A	N/A		1,84	5,95	N/A	N/A		8,72	4,750	N/A	N/A

4.3.3 Vegetation cover versus biomass

Table 4.2 and Figures A9-A12 outline the relationship between grassland vegetation cover and biomass (g.0,2m^{-2}) in the LPRC and the GRC. The R^2 values for the LPRC increase from October 2018 (0,057) to peak in January 2019 (0,214) and fall again in April 2019 (0,152) however all the R^2 values indicate weak positive relationships. The R^2 values for the GRC range from 0,084 to 0,202 to 0,07 in October 2018, January 2019 and April 2019 respectively.

The R^2 value (0,208) of the LPRC over the whole wet season of 2018-2019 is slightly higher than that of the R^2 value (0,149) of the GRC however the values indicate weak positive relationships. The vegetation cover from the 80 ground-truthing sites in the LPRC ranges from 20% to 100% whereas in the 80 ground-truthing sites in GRC the vegetation cover ranges from 30% to 100% (Figure A4). The biomass ranged from 1 to 60 g.0,2m^{-2} at the 80 ground-truthing site in the LPRC whereas the biomass ranged from 1 to 39 g.0,2m^{-2} in the GRC (Figure A8).

The mean biomass found at the 80 ground-truthing sites in the LPRC increases throughout the wet season from 9,45 ± 5,56 g.0,2m^{-2} in October 2018 to 21,93 ± 12,73 g.0,2m^{-2} in April 2019 (Table 4.3), however, there is no significant difference between the biomass found on any of the geologies and aspects at the 80 ground-truthing sites. Similarly, in the GRC, the mean biomass found at the 80 ground-truthing sites increases throughout the wet season from 6,8 ± 3,50 g.0,2m^{-2} in October 2018 to 14,09 ±7,20 g.0,2m^{-2} in April 2019 (Table 4.4). However, there is also no significant difference between the biomass found on any of the geologies and aspects at the 80 ground-truthing sites (Table 4.4). The mean biomass found at the 80 ground-truthing sites in the LPRC was higher than the mean biomass found in the GRC by between 2,5 and 7 ± 10,8 g.0,2m^{-2}

4.3.4 NDVI versus soil surface hardness, biocrust and slope

The relationships between NDVI and soil surface hardness as well as between biocrust and slope are all very weak negative relationships. The R^2 values for the relationship between NDVI and soil surface hardness in the LPRC (Table 4.2 and Figures A13-A16) are 0,00007, -0,0173, -0,1627 and -0,0262 for October 2018, January 2019, April 2019 and throughout the whole wet season respectively. The negative relationship is shown by soil surface hardness increasing with decreasing NDVI values. The R^2 values for the relationship between NDVI and soil surface hardness in the GRC (Table 4.2 and Figures A13-A16) are -0,0869, 0,0004, -0,0462 and -0,0136 for October 2018, January 2019, April 2019 and throughout the whole wet season respectively.

The R^2 values for the relationship between NDVI and biocrust in the LPRC (Table 4.2 and Figures A17-20) are -0,064, -0,0116, -0,096, -0,0054 for October 2018, January 2019, April 2019 and throughout the whole wet season respectively. The negative relationship is shown by biocrust increasing with decreasing NDVI values. The R^2 values for the relationship between NDVI soil surface hardness in the GRC (Table 4.2 and Figures A17-A20) are -0,0311, -0,0893, -0,1753 and -0,0214 for October 2018, January 2019, April 2019 and throughout the whole wet season respectively.

The R^2 values indicating the relationship between NDVI and slope for the 80 ground-truthing sites in the LPRC (Table 4.2 and Figures A21-24) are -0,0405, -0,0306, -0,0018 and -0,0054 for October 2018, January 2019, April 2019 and throughout the whole wet season respectively. The negative relationship is shown by slope increasing with decreasing NDVI values. This negative relationship at the finer plot-scale does not reflect the results found in Figure 4.6 at the catchment-scale where the relationship was positive and the NDVI values were taken from all NDVI pixels in grassland areas in the LPRC and not just the 80 ground-truthing sites. The R^2 values for the relationship between NDVI soil surface hardness in the GRC (Table 4.2 and Figures A21-A24) are -0,0465, -0,103, -0,0124 and -0,0032 for October 2018, January 2019, April 2019 and throughout the whole wet season respectively.

4.3.5 Influence of rock type and aspect on soil surface hardness

The soil surface hardness is always greater throughout the 2018-2019 wet season on the Clarens Formations (sandstones) than the Elliot Formations (mudstone) in the LPRC for the 80 sites measured. In the GRC, the soil surface hardness of Tarkastad Formations was always greater than that of the Molteno Formations for the 80 sites measured. There is no trend in soil surface hardness for north- and south-facing slopes in both the LPRC and GRC (Table 4.3 and 4.4). Similarly, there are no apparent trends for the means of the soil surface hardness over the 2018-2019 wet season in both catchments, however, there are significant differences between the two main aspects and geologies (Table 4.3 and 4.4). In the LPRC there was a significant difference in soil surface hardness between the Clarens and Elliot Formations in both October 2018 ($p<0,05$) and April 2019 ($p<0,05$); the Clarens Formations were found to be significantly harder than Elliot Formations. In the LPRC, soil surface hardness of south-facing slopes were found to be significantly harder than north-facing slopes ($p<0,05$) in January 2019 (Table 4.3). In the GRC, only in October 2018, was the soil surface hardness between the Tarkastad and Molteno Formations significantly different ($p<0,05$) in (Table 4.4).

4.3.6 Influence of rock type and aspect on biocrust

The mean biocrust cover in the LPRC consistently decreased through the wet season: 5,18% to 4,7% to 4,56% in October 2018, January 2019 and April 2019 respectively (Table 4.3). There are, however, significant differences in biocrust cover between north- and south-facing slopes in the LPRC in both October 2018 and January 2019. In October 2018 the south-facing slopes have significantly higher ($p<0,05$) percent of biocrust cover and in January 2019 north-facing slopes have significantly higher ($p<0,05$) percent of biocrust cover.

In the GRC, the mean biocrust cover in the GRC increased from 0,63% to 0,95% to 1,84% in October 2018, January 2019 and April 2019 respectively (Table 4.4), with no evidence of aspect influencing biocrust development here.

4.3.7 Influence aspect on slope

The south-facing slopes were significantly steeper than the north-facing slopes in the LPRC for the 80 ground-truthing sites that were measured (Table 4.3), however, in the GRC the north-facing slopes were slightly steeper than the south-facing slopes for the 80 ground-truthing sites that were measured (Table 4.4).

4.3.8 Relationships between other field variables

The relationships between 1) soil surface hardness and biomass (Figure A25-28); 2) soil surface hardness and vegetation cover (Figure A29-32); 3) vegetation cover and slope (Figure A33-36) and 4) vegetation cover and biocrust (Figure A37-A40) in both the LPRC and GRC are all weak, as indicated by their low R^2 values in Table 4.2.

The relationship between soil surface hardness and biomass in the LPRC, as indicated by the R^2 values, are -0,001, -0,117, -0,164 and -0,055 for October 2018, January 2019, April 2019 and the whole wet season respectively (Table 4.2) indicating weak negative relationships as soil surface hardness decreases while biomass increases. The R^2 values for the soil surface hardness versus biomass in the GRC are -0,018, -0,0007, -0,088 and -0,027 for October 2018, January 2019, April 2019 and the whole wet season respectively (Table 4.2) indicating weak negative relationships.

The R^2 values for the soil surface hardness versus vegetation cover in the LPRC are 0,002, 0,0006, -0,117 and -0,007 for October 2018, January 2019, April 2019 and the whole wet season respectively (Table 4.2) indicating weak relationships.

The R^2 values for the soil surface hardness versus vegetation cover in the GRC are -0,016, -0,0007, -0,155 and -0,0005 for October 2018, January 2019, April 2019 and the whole wet season respectively (Table 4.2) indicating weak negative relationships as soil surface hardness decreases while vegetation cover increases.

The relationship between vegetation cover and slope in the LPRC, as indicated by the R^2 values, are -0,304, -0,157, -0,107 and -0,155 for October 2018, January 2019, April 2019 and the whole wet season respectively indicating a weak negative relationship (Table 4.2). As slope angle increases, vegetation cover decreases. The R^2 values for the vegetation cover versus slope in the GRC are -0,087, -0,101, -0,128 and -0,045 for October 2018, January 2019, April 2019 and the whole wet season respectively (Table 4.2).

The relationship between vegetation cover and biocrust in the LPRC, as indicated by the R^2 values, are 0,144, 0,215, 0,178 and 0,054 for October 2018, January 2019, April 2019 and the whole wet season respectively (Table 4.2) indicating weak positive relationships. As vegetation cover increases biocrust cover decreases. The R^2 values for the vegetation cover versus slope in the GRC are -0,037, -0,180, -0,324 and -0,324 for October 2018, January 2019, April 2019 and the whole wet season respectively (Table 4.2) indicating weak negative relationships.

There are various interactions between field variables and how they influence the system dynamics and so the following description pertains to the LPRC and Figure 4.7. The first four principal components explain 73,26% of the total variation among the data of field variables (Table C1). Principal component one explains 30,3% of the total variation with vegetation cover being the main determinant followed by NDVI and biomass (Figure 4.7 and Table C2). Principal component two explains 16,1% of the total variation with soil surface hardness being the main determinant followed by geology (Figure 4.7 and Table C2).

The following description pertains to the GRC and Figure 4.8. The first four principal components explain 66,4% of the total variation among the data of field variables (Table C4). Principal component one explains 22,6% of the total variation with NDVI being the main determinant followed biomass and vegetation cover (Figure 4.8 and Table C5). Principal component two explains 18,3% of the total variation with soil slope being the main determinant followed geology, soil surface hardness and biomass (Figure 4.8 and Table C5).

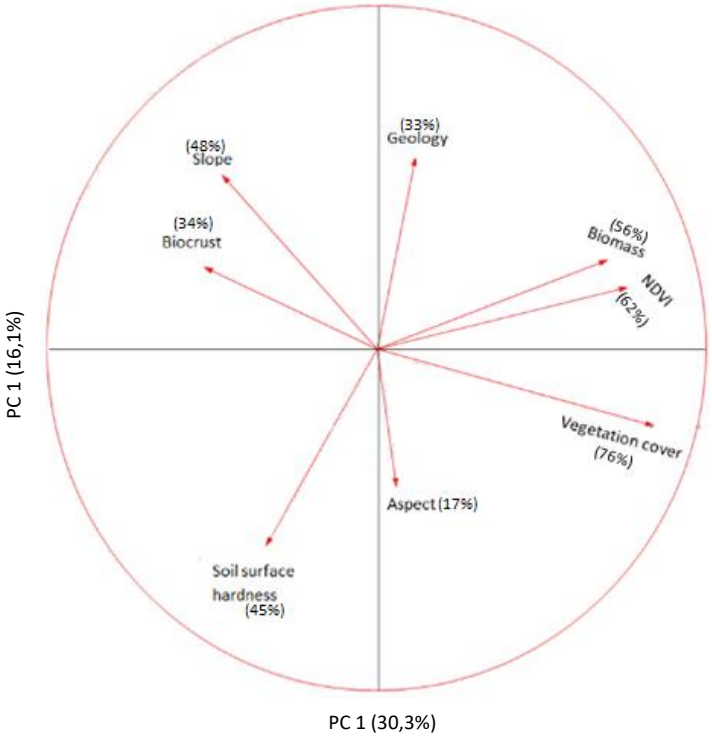

Figure 4.7: Principal component analysis monoplot showing the first two principal components, in the Little Pot River catchment.

Figure 4.8: Principal component analysis monoplot showing the first two principal components, in the Gqukunqa River catchment.

4.4 Rainfall and sediment data

This section presents the rainfall data and sediment data in various forms and displays the relationships between the two factors as well as the NDVI trends during the wet season. The annual rainfall totals for the LPRC are 707,8 mm; 1033,6 mm, 596 mm and 841 mm for 2015, 2016, 2017 and 2018 respectively. Of the past four years, 2016 was the wettest year and 2017 was the driest year in the LPRC. The annual rainfall totals for the GRC and surrounds was 772 mm, 642 mm and 329 mm for 2016, 2017 and 2018 respectively. There was not enough rainfall data available for 2015 and 2019 in the GRC to include those years in the results and analyses. The wettest year out of the last three years in the GRC was 2016 and the driest year was 2018.

4.4.1 Seasonality of the daily and high-intensity rainfall, NDVI and average daily sediment flux

Figure 4.9 displays the results for the daily rainfall (mm), average daily sediment flux ($t.day^{-1}$), the erosive rainfall events and the mean monthly NDVI values for the grassland areas in the LPRC over the period of January 2016 to January 2019. NDVI and daily rainfall (mm) follow the same trend each wet season in that they both increase steadily from October until February/March where they both peak and then both decrease in April and onwards into the dry season and increase again in October. Sediment data was only available from January 2016 until August 2016 but the trend for this available sediment data is that sediment flux is highest in January and decreases until April and onwards into the dry season.

During the wet season of 2015-2016; 2016-2017 and 2017-2018 there were seven, five, and ten erosive rainfall events respectively in the LPRC. The general visible trend is that the erosive rainfall events in the LPRC occur from the mid to late wet season and that the greatest erosive events occur in the months of January to March.

During the period for which the sediment data were available there were four events that exceeded 25 $t.day^{-1}$. These events were the four highest daily sediment flux events during the study time period. These days/events were: 19 January 2016 (144,31 t/day) (Table B3), 24 January 2016 (80,62 t/day), 26 January 2016 (40,34 t/day) and 19 February 2016 (28,79 t/day) (hereafter 'LPRC sediment event one through to four').

LPRC sediment event one occurred on the same day as an erosive rainfall event (26,4 mm/hr) and after seven days of continuous rain that equated to 39,6 mm (1,2 mm, 4 mm, 13,4 mm, 3,4 mm, 0,8 mm, 3,4 mm and 13,4 mm) (Table B3). LPRC sediment event two did not directly result from an erosive rainfall event but instead, after four days of continuous rain prior to and including the day of the sediment event that equated to 26,4 mm (1,4 mm, 2,4 mm, 2,8 mm and 21,8 mm) (Table B4).

LPRC sediment event three experienced six days of rainfall prior to the sediment event, however, the day prior to the sediment event the LPRC experienced an erosive rainfall event, equating to 28,8 mm/hr. The sum of the six days of rainfall equated to 52 mm (1,4 mm, 2,4 mm, 2,8 mm, 21,8 mm, 21,2 mm and 2,4 mm) (Table B5). LPRC sediment event four did not directly result from an erosive rainfall event but instead, after seven days of rain prior to the sediment event and including rain on the day of the sediment event that equated to 60,6 mm (4 mm, 0,2 mm, 14,4 mm, 19 mm, 17,4 mm, 5,4 mm and 0,2 mm) (Table B6).

The data presented below in Figures 4.10 to 4.12 only displays rainfall data for the days that sediment data were available and not the entire study period. The R^2 value for daily sediment flux versus the maximum 5-minute rainfall intensity in the LPRC is 0,0276 which indicates a weak positive relationship (Figure 4.10) and the R^2 value for daily sediment flux versus daily rainfall in the LPRC is 0,0702 which also indicates a weak but positive relationship (Figure 4.11). The R^2 value for the daily sediment flux versus seven-day antecedent rainfall in the LPRC is 0,0960 which also indicates a weak positive relationship, however, the relationship is slightly stronger than the relationship between daily sediment flux and maximum intensity and daily rainfall (Figure 4.12).

The mean monthly NDVI values in the LPRC display a seasonal growth flux which is typical of a phenological response. They rise from the month of October (mean=0,31) to peak in the month of March (mean=0,57) and declining in the month of April (mean=0,52) (Figure 4.9 and Table B1) which follows the similar trends in monthly rainfall where monthly rainfall is highest from January to March.

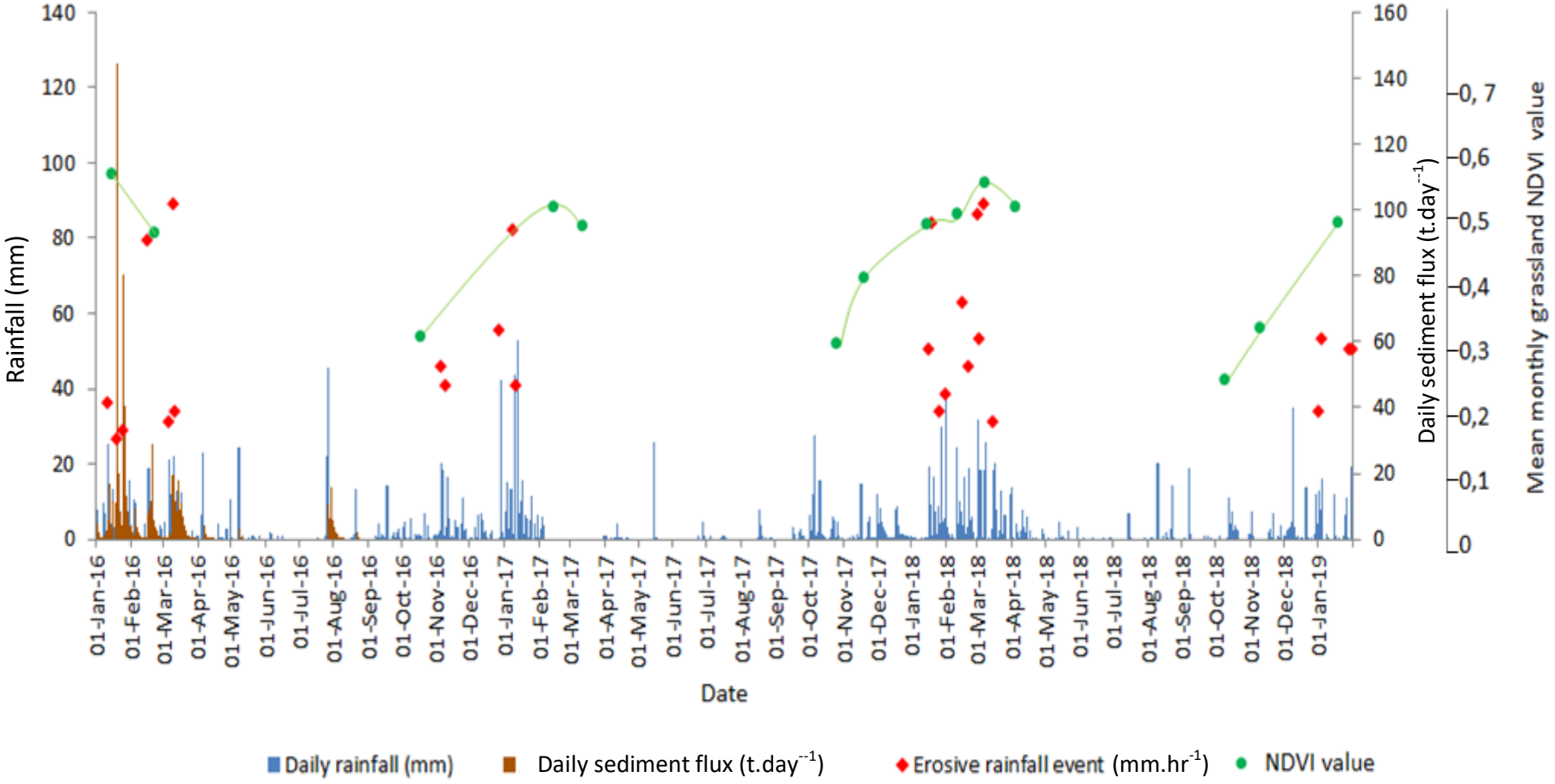

Figure 4.9: The seasonality of daily rainfall, erosive rainfall events, NDVI and daily sediment flux in the Little Pot River catchment from January 2016 to January 2019.

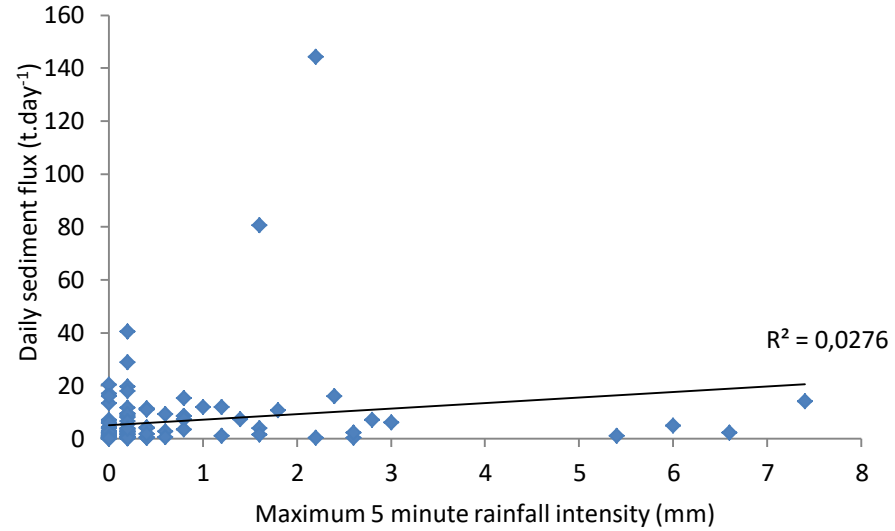

Figure 4.10: Relationship between daily sediment flux and rainfall intensity in the Little Pot River catchment.

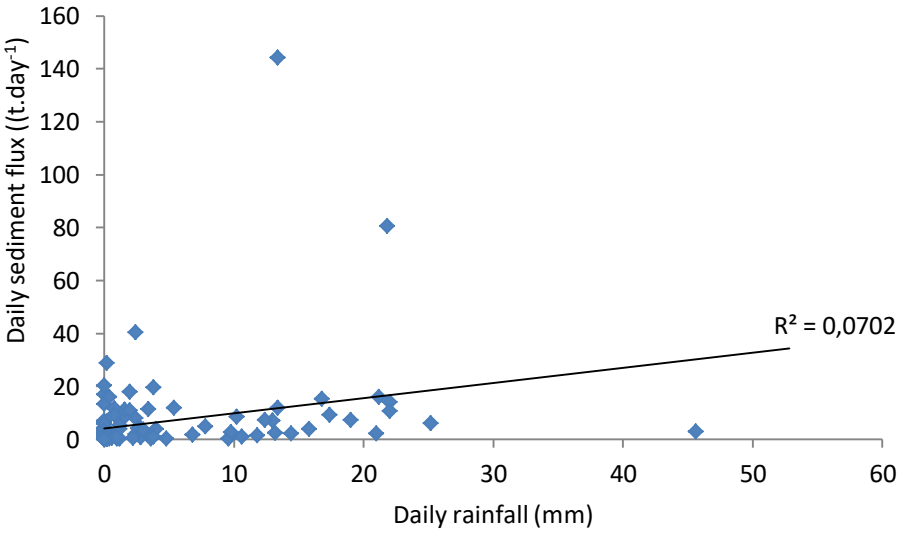

Figure 4.11: Relationship between daily sediment flux and daily rainfall in the Little Pot River catchment.

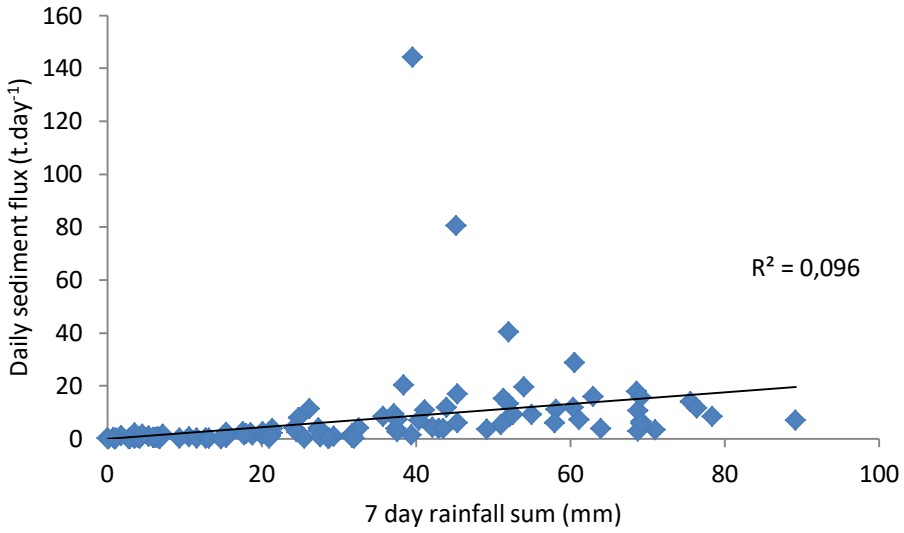

Figure 4.12: Relationship between daily sediment flux and antecedent rainfall in the Little Pot River catchment.

Figure 4.13 displays the results for the daily rainfall (mm), average daily sediment flux (t.day^{-1}), the erosive rainfall events and the mean monthly NDVI values for the grassland areas in the GRC over the period of October 2015 to January 2019. NDVI and daily rainfall (mm) follow the same trend each wet season as the LPRC in that they both increase steadily from October until February/March where they both peak and then both decrease in April and onwards into the dry season and increase again in October. The daily sediment flux in the GRC is low at the start of the wet season and only peaks in January-March and decreases onwards into the dry season.

During the wet season of 2015-2016; 2016-2017 and 2017-2018 there were seven, five, and six erosive rainfall events respectively. The general trend in erosive rainfall events is that the first erosive event occurred earlier on in the wet season and is not as high as the second event which is always the largest erosive rainfall event in the GRC. After the second erosive event the size of the following events decreased steadily

During the period for which the sediment data were available there were five events that exceeded 2800 t.day^{-1}. These events were the five highest daily sediment flux events during the study time period. These days/events were: 8 March 2016 (2863 t.day^{-1}), 19 February 2017 (3887 t.day^{-1}), 1 February 2017 (6449 t.day^{-1}), 16 February 2018 (5455 t.day^{-1}) and 18 March 2018 (6863 t.day^{-1}) (hereafter, 'GRC sediment event one through to five').

Only one sediment event in the GRC resulted from a single erosive event, with the majority due to continuous rainfall over >2 days. GRC sediment event one resulted from three days of continuous rain that equated to 43,6 mm (3,2 mm, 15,8 mm and 24,6 mm) (Table B7). Only GRC sediment event two resulted from a single erosive rainfall event the previous day (45,6 mm/hr) and 14,6 mm of rain on the day of the sediment event (Table B8). GRC sediment event three also resulted after three days of continuous rain that equated to 53,6 mm (16,4 mm, 34,2 mm and 3 mm) (Table B9), with GRC sediment event four and five, after seven days and five days of continuous rain equating to 40,6 mm (8,6 mm, 5,4 mm, 13 mm, 3,6 mm, 5,6 mm, 3,4 mm and 1 mm) (Table B10) and 45,8 mm (8,8 mm, 12,2 mm, 16,6 mm, 4,2 mm, 4 mm) (Table B11) respectively.

The data presented below in Figures 4.14 to 4.16 only displays rainfall data for the days that sediment data were available and not the entire study time period. The R^2 value for daily sediment flux versus maximum 5-minute rainfall intensity in the GRC is 0,0119 which indicates a weak but positive relationship (Figure 4.14) and the R^2 value for daily sediment flux versus daily rainfall in the GRC is 0,1131 which also indicates a weak but positive relationship (Figure 4.15). The R^2 value for the daily sediment flux versus seven-day antecedent rainfall (Figure 4.16) in the GRC is 0,1455 which also indicates a weak positive relationship, however, the relationship is slightly stronger than the relationship between daily sediment flux and daily rainfall.

The mean monthly NDVI values in the GRC display a seasonal growth flux which is typical of a phenological response. They rise from the month of October (mean=0,55) to peak in the month of March (mean=0,55) and declining in the month of April (mean=0,50) (Figure 4.13 and Table B2) which follows the similar trends in monthly rainfall where monthly rainfall is highest from January to March.

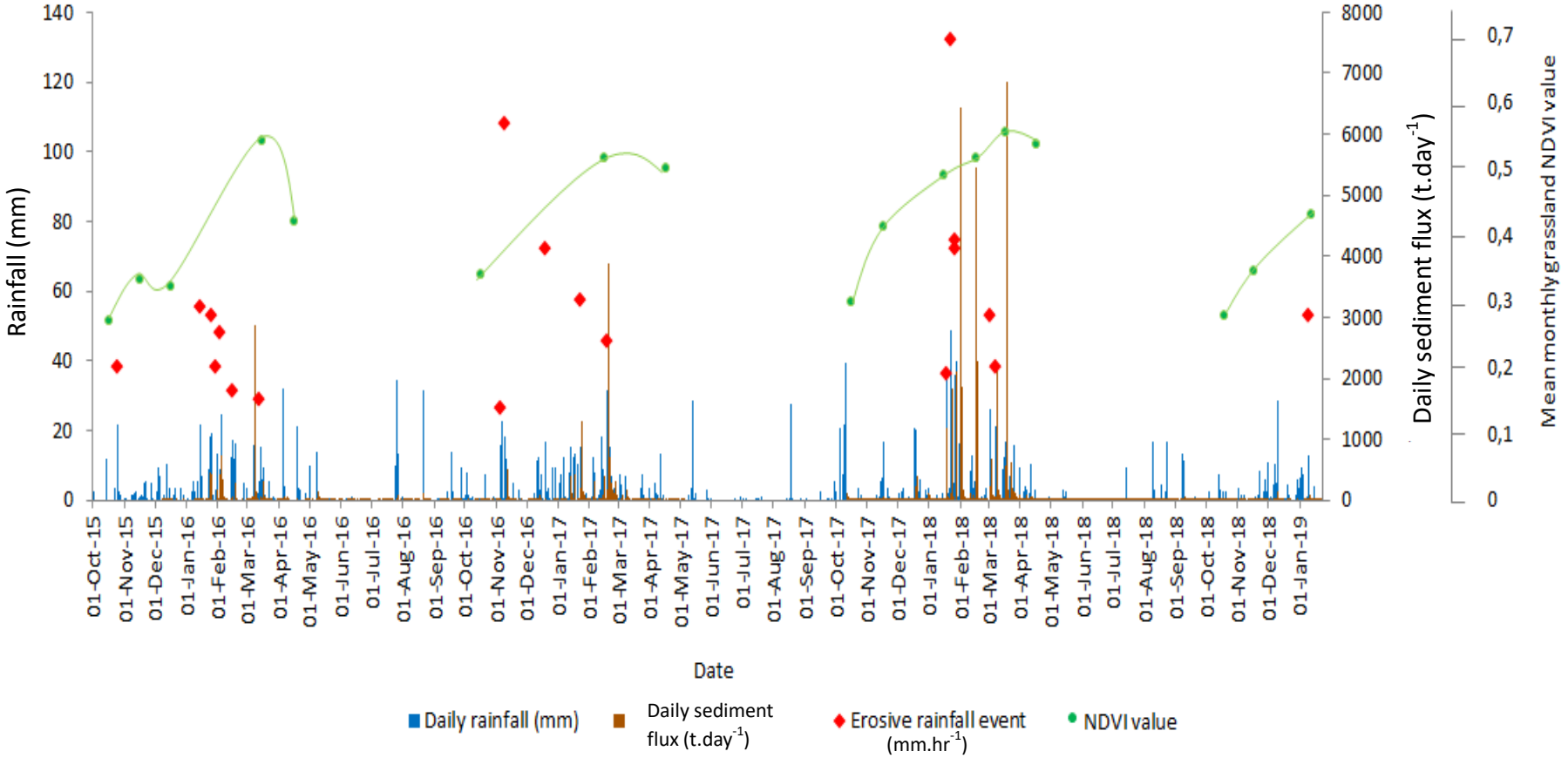

Figure 4.13: The seasonality of daily rainfall, erosive rainfall events, NDVI and daily sediment load in the Gqukunqa River catchment from January 2016 to January 2019.

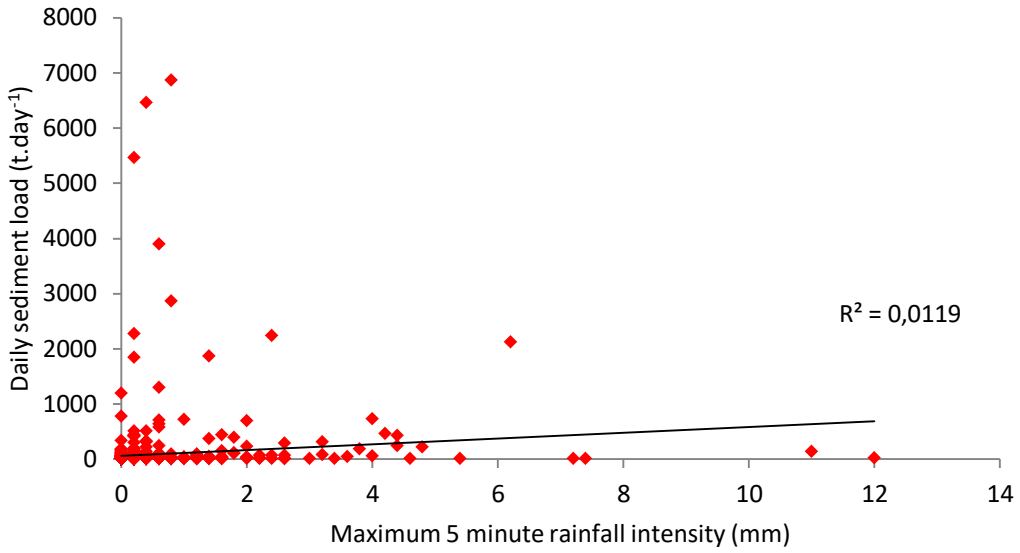

Figure 4.14: Relationship between daily sediment flux and rainfall intensity in the Gqukunqa River catchment.

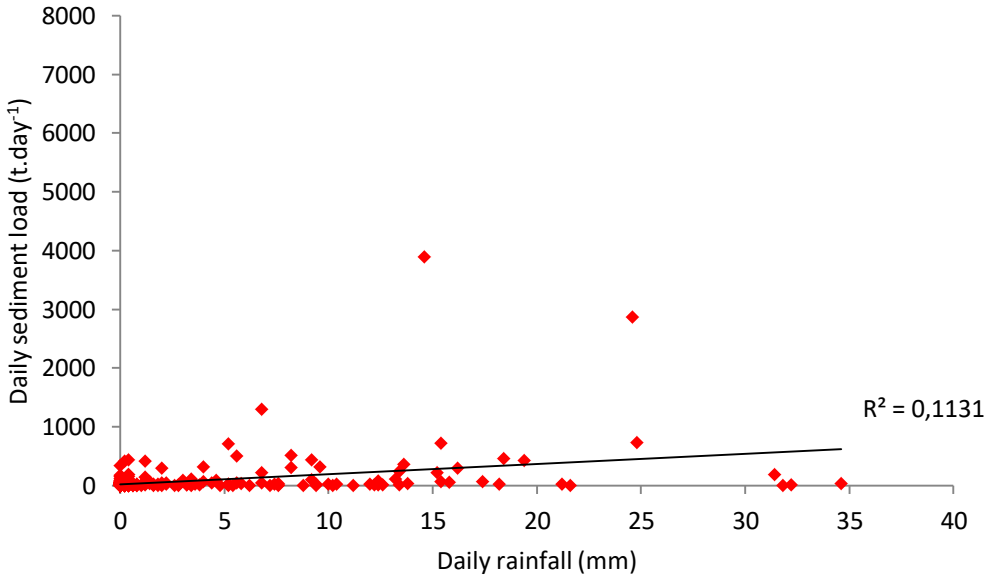

Figure 4.15: Relationship between daily sediment flux and daily rainfall in the Gqukunqa River catchment.

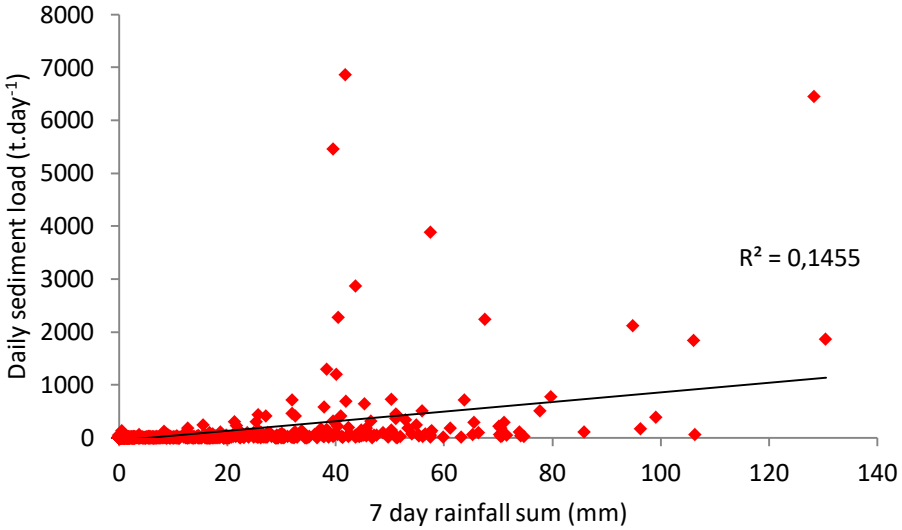

Figure 4.16: Relationship between daily sediment flux and antecedent rainfall in the Gqukunqa River catchment.

Chapter 5: Discussion

5.1 Introduction

This section discusses and gives explanations for the findings in the results in Chapter 4: Results. Remote sensing data and NDVI trends/results are identified and discussed as well as the relationships and trends between and within the field variables. Furthermore, the relationships between daily rainfall, high-intensity rainfall and daily sediment flux are discussed including the trends between them.

5.2 Remote sensing and NDVI trends

The mean monthly NDVI values of the grassland areas in both the LPRC and GRC increased throughout the course of the 2018-2019 wet season and peaked between January 2019 and April 2019 (towards the end of the wet season). The peak in NDVI values is caused by high levels of photosynthetic activity which is a result of various factors: 1) soil moisture content, caused by rainfall (Pandey and Singh, 2007); 2) daylight hours/photoperiod (Adole *et al*., 2019) and 3) higher temperatures (Adole *et al*., 2019). For Southern Africa in particular, Fuller and Prince (1996) and Zhang *et al* (2005) found that the average threshold amount of cumulative rainfall that is required to trigger grassland green-up is 49-50 mm after the dry season. This threshold was surpassed on 18 November 2018 and 27 November 2018 in the LPRC and GRC respectively thus there was a delayed effect in the green-up of the grasslands in both catchments. This delay in grassland green-up is likely to cause a delayed phenological response of the grasses which means that the grasses will only provide greater soil cover later in the wet season and into the early dry season, i.e. regardless of the rain that fell in October 2018, there was a month and half to nearly two months lag before the grass growth signal could be seen in the 2018-2019 wet season. Pandey and Singh (2007) found that total biomass volume was related to rainfall that fell later in the rainy season and not early in the rainy season. This was found because rainfall that occurs in the early wet season stimulates the growth of shoots, however, late rainfall during the wet season will sustain biomass accumulation (Pandey and Singh, 2007).

During the dry season the grasses in both the LPRC and GRC become senescent due to the change of seasons and the recycling of nutrients to use towards reproduction and the new season's growth (Yang and Udvardi, 2018). These senescent grasslands produce lower NDVI values in the dry season (Sarath *et al*., 2014), entering into the wet season. The areas with the greatest amount of variation in NDVI in the LPRC and GRC (Figure 4.2 and 4.3) are those which have low values at the start of the wet season and are likely to be senescent grasslands thus allowing for a large increase in plant

growth and thus an increase in NDVI over the course of the wet season. The areas with the smallest amount of variation in NDVI values in the LPRC (Figure 4.2) can be explained by the low reflectance values from rocky outcrops and bare patches of soil. Here the low vegetation cover, rocky outcrops and bare patches do not change much over the course of a wet season.

Throughout the course of the 2018-2019 wet season in both the LPRC and the GRC, the total size of grassland areas with NDVI values above the catchment mean increase steadily (Figure 4.4). As a result the system productivity therefore increases over the course of the wet season. At the start of the wet season after the threshold of 50 mm (Fuller and Prince, 1996; Zhang *et al.,* 2005) has been surpassed and there are longer sunlight hours the area of new active plant cells expand rapidly (Yang and Udvardi, 2018). When this happens the senescent leaves become active again thus the grasses become greener faster. The grassland areas that do not green-up as much over the course of the wet season are likely to be low in vegetation cover/biomass and may also be possible erosion hotspots or areas with bare soil which have lower NIR reflectance values than grasslands (Myneni and Williams, 1994).

5.2.1 Trends between aspect and NDVI at catchment-scale

The mean monthly NDVI values are higher on south-facing slopes than the north-facing slopes at the broader catchment-scale in both the LPRC and GRC for the 2018-2019 wet season. This supports the findings from Jin *et al* (2006) and Mokarram and Sathyamoorthy (2015) who found that the best vegetation growth is on the shady side of the mountain slopes due to lower evapotranspiration levels and the resultant higher retention levels of soil moisture. In the Southern Hemisphere, north-facing slopes are generally less steep in this area as they are exposed to more direct insolation which dries up the north-facing slopes faster than south-facing slopes, and exposes the north-facing slopes to deeper cycles of heating and cooling and wetting and drying (Sumner *et al*., 2009). Where sandstone particles are loosely packed and where there is a high content of clay, weathering is expected to occur mainly as a result of wetting and drying cycles. This leaves the north-facing slopes with lower moisture retention levels and less vegetation cover which leads to increased erosion, as found by Francis and Thornes (1990), and reduces the slope angle.

5.2.2 Trends between slope angle and NDVI at catchment-scale

In only the LPRC, the mean monthly NDVI values at the broader catchment-scale followed a trend of a slight increase with increasing slope angle. Cook (1966) and Ford (2015) found that on commercial farms there was a tendency for livestock grazing to be concentrated on gentler slope gradients than on steeper slopes. Whilst grazing intensity was not assessed, the anecdotal evidence from field trips

showed that stock preference in the LPRC was on the gentle slopes which are the easily accessible slopes for livestock. Steeper slopes are more difficult for livestock to access and thus in the LPRC they tend to prefer to graze on gentler slopes. This puts less grazing pressure on the grasses on the steeper slopes and allows the grasses to grow with less grazing pressure and reproduce easier.

In contrast, in the GRC at both the broader catchment-scale and at plot-scale the mean monthly NDVI values followed a trend of a slight decrease with increasing slope angle indicating lower active plant growth of the grasses on steeper slopes (Yang and Udvardi, 2018). Wilcox *et al* (1998) found that infiltration of water decreased on steeper slopes where livestock grazing was present owing to compaction and harder surfaces resulting in lower infiltration rates and higher runoff rates. Photosynthetic activity, which influences NDVI value, is a function of soil moisture (Pandey and Singh, 2007). Thus the lower soil moisture levels and grazing pressure on steeper slopes are likely to be a cause of the lower NDVI values on steeper slopes.

5.3 Field measured variables

The majority of the field variables had weak relationships, portrayed by the low R^2 values (Table 4.2). However, the scatter plots (Figure A1-A40) are useful in indicating the trend of the relationship (positive/negative). This section discusses the relationships between the variables and the trends within the variables over the course of the 2018-2019 wet season.

5.3.1 Vegetation cover and NDVI

The relationship between grassland vegetation cover and NDVI ranges from weak to moderate in both catchments, with the only moderate relationship found in April 2019 in the GRC. Many researchers have found that NDVI is a good proxy for biomass/vegetation cover (Coe *et al*., 1976; Fynn and Connor, 2000; Pandey and Singh, 2007). However, the results from this study do not reflect these findings.

Reasons for this could include: 1) the grassland vegetation cover percentage value may be high but the grasses could be short and grazed which may result in a lower NDVI value due to less vegetation cover caused by grazing (Ratsele, 2013); 2) the presence of bare soil patches can decrease pixel-based NDVI values as found by Myneni and Williams (1994) as the bare patches amongst very green grass result in mixed pixel NDVI signatures that will be lower than anticipated if spatial resolution of the sensor only captured the grass tuft; 3) the studies done by Coe *et al* (1976), Fynn and Connor (2000) and Pandey and Singh (2007) were not conducted in the Eastern Cape of South Africa and it may be that NDVI is not a good predictor of vegetation cover in the sub-humid climate of the study

area; and 4) many areas had recently been burnt in both catchments during the October 2018 field trip with small green shoots (and thus low biomass) visible in the burnt landscape, artificially altering the phenological response of the grassland, which may have negatively influenced the relationship of vegetation cover and NDVI across the whole 2018-2019 wet season.

In October 2018, in both catchments, the vegetation cover was higher on north-facing slopes, however, as the season progressed, this relationship switched. In January 2019 and April 2019 the vegetation cover was higher on south-facing slopes. Vegetation cover is a factor of soil moisture (Fay and Schultz, 2009) thus the higher vegetation cover on south-facing slopes could be caused by the moisture retention that would increase plant growth. Radcliffe (1982) found that south-facing slopes in the Southern Hemisphere have more palatable grasses in the winter months due to north-facing slopes having higher quantities of dead plant leaf litter caused by more rapid evaporation on north-facing slopes thus reducing soil moisture. The higher vegetation cover on north-facing slopes in October 2018 in both catchments could be explained by the fact that south-facing slopes have more palatable grasses during the winter which has the potential to reduce vegetation cover on south-facing slopes in the winter.

Geology did not have a significant effect on the vegetation cover and NDVI at the plot-scale in the GRC. Vegetation cover was the same on both the Tarkastad and Molteno Formations which does not reflect the findings of Finca (2012) who found that vegetation cover and biomass were lower on mudstone Formations. However, the Molteno Formation has thick layers of mudstones and is not a true sandstone (Pretorius, 2016) which may have caused the similarities in vegetation cover between the Tarkastad and Molteno Formations. More field sites and a longer temporal monitoring period (beyond only one season), would explore this further.

5.3.2 Biomass

Biomass and NDVI showed weak positive relationships in both the LPRC and GRC, which does not reflect the findings of Coe *et al* (1976) who determined that biomass and NDVI have strong positive relationships. At the beginning of the wet season the grasses were observed to be predominantly brown/senescent due to the lack of active chlorophyll in their leaves (Yang and Udvardi, 2018), thus reflect a lower NDVI signature/value which is likely a cause of the skewed relationship between biomass and NDVI across the 2018-2019 wet season.

However, the LPRC has a slightly stronger relationship between biomass and NDVI than the GRC. This could be explained by the more intense and uncontrolled grazing that the grasses in the GRC

receive from livestock, compared to the rotational grazing that is practised in the LPRC. Pandey and Singh (2007) found that grazing stimulates 4-45% greater active plant growth where the grazing was light to moderate which is found in the LPRC. In contrast, the GRC stocking rates are high and there is little practise of livestock rotation which, according to Fynn and Connor (2000), has a deleterious effect on active plant growth and biomass, leaving the land vulnerable to erosion.

Biomass and percentage of vegetation cover had a weak positive relationship in both the LPRC and GRC. The weak relationship between the two field variables could be explained by the fact that high vegetation cover does not necessarily mean high biomass and, in contrast, high biomass might not necessarily mean high vegetation cover. At a catchment-scale this can be explained by the preferred grazing of more palatable grasses compared to less palatable grasses which promote high vegetation cover and low biomass in certain grass species. The empirical evidence showed that some of the 80 ground-truthing sites (5 x 5 m quadrats), as well as areas all over each catchment, had 100% vegetation cover but the grass was short and clearly grazed (biomass removal). In contrast, some sites had large clumps of grass (high biomass) with bare patches in between. Both of these reasons could contribute to the weak relationship between vegetation cover and biomass.

In support of the vegetation cover findings, biomass is greater on south-facing slopes in January 2019 and April 2019 in both the LPRC and GRC. However, biomass is only marginally greater on north-facing slopes in October 2018. The difference in biomass on the two aspects in January 2019 and April 2019 can be explained by the moisture retention on south facing slopes that would improve plant growth (Fay and Schultz, 2009). The higher biomass on north-facing slopes in October 2018 could be explained by the more palatable grass species being found on south-facing slopes (Radcliffe, 1982) which leaves the grasses on the north-facing slopes to grow. The south-facing slopes in winter in both catchments will also become colder than north-facing slopes and will not receive as much sunlight as the north-facing slopes (Vetter *et al*., 2006). These two factors will stunt plant growth in winter on south-facing slopes in the two catchments more so than on north-facing slopes, thus contributing to higher biomass on north-facing slopes after the winter months and before much rain has fallen.

5.3.3 NDVI versus slope at a finer plot-scale

The relationship between NDVI and plot-scale slope angle in both catchments is negative which does not follow the catchment-wide trend for the LPRC discussed above in section 5.2.2. This could be due to: 1) the slope angles are binned into classes and thus may not predict the most accurate

representation of the relationship between NDVI and slope, whereas here the NDVI was plotted against an exact slope angle and not against a slope class, 2) there are only 80 points from each catchment represented in the scatter plot of NDVI versus slope angle (Figure A24) compared to thousands of NDVI pixels with associated slope classes in the analyses discussed in 5.2.2. This second reason alludes to the issue of scale and how the finer scale results deviate from the catchment-scale observations. Chase *et al* (2018) explored the effect of scale on biodiversity in response to ecological drivers and found that the changes in biodiversity were frequent and scale-dependent. Of the studies reviewed, the authors determined that biodiversity responses to the drivers of system behaviour, 'switched' responses when considered at varying scales. Potentially this has implications here, for the upscaling of trends observed at the plot-scale to outcomes for catchment-scales. Given the 80 sampling plots, the catchment-wide scale/trend found between NDVI and slope is more likely to be representative of the catchment than the plot scale used.

5.3.4 Soil surface hardness

Soil surface hardness affects the infiltration rate of precipitation where harder soil surfaces will result in greater runoff and incur greater erosional energy. The soil surface hardness in the LPRC was found to be greater throughout the 2018-2019 wet season on sandstone Formations (Clarens Formations) than mudstone Formations (Elliot Formations). Mudstones are comprised of smaller clay particles than the sand particles in sandstones and the clay minerals in mudstones are able to attract and absorb water which results in swelling and softening of the mudstone soils when they get wet (O'Byrne, 1967; Zhang *et al*., 2010). It had rained before, or during, every field trip that was conducted and the rain is likely to have caused the mudstone soils to swell and result in the clay particles to be pushed further apart which is likely to lead to softer soil surface hardness. This means that mudstones are likely to be more sensitive to trampling by livestock during the wet season. When these soils become dry they shrink again becoming harder at the surface (Zhang *et al*., 2010).

The soil surface hardness in the GRC was found to be greater on Tarkastad Formations than Molteno Formations throughout the 2018-2019 wet season. Both the Tarkastad and Molteno Formations consist of mudstone and sandstone, however, the Tarkastad Formation has a higher ratio of mudstone to sandstone and the Molteno Formation has a higher ratio of sandstone to mudstone. Due to the rain experienced in the GRC directly before, or during, the soil surface hardness measuring, it would be expected that the mudstones would swell and become softer, however, this was not found to be true as it was in the LPRC. This could be caused by the duplex soils in the Molteno and Tarkastad Formations found in the GRC. Duplex soils have clear distinction between the topsoil and sub-soil layers which is owed to the higher clay content that is found in the sub-soil

caused by leaching (Fey, 2010). As a result of the leaching in the duplex soils in the GRC, the surface soils in the GRC may possibly have a lower clay content and undergo less swelling and shrinking which will not result in softer mudstone surface soils after wetting.

There is no visible trend in the soil surface hardness between north and south-facing slopes in the GRC which could be attributed to the swelling and shrinking mudstone soils with varying wetness during field measurements.

5.3.5 Biocrust

Biocrust plays a role in soil protection from wind and water erosion with greater biocrust cover on bare patches of soil resulting in reduced soil erosion (Zhang *et al.,* 2006; Bowker *et al.,* 2008; Chamizo *et al*., 2017). However, the percentage of biocrust cover in both the LPRC and GRC is most likely to be too low to prevent a significant amount of soil erosion from occurring. What is important to note is that the LPRC had +-5% biocrust cover in each month that fieldwork was conducted however the GRC had +-1% biocrust cover throughout the wet season. The low percentage of biocrust cover in the GRC could be linked to removal of biocrust via trampling from the high stocking rates of livestock as was found by Eldridge (1998) and Read *et al* (2011). Biocrust is brittle and weakly attached to the surface of the soil and thus rapidly disintegrates and breaks off in chunks when trampled by livestock (Eldridge, 1998).

A slight decreasing trend in biocrust cover in the LPRC over the course of the 2018-2019 wet season. This could be attributed to the fact that vegetation cover and biomass increase over the course of the wet season which reduces the amount of visible bare soil patches and thus reduces space for biocrust growth (Chamizo *et al*., 2017). The opposite trend was found in the GRC where there was an increasing trend in biocrust cover over the course of the 2018-2019 wet season. This is unexpected in this catchment because of the heavy stocking rate and trampling of biocrust by livestock. Another contributing factor to this is that perhaps the human-derived sampling method is not sensitive enough to minute changes (which are likely within the measurement error of the visual assessment) and capturing biocrust in this type of system and that machine-driven sampling or alternative methods may be more precise in biocrust cover sampling.

5.4 Relationship between rainfall and daily sediment flux

Although NDVI has been found by this study not to have a very strong relationship with biomass and grass cover, it was found in both the LPRC and GRC that NDVI followed the same trend as daily rainfall in that they both increased steadily from October and peaked between January and April. This trend holds true for biomass and daily rainfall as biomass increased over the course of the 2018-

2019 wet season however no field work was conducted in February or March to determine if biomass peaked in February, March or April. However, the results do reflect the findings of various authors (Coe *et al*., 1976; Fynn and Connor, 2000; Pandey and Singh, 2007) in that biomass has a positive relationship with rainfall. Ground cover is highest during periods of high rainfall, thus protecting the soils to some extent. The mean monthly NDVI values were highest during the months which received the highest amount of rainfall which supports the research done by Pandey and Singh (2007) and Deshmukh (2008) in that "green" biomass is a function of soil moisture.

In the LPRC the erosive rainfall events, as classified by Stocking and Elwell (1976), did not show a clear trend but mostly occurred from the mid to late wet season which is also when the highest sediment flux events took place in early 2016. The erosive rainfall events in the GRC, however, followed more of a visible trend each wet season which was seen by the second erosive rainfall event always being the largest, followed by a decrease in intensity of the following events in the wet season. The erosive rainfall events in the GRC were, in general, greater in intensity than those that occurred in the LPRC.

Suspended sediment data for the Little Pot River is only available from January 2016 until August 2016 so inferences are made from what sediment data are available. Sediment data collection in the LPRC only began in January 2016, however, due to the prolonged drought in the Eastern Cape and the UTRC the larger rainfall events in the 2015-2016 wet season only began in January 2016 (Bannatyne, 2019, *pers. comm*.). Due to the larger rainfall events only starting from January 2016 onwards, it is likely that no major sediment events occurred before then, thus no vital sediment-rainfall relationship data was lost prior to sediment sampling beginning.

The GRC has a significantly higher sediment yield than the LPRC with sediment flux events that are between one and two orders of magnitude larger than those found in the LPRC. This is largely due to the dispersive soils that are found in the GRC and the source of the majority of the sediment is thought to be the gullies found in the GRC which agrees with the findings of Pretorius (2016). Pretorius (2016) found that gullies in the UTRC account for up to 70 times more annual sediment yield than sheet and rill erosion. There are large and active gully systems in the GRC that are widely spread throughout the catchment and are likely to contribute large amounts of sediment to the Gqukunqa River during periods of significant rainfall.

The maximum five-minute rainfall intensity and daily sediment flux have a very weak positive relationship in both catchments. This differs from the findings of Gallart *et al* (2002) and Chirino *et al* (2006) who found that rainfall intensity is more strongly related to erosion and that most of the

sediment that is exported from a catchment is created during high-intensity rainfall events. However, the erosion, which was not measured in this study, may only occur during the high intensity events and the eroded soil may only reflect in the rivers during the larger very wet conditions when hillslope channel connectivity is activated. Gallart *et al* (2002) found that sediment delivery to river systems was controlled by the role of saturated areas during high-intensity storm events and that the rivers in catchments with heavily eroded landscapes had very high suspended sediment concentrations. The empirical evidence from the LPRC reveals that the LPRC has a high percentage cover of grassland protecting the soil from erosion with very few areas of bare soil and the high percentage grass cover promotes infiltration (Joshi and Tambe, 2010). The high rates of infiltration will result in lower surface runoff rates and reduce the sediment connectivity in the catchment.

The daily sediment flux also had a very weak positive relationship with daily rainfall in both catchments, however, this relationship is slightly stronger than the relationship between maximum five-minute rainfall intensity and daily rainfall in both catchments. This alludes to the idea that it is less likely to be the intensity of a rainfall event that determines most of the erosion and sediment transport in this landscape but rather the volume and the length of rainfall period. The slightly stronger relationship between daily sediment flux and daily rainfall could be explained by the saturation of the duplex soils present in these catchments during rainfall events. Duplex soils have poor infiltration rates, slow internal drainage and are susceptible to waterlogging, all of which leads to soils that can become easily saturated during rainfall events (Seitlheko, 2003). In duplex soils, the rate at which infiltration occurs in the topsoil/surface soil is generally quicker than the clay sub-soil which results in saturated topsoils and sub-surface lateral flows (Brooksbank *et al*., 2011). Scott and Van Wyk (1990) found that hillslope soil erosion was caused by rainfall storms that had a low intensity but a long duration. Scott and Van Wyk (1990) also found that if the rate at which the rainfall infiltrated the soil was lower than the rainfall intensity then the surface soil would ultimately become saturated which resulted in saturated overland flow, carrying sediment into the river system.

Four out of five of the highest daily sediment fluxes (daily load, t/day) in the LPRC resulted from four to seven days of continuous rainfall and not directly from an erosive rainfall event. Only one of the five highest sediment flux events occurred on the same day as an erosive rainfall event. Four out of five of the largest sediment events (daily load, t/day) in the GRC resulted from two to seven days of continuous rainfall and not directly from an erosive rainfall event. Only one of the five highest daily sediment fluxes occurred on the same day as an erosive rainfall event which alludes to the fact that

there could be a lag effect in the resultant sediment flux in the rivers after erosive rainfall events. The sediment events in each catchment did not occur on the same dates thus indicating that the sediment events were caused by local rainfall events that were restricted to the respective catchments despite them being ± 40 km apart.

Daily sediment flux and daily rainfall may be poorly related in both catchments but sediment flux and threshold values of rainfall after continuous days of rainfall are what is important here. This is supported by Figures 4.12 and 4.16 which show that there is a slightly stronger relationship between the sum of seven days of rainfall (antecedent rainfall) and daily sediment flux. This means that eroded sediment only travels through the catchment and river systems to the monitoring sites during wet periods when hillslope-channel and longitudinal connectivity peaks. This is supported by Fryirs *et al* (2007) who found that it is usually the larger rainfall events and prolonged periods of wetness that are responsible for hillslope-channel connectivity.

In the LPRC there is generally good vegetation cover year-round with very few gullies present that are able to contribute to high sediment fluxes in the Little Pot River. The high-intensity rainfall events have, as mentioned above, poor relationships with sediment flux in the Little Pot River which means there is most likely another mechanism and cause for the highest sediment flux events here. Beckedahl (1996) explored sub-surface soil erosion phenomena and found that under particular circumstances the amount of sediment lost via surface erosion could be increased by up to a further 77% by sub-surface erosion. Rainfall intensities that are below the infiltration capacity of the soil will result in partly saturated soils where the infiltrated water can cause chemical weathering of the sub-soil and lead to through-flow (Beckedahl, 1996). This through-flow transports soil material beneath the surface of the land and ultimately contributes suspended sediment to the river system, thus increasing the daily sediment flux during periods of low rainfall volume or intensity. The high sediment fluxes in the Gqukunqa River after multiple days of rain are likely to be caused by and enhanced by sub-surface soil erosion phenomena as described by Beckedahl (1996).

Chapter 6 Conclusion

6.1 Concluding remarks

This project was aimed at determining the seasonal trends of rainfall, ground cover and sediment dynamics in the Little Pot River and Gqukunqa River catchments. A variety of field methods and desktop methods/analyses were used to achieve this at two different scales, i.e. at the finer scale of 5 x 5 m quadrats and at the catchment-scale. Field variables measured were grassland biomass, grassland vegetation cover, soil surface hardness, biocrust cover and slope. Desktop methods and analyses included the creation of NDVI maps and analyses of rainfall and sediment data for both catchments. This section gives a summary of the conclusions of the results and the implications thereof for the overarching purpose of the study.

It was originally thought that in order to fulfil the first objective, NDVI would be an accurate predictor/proxy for grassland vegetation cover and above-ground biomass at the plot-scale, however, it was found that the relationships between these factors in the two study catchments are relatively weak and that NDVI is better at indicating phenological changes at the catchment-scale over a wet season. Rainfall is a key driver of rangeland vegetation dynamics, however, other researchers found that livestock grazing plays an important role in vegetation change and that rangelands may display multiple equilibrial and non-equilibrial system responses at a variety of temporal and spatial scales. This study was not conducted under controlled conditions and livestock were left to graze under their normal conditions in each respective study catchment by their owners/farmers/shepherds. Grazing and governance are major system disturbance drivers in the UTRC, both of which play a major role in shaping the responses of vegetation in both catchments and cannot be ignored as they can have mediating effects on the relationships between NDVI, vegetation cover and biomass. Daily rainfall, NDVI, biomass and vegetation cover all follow the same trend in the wet season in both catchments in that they increase over the course of the wet season to peak between January and April. It was not able to be determined what exact month biomass and vegetation cover peaked as measurements were only taken in October 2018, January 2019 and April 2019 making it difficult to full achieve objective one.

NDVI, vegetation cover and biomass were found to be higher on south-facing slopes compared to north-facing slopes which implies that active plant growth is a function of soil moisture that is retained better on south-facing slopes. This also supports models of higher erosion rates on north-facing slopes (in the Southern Hemisphere) due to greater moisture and temperature extremes (enhancing weathering processes) and supports less vegetation/poorer cover (poor protection from

erosive rainfall). Vegetation cover and biomass on south-facing slopes were higher on south-facing slopes in both catchments for the majority of the wet season which means that vegetation cover and plant growth on north-facing slopes should be promoted and conserved in the future.

Scale effects were evident form measurements at the plot and catchment-scale. The relationship between NDVI and slope for the whole catchment of grassland areas compared to the relationship between NDVI and slope for the 80 ground-truthing sites per catchment reflected contrasting results. Therefore, scaling should be handled with caution.

Biocrust cover is relatively low in both catchments and increases with a reduction in vegetation cover. The biocrust in both catchments are sensitive to continuous grazing caused by the trampling from livestock.

The soil surface hardness was harder on sandstone Formations in the LPRC, owing to swelling and softening of the soils on mudstone Formations after rainfall periods before or during field trips. In contrast, the Tarkastad Formation (consisting of a high ratio of mudstones) in the GRC had harder surface soils which was likely caused by leaching in duplex soils which reduces the clay content resulting in less swelling and softening of mudstone surface soils.

In both catchments, the majority of the erosive rainfall events occurred during the months of January to March each wet season, fulfilling objective two. These erosive events occurred during the period in which vegetation cover and biomass were high and also where the highest daily sediment fluxes occurred. The timing of the majority of the erosive rainfall events in both catchments reiterates the precaution that vegetation cover must be promoted the entire year in order to protect the soils from erosion because the erosive rainfall events are intermittent and unpredictable. The reality of this practice is that it will be difficult to implement given the additional challenges of drought and fodder needs for livestock, however, this practice should be exercised as much as possible, particularly in areas which are highly eroded and susceptible to erosion.

With regards to objective three, sediment loads increased during the wet season and peaked around January-March despite good vegetation cover. The daily sediment load was not strongly linked to individual high intensity events, but more to wet periods over several days. This supports the notion of sediment delivery being optimised when most of the catchment surface is connected hydrologically during the extreme wet periods. The LPRC and GRC both have very different sediment yields where the GRC has a much larger sediment yield output than the LPRC. The LPRC is higher in elevation and falls under freehold tenure where the land is farmed commercially by livestock farmers and livestock undergo routine and planned rotation in order to reap the optimum benefits

of each livestock camp. The soils in the LPRC are more stable and protected from erosion by vegetation cover thus alludes to the reason behind the low sediment yield in the Little Pot River. The GRC is lower in elevation and falls under communal land tenure where livestock graze freely, however, the livestock tend to graze mainly around the general vicinity of the homesteads thus causing erosion hotspots. Despite the GRC being more than double the size of the LPRC the very high sediment yield and very high daily sediment flux events in the GRC are likely owed to: 1) the dispersive soils in the catchment; 2) the large gully systems in the catchment; 3) the poor management of livestock in the catchment leading to vegetation destruction and bare soils and 4) a higher maximum rainfall intensity.

It is also likely that surface and gully erosion may not be the only source of sediment in the rivers and that sub-surface erosion phenomena and sub-surface chemical weathering of the soil may be another source of sediment in the rivers in both catchments. Sub-surface erosional processes and through-flow can transport large amounts of soil material to the river system even during low rainfall intensities. These sub-surface erosion phenomena should be further explored in the Upper Tsitsa River catchment to understand the more complex system responses and sediment sources in the UTRC.

This study has contributed a variety of knowledge to the Tsitsa Project including rainfall intensity, ground cover and sediment dynamics and the relationships between these factors. The findings of the weak positive relationships between NDVI and vegetation cover and biomass will help advise future students and researchers within the Tsitsa Project that NDVI is not the best proxy for vegetation cover and biomass within the greater study area. The finding of sediment events being larger after antecedent rainfall events rather than high-intensity rainfall events will help inform policy of grazing management practices in areas with dispersive soils.

6.2 Limitations and recommendations

Time constraints of this study was one of the major limiting factors in terms of gathering data about field variables, like vegetation cover and biomass, only over one wet season instead of over multiple wet seasons. This may have implications for the field variable results because this wet season may be an anomaly and not be representative of a normal year which may have had higher or lower rainfall that is one of the main drivers of the vegetation and sediment dynamics in the system. However, even though only one wet season was sampled this does not invalidate the results because the Eastern Cape has been facing a prolonged drought period and so the observed rainfall during this season is comparable to recent years as the last four years have been below the average

annual rainfall (Figure 1.4). A longer NDVI time series was also used to track the trends of NDVI in previous years. It is still, however, recommended that this type of data is collected over multiple wet seasons to get more representative data of vegetation dynamics and sediment dynamics.

In terms of sediment data there were multiple limiting factors: 1) In the LPRC the sediment is only available from January 2016 until August 2016 so it does not cover one full wet season nor available for the length of the study period; 2) there are gaps in the sediment data in both the LPRC and GRC as some suspended sediment samples could not be taken on certain days by citizen technicians due to personal reasons (e.g. multi-day funerals and sickness); 3) activities in ploughed areas and forestry areas might also impact the daily sediment flux data in the rivers which was not accounted for therefore ploughing and harvesting dates should be included in further studies and 4) some suspended sediment samples were not taken during the peak of the flood event due to some floods occurring at night and safety issues associated with night-time sampling (due to most citizen technicians not being able to swim so there is a risk at night with not being able to see and slipping into the river). In order to find the clearest relationship between high-intensity rainfall and suspended sediment flux, the sediment flux from the sediment event (and not the day) would be required however this was not possible due to the above reasons. While the emphasis in these catchments has been capacity development of local community members and creating employment opportunities (citizen technicians), the data collected by citizen technicians could be supported by embedding automated monitoring equipment at key flood points – triangulating data collection. This is, however, not feasible for this system because issues linked to crime/vandalism, and remoteness of these sites makes checking these data loggers impractical.

In terms of rainfall data, there were limiting factors: 1) the rain gauge in the GRC was only installed in January 2018 and as a result the rain gauge from the neighbouring catchment (the Lower Sinxaku catchment) had to be used to supplement the Gqukunqa River catchment rainfall data which is not ideal due to the high spatial variability of rainfall across the landscape; 2) the rain gauge on Woodcliffe Farm in the LPRC was partly blocked by bird droppings, which may have skewed the intensity data for the time period before it was cleared; and 3) the study fell during years with lower rainfall than the annual average (Figure 1.4) which will have resulted in lower sediment yields than usual.

The biomass readings at each quadrat in the field were not calibrated using the cut and dry method but rather from the regression curve established by Gwate (2017) who used the cut and dry method. The calibration of the DPM done by Gwate (2017) for commercial areas was done in a neighbouring catchment to the LPRC, however, the calibration of the DPM done for the communal areas was done

+-75 km away near Cala, Eastern Cape, which consisted of a different grassland classification (Southern Drakensberg Highland grassland) to the GRC (Drakensberg Foothill Moist grassland). Zambatis *et al* (2006) took nine DPM readings in multiple 2 x 2 m quadrats to calibrate biomass readings from the DPM to the cut and dried biomass from the 2 x 2 m quadrats. Although in this study five DPM readings were taken per 5 x 5 m quadrat, this does exclude the fine-scale spatial variation within each quadrat thus leading to potential inaccuracies in the biomass readings. In a catchment of this nature – there is a lot of fine-scale heterogeneity in plant communities at this scale with clumps of unpalatable grasses present amongst short grazed palatable grasses.

The soil surface hardness results were most likely to have been affected by the rainfall that the catchments had both received before or during each field trip which caused the mudstone soils to swell and soften. This resulted in inaccuracies in the soil surface hardness results and made it difficult to determine the true effect that soil surface had on other field variables. However, due to time constraints, the field trips could not be extended to allow for the soils to dry.

The low number of 80 ground-truthing sites per catchment may have been too few and could have affected the NDVI field-based correlations. Many relationships in both catchments were determined based on the 80 sites. However, 80 sites that represent these relationships at a catchment-scale might not be the most effective way to predict accurate catchment-scale relationships and extrapolations based on NDVI alone should be handled with caution. In order to improve the relationships between field variables and the NDVI field-based correlations over a single growing season, supplementary field surveys with more sites could be conducted in a controlled environment without grazing in order to account for the variability and inconsistencies in the results. To explore more in-depth the effect of vegetation cover on sediment dynamics in this type of landscape, a higher spatial resolution sensor should be used for NDVI calibration and more consistent field methods should be conducted during each month of the wet season to more accurately determine the vegetation cover dynamics.

The soils in the GRC are highly erodible, even during low intensity events. Grazing management and maintenance of good vegetation cover throughout the year is crucial to reduce soil loss from this landscape.

6.3 Future research agendas

There are a few research agendas that should be followed by future researchers who are aiming to conduct similar studies in the same greater study area of this research: 1) in order to remove the effect of erosion hotspots on NDVI readings, additional field validation of erosion hotspots will be required to identify erosion hotspots from an NDVI map in the future; 2) in order to determine which month the amount of vegetation and biomass peaks, future work would need to be done in every month of the wet season and not just at the beginning, middle and end of the wet season; 3) in order to increase the accuracy of the DPM readings relative to biomass values and given the error associated with use of regression curves, in future more biomass readings could be taken and calibrated using the cut and dry method in the exact study catchments for increased accuracy, instead of using regression curves from other catchments; 4) in order to improve the accuracy of the soil surface hardness and to determine the true effect of soil surface hardness on other field variables, dry soils should be tested for soil surface hardness in future; and 5) the role that senescent vegetation plays in soil protection should be explored because it does not show up in remotely sensed images due to lack of chlorophyll in the leaves. It is not green vegetation that protects soil from erosion.

A major addition and suggestion for future research on this topic would be to extend this study over a number of years, including the dry season so as to get a sense of how 'green up' and vegetation cover/biomass metrics are shifting during the growing season. This would have big implications for long term vegetation cover and its ties to potential for erosion.

References

Abrams, M.M., Jarrell, W.M. (1995). Soil-phosphorus as a potential non-point source for elevated stream phosphorus levels. *Journal of Environmental Quality*, 24, 132-138.

Abuzar, M., Sheffield, K., Whitfield, D., O'Connell, M., McAllister, A. (2014). Comparing inter-sensor NDVI for the analysis of horticulture crops in south-eastern Australia. *American Journal of Remote Sensing*, 2(1), 1-9.

Adole, T., Dash, J., Rodriguez-Galiano, V., Atkinson, P.M. (2019). Photoperiod controls vegetation phenology across Africa. *Communications Biology*, 2, 1-13.

Alatorre, L.C., Begueria, S., Lana-Renault, N., Navas, A., Garcia-Ruiz, J.M. (2012). Soil erosion and sediment delivery in a mountain catchment under scenarios of land use change using a spatially distributed numerical model. *Hydrology and Earth System Sciences*, 16, 1321-1334.

Ali, I., Fiona, C., Edward, E., Brian, B., Stuart, G. (2016). Satellite remote sensing of grasslands: From observation to management. *Journal of Plant Ecology*, 9(6), 649–671.

Anderson, K.L., Smith, E.F., Owensby, C.E. (1970). Burning bluestem range. *Journal of Range Management*, 23, 81-92.

Anderson, C.B. (2018). Biodiversity monitoring, earth observations and the ecology of scale. *Ecology Letters*, 21(10), 1572-1585.

Andrew, M., Fox., R. (2004). 'Undercultivation' and intensification in the Transkei: a case study of historical changes in the use of arable land in Nompa, Shixini. *Development Southern Africa*, 21(4), 688-706.

Archibald, S., Scholes, R.J. (2007). Leaf green-up in a semi-arid African savanna – separating tree and grass responses to environmental cues. *Journal of Vegetation Science*, 18, 583-594.

Bai, Z. G., Dent, D.L., Olsson, L., Schaepman, M.E. (2008). *Global Assessment of Land Degradation and Improvement. 1 . Identification by remote sensing*. Unpublished report for: World Soil Information. Wageningen: World Soil Information.

Bannatyne, L. J., Rowntree, K.M., van der Waal, B.W., Nyamela, N. (2017). Design and implementation of a citizen technician – based suspended sediment monitoring network : Lessons from the Tsitsa River catchment , South Africa. *WaterSA*, 43(3), 365–377.

Barcelona Field Studies Centre. (2019). *Measuring Slope Steepness.* [Online]. https://geographyfieldwork.com/SlopeSteepnessIndex.htm. [24/11/2019].

Bäse, F., Helmschrot, J., Schmied, H.M., Flugel, W. (2006). The impact of land use change on the hydrological dynamic of the semi arid Tsitsa catchment in South Africa. *Proc. 2nd Göttingen GIS and Remote Sensing*, 267-265.

Bartley, R., Corfield, J.P., Abbott, B.N., Hawdon, A.A., Wilkinson, S.N., Nelson, B. (2010a). Impacts of improved grazing land management on sediment yields, Part 1: Hillslope processes. *Journal of Hydrology*, 389, 238-248.

Bartley, R., Wilkinson, S.N., Hawdon, A.A., Abbott, B.N., Post, D.A. (2010b). Impacts of improved grazing land management on sediment yields. Part 2: Catchment response. *Journal of Hydrology*, 389, 249-259.

Beckedahl, H.R., Bowyer-Bower, T.A.S., Dardis, G.F., Hanvey, P.M. (1988). Geomorphic effects of soil erosion. *In* Moon, B.P., Dardis,G.F. (eds.) *The Geomorphology of Southern Africa*. Johannesburg: Southern Book Co., 249-276.

Beckedahl, H.R. (1996). *Subsurface soil erosion phenomena in Transkei and Southern Kwazulu-Natal, South Africa*. Pietermaritzburg: University of Natal (PhD Dissertation) [pdf].

Beinart, W. (2003). (ed). *The rise of conservation in South Africa: settlers, livestock and the environment 1770–1950.* Oxford: Oxford University Press.

Belay, K.T., Van Rompaey, A., Poesen, J., Van Bruyssel, S., Deckers, J., Amare, K. (2014). Spatial Analysis of Land Cover Changes in Eastern Tigray (Ethiopia) from 1965 to 2007: Are there signs of a Forest Transition? *Land Degradation and Development*, 26, 680-689.

Blake, W.H., Walsh, R.P.D., Barnsley, M.J., Palmer, G., Dyrynda, P., James, J.G. (2003). Heavy metal concentrations during storm events in a rehabilitated industrialised catchment. *Hydrological Processes*, 17, 1923-1939.

Bonilla, C. A., Johnson, O. I. (2012). Soil erodibility mapping and its correlation with soil properties in Central Chile. *Geoderma*, 189, 116–123.

Bovee, K.D., Milhous, R. (1978). *Hydraulic simulation in instream flow studies: theory and techniques.* Cooperative Instream Flow Service Group. Fort Collins: U.S. Fish and Wildlife Service, Office of Biological Services.

Bowker, M.A., Belnap, J., Chaudhary, V.B., Johnson, N.C. (2008). Revisiting classic water erosion models in drylands: the strong impact of biological soil crusts. *Soil Biology & Biochemistry*, 40, 2309–2316.

Bransby, D.J. Tainton, N.M. (1977). The disc pasture meter: possible applications in grazing management. *Proceedings of the Grassland Society of Southern Africa*, 12, 115–118.

Brooksbank, K, White, D.A., Veneklaas, E.J., Carter, J.L. (2011). Hydraulic redistribution in Eucalyptus kochii subsp. borealis with variable access to fresh groundwater. *Trees*, 25, 735–744.

Brown, M.E., Pinzon, J.E., Didan, K., Morisette, J.T., Tucker, C.J. (2006). Evaluation of the consistency of long-term NDVI time series derived from AVHRR, SPOT-vegetation, SeaWiFS, MODIS, and Landsat ETM+ sensors. *IEEE Transactions on Geoscience and Remote Sensing*, 44, 1787– 1793.

Buhmann, C., Rapp, I., Laker, M. C. (1996). Differences in mineral ratios between disaggregated and original clay fractions in some South African soils as affected by amendments. *Soil Research*, 34, 909-923.

Burke, I. C., Schimel, D.S., Yonker, C. M., Parton, W.J., Joyce, L.A., Lauenroth, W.K. (1990.) Regional modeling of grassland biogeochemistry using GIS. *Landscape Ecology*, 4, 45-54.

Butterfield, H. S., Malmström, C. M. (2009). The effects of phenology on indirect measures of aboveground biomass in annual grasses. *International Journal of Remote Sensing*, 30(12), 3133–3146.

Camp, K. (1995). Republic of South Africa. Department of Agriculture. *Cedara Report*: *Valley Bushveld of KwaZulu-Natal: Natural resources and management, KwaZulu-Natal*. Cedara: Department of Agriculture.

Chamizo, S., Rodruguez-Caballero, E., Roman, J.R., Cantón, Y. (2017). Effects of biocrust on soil erosion and organic carbon losses under natural rainfall. *Catena*, 148, 117-125.

Chase, J.M., McGill, B.J., McGlinn, D.J., May, F., Blowes, S.A., Xiao, X., Knight, T.M., Purschke, O., Gotelli, N.J. (2018). Embracing scale-dependence to achieve a deeper understanding of biodiversity and its change across communities. *Ecology Letters*, 21, 1737-1751.

Chirino, E. Bonet, A., Bellot, J., Sanchez, J.R. (2006). Effects of 30-year-old Aleppo pine plantations on runoff, soil erosion, and plant diversity in a semi-arid landscape in south eastern Spain. *Catena*, 65(1), 19–29.

Clevers, J., van Der Heijden, G., Verzakov, S. (2007). Estimating grassland biomass using SVM band shaving of hyperspectral data. *Photogrammetic Engineering and Remote Sensing*, 73, 1141.

Coastal and Environmental Services. (2009). Tsitsa River Basin Land Use And Environmental Management Plan. Unpublished report for ASGISA Eastern Cape. Grahamstown: Coastal and Environmental Services.

Coe, M. J., Cummings, J., Phillipson, J. (1976). Biomass and production of large herbivores in relation to rainfall and primary production. *Oecologia*, 22, 341–354.

Coetzee, A. (2016). *The geometry of Karoo dolerite dykes and saucers in the Highveld Coalfield: constraints on emplacement processes of mafic magmas in the shallow crust*. Stellenbosch: Stellenbosch University (MSc dissertation) [pdf].

Compton, J.S., Maake, L. (2007). Source of the suspended load of the upper Orange River, South Africa. *South African Journal of Geology*, 110, 339–48.

Compton, J.S., Herbert, C.T., Hoffman, M.T., Schneider, R.R., Stuut, J. (2010). A tenfold increase in the Orange River mean Holocene mud flux: implications for soil erosion in South Africa. *The Holocene*, 115-122.

Cook, C.W. (1966). Factors affecting utilization of mountain slopes by cattle. *Journal of Range Management*, 19, 200-204.

Cosandey, C., Andreassian, V., Martin, C., Didon-Lescot, J.F., Lavabre, J., Folton, N., Mathys, N., Richard, D. (2005). The hydrological impact of the Mediterranean forest: a review of French research. *Journal of Hydrology*. 301, 235–249, 2005.

Council for Geoscience. (2008). *Map download*. [Online]. http://geoscience.org.za/cgs/. [06/06/2018].

Davies-Colley, R. J., Hickey, C.W., Quinn, J.M., Ryan, P.A. (1992). Effects of clay discharges on streams: 1. Optical properties and epilithon. *Hydrobiologia*, 248, 215–234.

Dearing, J. A. (1992). Sediment yields and sources in a Welsh upland lake catchment during the past 800 years. *Earth Surface Processes and Land forms*, 17, 1–22.

D'Oleire-Oltmanns, S. Irene, M., Dirk, T. Blashcke, T. (2014). Detection of gully-affected areas by applying object-based image analysis (OBIA) in the region of Taroudannt, Morocco. *Remote Sensing*, 6(9), 8287–8309.

Deshmukh, I.K. (2008). A common relationship between precipitation and grassland peak biomass for East and Southern Africa. *African Journal of Ecology*, 22(3), 181-186.

Droppo, I.G. (2001). Rethinking what constitutes suspended sediment. *Hydrological Processes*, 15, 1551–1564.

Duma, M.F. (2000). A comparative study of soil degradation between rangelands under communal grazing and controlled grazing in Alice, Eastern Cape. Grahamstown: Rhodes University (MSc dissertation) [pdf].

Dumitrascu, N., Florian, S., Lustina, L. (2016). Analysis of land cover and land use changes using Sentinel-2 images*. Present Environment and sustainable Development*, 10(2), 161-172.

Eldridge, D.J. (1998). Trampling of microphytic crusts on calcareous soils and its impact on erosion under rain-impacted flow. *Catena*, 33, 221–239.

Elwell, H.A., Stocking, M.A. (1976). Vegetal cover to estimate soil erosion hazard in Rhodesia. *Geoderma*, 15, 61-70.

ESA – see European Space Agency. (2019). *Product types.* [Online]. https://sentinel.esa.int/web/sentinel/user-guides/sentinel-2-msi/product-types. [07/09/2019].

ESRI. (2016). ArcGIS - ArcMap 10.5.1. Released: December 2016.

Fabricius, C., Biggs, H., Powell, M. (2016). *Ntabelanga Lalini Ecological Infrastructure Project Research Investment Strategy.* Unpublished report for: Department of Environmental Affairs. Pretoria: Department of Enviromental Affairs.

FAO – see Food and Agriculture Organization of the United Nations. (2010). *Land degradation assessment in drylands (LADA): assessing the status causes and impact of land degradation.*Unpublished report for Food and Agriculture Organization of the United Nations. Rome: Land Degradation Assessment in Drylands.

Farnsworth, K.L., Milliman, J.D. (2003). Effects of climatic and anthropogenic change on small mountainous rivers: the Salinas River example. *Global and Planetary Change*, 39, 53-64.

Fay, P.A., Schultz, M.J. (2009). Germination, survival, and growth of grass and forb seedlings: Effects of soil moisture variability. *Acta Oecologica,* 35, 679-684.

Feeny, D., Berkes, F., McCay, B.J., Acheson, J.M. (1990). The Tragedy of the Commons: Twenty-Two Years Later. *Human Ecology*, 18, 1-19.

Fey, M. (2010). *Soils of South Africa*. Cape Town: Cambridge University Press.

Finca, A. (2012). *Modelling trends of evapotranspiration using MODIS LAI in selected grasslands catchment of the Eastern Cape*. Port Elizabeth: Nelson Mandela Metropolitan University (MSc dissertation [pdf].

Fleming, A., Summerfield, M.A., Stone, J.O., Fifield, L.K., Cresswell, R.G. (1999). Denudation rates for the southern Drakensberg, SE Africa, derived from in-situ-produced cosmogenic ^{36}CI: initial results. *Journal of the Geological Society of London*, 156, 209-212.

Flugel, W. A., Marker, M., Moretti, S., Rodolfi, G., Sidrochuk, A. (2003). Integrating geographical information systems, remote sensing, ground truthing and modelling approaches for regional erosion classification of semi-arid catchments in South Africa. *Hydrological Processes*, 17, 929- 942.

Flynn, E.S., Dougherty, C.T, Wendroth, O. (2008). Assessment of pasture biomass with the normalized difference vegetation index from active ground-based sensors. *Agronomy Journal*, 100, 114-121.

Ford, R.M. (2015). *The effects of fire and grazing management on climax grasslands dominated by Hyparrhenia hirita and Cymbopogon validus*. Pretoria: University of Pretoria (MSc dissertation) [pdf].

Foster, I.D.L., Charlesworth, S.M. (1996). Heavy metals in the hydrological cycle: trends and explanation. *Hydrological Processes*, 10, 227–261.

Francis, C.F., Thornes, J.B. (ed). (1990). *Runoff Hydrographs from Three Mediterranean Vegetation Cover Type in Vegetation and Erosion.* Chichester: J.B. Thornes, John Wiley and Sons.

Fryirs, K., Brierley, G.J., Preston, N.J., Kasai, M. (2007). Buffers, barries and blankets: The (dis)connectivity of catchment-scale sediment cascades. *Catena*, 70, 49-67.

Fynn, R., Connor, T.G.O. (2000). Effect of stocking rate and rainfall on rangeland in a semi-arid and cattle performance dynamics savanna , South Africa. *Journal of Applied Ecology*, 37(3), 491–507.

Fuller, D.O., Prince, S.D. (1996). Rainfall and foliar dynamics in tropical southern Africa: Potential impacts of global climatic change on savanna vegetation, *Climatic Change*,33, 69–96.

Furumai, H., Kondo, T., Ohgaki, S. (1989). Phosphorus exchange kinetics and exchangeable phosphorus forms in sediments. *Water Research*, 23, 685-691.

Gallart, F., Llorens, P., Latron, J., Regues, D. (2002). Hydrological processes and their seasonal controls in a small Mediterranean mountain catchment in the Pyrenees. *Hydrology and Earth System Sciences*, 6(3), 527–537.

Gao, L., Bowker M.A., Xu, M., Sun, H., Tuo, T., Zhao, Y. (2017). Biological soil crusts decrease erodibility by modifying inherent soil properties on the Loess Plateau, China. *Soil Biology & Biochemistry*, 105, 49-58.

Garcia-Ruiz, J. M. (2010). The effects of the land use on soil erosion in Spain: A review. *Catena*, 81, 1–11.

Garcia-Ruiz, J.M., Lasanta, T., Ortigosa, L., Ruiz-Flano, P., Marti, C., Gonzalez, C. (1995). Sediment yield under different land uses in the Spanish Pyrenees. *Mountain Research and Development*, 15(3), 229-240.

Garland G.G., Hoffman T. and Todd S. (2000). Soil degradation. *In* Hoffman, T., Todd, S., Ntshona, Z., Turner, S. (eds.), A national review of land degradation in South Africa, unpublished report. Pretoria: South African National Biodiversity Institute.

Gao, J. (2006). Quantification of grassland properties: how it can benefit from geoinformatic technologies? *International Journal of Remote Sensing*, 27(7), 1351-1365.

Gordon, N.D., McMahon, T.A., Finlayson, B.L., Gippel, C.J., Nathan, R.J. (2004). *Stream Hydrology An Introduction for Ecologists* (2e). West Sussex: John Wiley & Sons.

Graham, A. A. (1990). Siltation of stone-surface periphyton in rivers by clay-sized particles from low concentrations in suspension. *Hydrobiologia*, 199, 107-115.

Gu, Y., Brown, J.F., Verdin, J.P., Wardlow, B. (2007). A five-year analysis of MODIS NDVI and NDWI for grassland drought assessment over the central Great Plains of the United States. *Hydrology and Land Surface Studies*, 34(6), 1-6.

Guay, K. C. Beck, P.S.A., Bemer, L.T., Goetz, S.J., Baccini, A., Buermann, W. (2014). Vegetation productivity patterns at high northern latitudes: A multi-sensor satellite data assessment. *Global Change Biology*, 20(10), 3147–3158.

Gwate, O. (2017). *Modelling plant water use of the grassland and thicket biomes in the Eastern Cape, South Africa: towards an improved understanding of the impact of invasive alien plants on soil chemistry, biomass production and evapotranspiration*. Grahamstown: Rhodes University (PhD dissertation) [pdf].

Gyozo, J., van Rompaey, A., Szilassi, P., Csillang, G., Mannaerts, C., Woldai, T. (2005). Historical land use changes and their impact on sediment fluxes in the Balaton basin (Hungary). *Agriculture Ecosystems and Environmen*t, 108, 119–133.

Hardin, G. (1968). The tragedy of the commons. *Science*, 162, 1243-1248.

Hoffman, M.T., Todd, S., Ntshona, Z., Turner, S. (eds). (1999). *Land degradation in South Africa.* Pretoria: Department of Environment Affairs and Tourism.

Hoffman, T.M., Todd, S. (2000). A National Review of Land Degradation in South Africa: The Influence of Biophysical and Socio-economic Factors. *Journal of Southern African Studies*, 26, 743-758.

Huchzermeyer, N., Sibiya, S., Schlegel, P., van der Waal, B. (2018). *Cultivated Lands in the Upper Tsitsa River Catchment T35 A-E. Cultivated land mapping: level of degradation and vulnerability to erosion*. Unpublished report for Tsitsa Project. Grahamstown: Tsitsa Project.

Huggett, R.J. (2007). *Fundamentals of geomorphology* (2e). New York: Routledge, London and New York.

Huntley, B. J., B. H. Walker. (1982). *Ecology of tropical savannas.* Berlin: Springer-Verlag.

Hurni, H. (1990). Degradation and conservation of the soil resources in the Ethiopian highlands. *In* Messerli, B. and Hurni, H. (eds). *African Mountains and Highlands: Problems and Perspectives. Marceline*. Missouri: African Mountains Association, 51-64.

Huston, M.A., Wolverton, S. (2009). The global distribution of net primary production: resolving the paradox. *Ecological Monographs*, 79(3), 434-377.

Scholes, R., Montanarella, L., Brainich, A., Barger, N., ten Brink, B., Cantele, B., Erasmus, B., Fisher, J., Gardner, T., Holland, T.G., Kohler, F., Kotiaho, J.S., Von Maltitz, G., Nangendo, G., Pandit, R., Parrotta, J., Potts, M.D., Prince, S., Sankaran, M., Willemen, L. (2018). Summary for policymakers of the assessment report on land degradation and restoration of the Intergovernmental Science - Policy Platform on Biodiversity and Ecosystem Services. Bonn: IPBES.

Jianlong, L., Tiangang, L., Quangong, C. (1998). Estimating grassland yields using remote sensing and gis technologies in China. *New Zealand Journal of Agricultural Research*, 41(1), 31–38.

Jin, Y. Yang, X., Qiu, J., Li, J., Gao, T., Wu, Q., Zhao, F., Ma, H., Yu, H., Xu, B. (2014). Remote sensing-based biomass estimation and its spatio-temporal variations in temperate Grassland, Northern China. *Remote Sensing*, 6(2), 1496–1513.

Joshi, V.U., Tambe, D.T. (2010). Estimation of infiltration rate, run-off and sediment yield under simulated rainfall experiments in upper Pravara Basin, India: Effect of slope angle and grass-cover. *Journal of Earth System Science*, 119, 763-773.

Kakembo, V, Rowntree, K.M. (2003). The relationship between land use and soil erosion in the communal lands of Peddie district, Eastern Cape, South Africa. *Land Degradation and Development*, 14, 39-49.

Kim, L., Choi, E., Stenstrom, M.K. (2003). Sediment characteristics, phosphorus types and phosphorus release rates between river and lake sediments. *Chemosphere*, 50, 53-61.

Kirkland, T., Hunter, l., Twine, W. (2007). "The Bush is No More": Insights on Institutional Change and Natural Resource Availability in Rural South Africa. *Society and Natural Resources*, 20(4), 337-350.

Kort, J., Collins, M., Ditsch, D. (1998). A review of soil erosion potential associated with biomass crops. *Biomass and Bioenergy*, 14(4), 351-359.

Kondolf, G.M. (1997). Hungry water: effects of dams and gravel mining on river channels. *Environmental Management*, 21, 533-551.

Laker, M. C. (2004). Advances in soil erosion, soil conservation, land suitability evaluation and land use planning research in South Africa, 1978–2003. *South African Journal of Plant and Soil*, 21(5), 345–368.

Lange, R.T. (1969). The Piosphere: Sheep Track and Dung Patterns. *Journal of Range Management*, 22(6), 396-400.

Le Roux, J.S. (1990). Spatial variations in the rate of fluvial erosion (sediment production) over South Africa. *Water SA*, 16, 185–94.

Le Roux, J. J., Newby, T. S., Sumner, P. D. (2007). Monitoring soil erosion in South Africa at a regional scale: Review and recommendations. *South African Journal of Science*, 103(7–8), 329–335.

Le Roux, J.J., Mashimbye, Z.E, Weepner, H.L., Newby, T.S. (2008). *Erosion Status of Priority Tertiary*

Catchment Areas Identified by the Soil Protection Strategy of the Department of Agriculture. Unpublished report for the Department of Agriculture. Pretoria: Institute for soil, climate and water.

Le Roux, J.J. (2011). *Monitoring soil erosion in South Africa at a regional scale*. Unpublished report for the Council of Geoscience. Pretoria: Agricultural Research Council Institute for Soil, Climate and Water Private.

Le Roux, J.J., Sumner, P.D. (2011). Factors controlling gully development: Comparing continuous and discontinuous gullies. *Land Degradation and Development*, 23(5), 440-449.

Le Roux, J.J. (2014). *Soil erosion in South Africa – its nature and distribution.* [Online]. https://www.grainsa.co.za/soil-erosion-in-south-africa---its-nature-and-distribution. [27/02/2020].

Le Roux, J.J., Barker, C.H., Weepner, H.L., van den Berg, E., Pretorius, S.N. (2015). *Sediment Yield Modelling in the Mzimvubu River Catchment*. WRC Report No: 2243/1/15. Water Research Commission, Pretoria.

Le Roux, J. J. (2017). Sediment yield potential in South Africa's only large river network without a dam: implications for water resource management. *Land Degradation and Development*, 29, 765-775.

Mararakanye, N., Nethengwe, N. S. (2012). Gully Erosion Mapping Using Remote Sensing Techniques in the Capricorn District, Limpopo. *South African Journal of Geomatics*, 1(2), 109–118.

Mason, S.J. Jury M.R. (1997). Climatic variability and change over southern Africa: a reflection on underlying processes. *Progress in Physical Geography*, 21, 23–50.

Meadows, M. E., Hoffman, M. T. (2002). The nature, extent and causes of land degradation in South Africa: legacy of the past, lessons for the future?. *Area*, 34(4), 428–437.

Mirzabaev, A., Nkonya, E.M., Goedecke, J., Johnson, T., Anderson, W. (2016). Global drivers of land degradation and improvement. *In* Nkonya, E., Mirzabaev, A., von Braun, J. (eds.), *Economics of land degradation and improvement- A global assessment for sustainable development*. Bonn: Springer Open, 167 - 195.

Miura, T., Yoshioka, H., Fujiwara, K., Yamamoto, H. (2008). Inter-Comparison of ASTER and MODIS Surface Reflectance and Vegetation Index Products for Synergistic Applications to Natural Resource Monitoring. *Sensors*, 8(4), 2480-2499.

Mokarram, M., Sathyamoorthy, D. (2015). Modelling the relationship between elevation, aspect and spatial distribution of vegetation in the Darab Mountain, Iran using remote sensing data. *Modelling Earth Systems and Environment*, 1 (4), 1-6.

Moore, L.M. (1996). The Basic Practice of Statistics, *Technometrics*, 38(4).

Moore, N. J. (2016). *Rainfall Erosivity in the Tsitsa Catchment , Eastern Cape , South Africa.* Grahamstown: Rhodes University (Honours research project) [pdf].

Morgan, R.P.C. (2005). *Soil Erosion & Conservation* (3e). Oxford: Blackwell Publishing.

Morrison, L. (2016). Observer error in vegetation surveys: A review. *Journal of Plant Ecology*, 9(4), 367-379.

Mucina, L., Rutherford, M. C. (2006). *The Vegetation of South Africa, Lesotho and Swaziland.* Pretoria: South African National Biodiversity Institute.

Myneni, R., Williams, D.L. (1994). On the relationship between FAPAR and NDVI. *Remote Sensing of Environment*, 49(3), 200-211.

National Geospatial Information. (2017). *Elevation data.* [Online]. http://www.ngi.gov.za/images/stories/pdfs/5m_contours_available_June_2017_300dpi_Geo.pdf. [15/06/2018].

Nel, W., Sumner, P. D. (2007). Intensity, energy and erosivity attributes of rainstorms in the KwaZulu-Natal Drakensberg, South Africa. *South African Journal of Science*, 103(9–10), 398–402.

Nearing, M. A., Lane, L. J., Lopes, V. L. (1994). Modelling soil erosion. *Soil Erosion Research Methods*, 2, 127-156.

Noble, J.C., Cunningham, G.M., Mulham, W.E. (1984). Rehabilitation of degraded land. *In* Harrington, G.N., Wilson, A.D., Young, M.D. (eds.), *Management of Australia's Grasslands*. Melbourne: CSIRO, 171–186.

O'Connor, T.G., Puttick, J.R., Hoffman, M.T. (2014). Bush encroachment in southern Africa: changes and causes. *African Journal of Range & Forage Science*, 31(2), 67-88.

O'Byrne, T.N. (1967). A correlation of rock types with soils, topography, and Erosion in the Gisborne-East Cape region, New Zealand. *Journal of Geology and Geophysics*, 10(1), 217-231.

O'Reagan, P.J., Turner, J.R. (1992). An evaluation of the empirical basis for grazing management recommendations for rangeland in southern Africa. *Journal of Grassland Society of South Africa*, 9(1), 39-49.

Owens, P.N, Walling, D.E., Carton, J., Meharg, A.A., Wright, J., Leeks, G.J.L. (2001). Downstream changes in the transport and storage of sediment- associated contaminants (P, Cr and PCBs) in agricultural and industrialised drainage basins. *The Science of the Total Environment*, 266, 177-186.

Owens, P.N., Batalla, R.J., Collins, A.J. Gomez, B., Hicks, D.M., Horowitz, A.J., Kondolf, G.M., Marden, M., Page, M.J. Peacock, D.H., Petticrew, E.L., Salomonsk, W., Trustrum, N.A. (2005). Fine-grained sediment in river systems: environmental significance and management issues. *River Research and Applications*, 21, 693-717.

Palmer, A. R. Bennett, J. E. (2013). Degradation of communal rangelands in South Africa: towards an improved understanding to inform policy. *African Journal of Range and Forage Science*, 30(1–2), 57–63.

Pandey, C. B., Singh, J. S. (2007). Rainfall and Grazing Effects on Net Primary Productivity in a Tropical Savanna , India. *Ecology*, 73(6), 2007–2021.

Pereira, P., Cerda, A., Lopez, A.J., Zavala, L.M., Mataix-Solera, J., Arcenegui, V., Misiune, L., Keestra, S., Novara., A. (2016). Short-Term Vegetation Recovery after a Grassland Fire in Lithuania: The Effects of Fire Severity, Slope Position and Aspect. *Land Degradation and Development*, 27, 1523-1534.

Phillips, S.M. Clarke, S.E. (1971). The calibration of a weighted disc against pasture dry matter yields. *Proceedings of the New Zealand Grassland Association*, 33, 68–75.

Piegay, H., Walling, D.E., Landon, N., He, Q., Liebault, F., Petiot, R. (2004). Valley landscape, morphology and sedimentation as indicators of recent changes in sediment yield in an Alpine montane basin (The Upper Drome in France). *Catena*, 55, 183–212.

Pile, K. (1996). Soil erosion, policy and people's perceptions in a rural community in KwaZulu Natal. *South African Geographical Journal*, 39, 59–64.

Pretorius, S. (2016). *Sediment yield modelling in the upper Tsitsa Catchment, Eastern Cape, South Africa*. Pretoria: University of Pretoria (MSc dissertation) [pdf].

Qi, J., Wallace, O. (2002). Biophysical attributes estimation from satellite images in arid regions. *IEEE International Geoscience and Remote Sensing Symposium*, 4, 2000–2002.

Radcliffe, J.E. (1982). Effects of aspect and topography on pasture production in hill country. *New Zealand Journal of Agricultural Research*, 25(4), 485-496.

Ratsele, C. (2013). *Long-Term Ecological Effects of Rangeland Burning, Grazing and Browsing on Vegetation and Organic Matter Dynamics*. Alice: University of Fort Hare (PhD Dissertation) [pdf].

Reid, R., Galvin, K.A., Kruska, R. (2008). Global significance of extensive grazing lands and pastoral societies: an introduction. *In* Galvin, K.A, Reid, R., Behnke, R.H., Hobbs, N.T. (eds), *Fragmentation in arid and semi-arid landscapes: consequences for human and natural systems*. Dordrecht: Springer, 1–24.

Richards, C., Bacon, K.L. (1994). Influence of fine sediment on macroinvertebrate colonization of surface and hyporheic stream substrates. *Great Basin Naturalist*, 54, 106-113.

Robertson, G. (1998). Effect of rainfall on biomass, growth and dieback of pastures in an arid grazing system. *Austral Ecology,* 13(4), 519-528.

Rowntree, K., Duma, M., Kakembo, V., Thornes, J. (2004). Debunking the myth of overgrazing and soil erosion. *Land Degradation and Development*, 15, 203–214.

SANBI – see South African National Biodiversity Institute. (2009). *Archived National Land Cover 2009* (vector geospatial dataset). [Online]. http://bgis.sanbi.org/SpatialDataset/Detail/345. [06/06/2018].

SANBI – see South African National Biodiversity Institute. (2012). *Vegetation Map of South Africa, Lesotho and Swaziland* (vector geospatial dataset). [Online]. http://bgis.sanbi.org/SpatialDataset/Detail/18 [06/06/2018].

SIC – see Satellite Imaging Corporation. (2019). *Satellite Sensors.* [Online]. www.satimagingcorp.com/satellite-sensors/. [9/05/2019].

Sarath, G., Baird, L.M., Mitchell, R.B. (2014). Senescence, dormancy and tillering in perennial C_4 grasses. *Plant Science*, 217, 140-151.

Sayre, N.F., Davis, D.K., Bestelmeyer, B., Williamson, J.C. (2017). Rangelands: Where Anthromes Meet Their Limits. *Land*, 6.

Schroter, D., Cramer, W., Leemans, R., Prentice, I.C., Araujo, M. B., Arnell, N.W., Bondeau, A., Bugmann, H., Carter, T.R., Gracia, C.A., de la Vega-Leinert, A.C., Erhard, M., Ewert, F., Glen-dining, M., House, J.I., Kankaanpaa, S., Klein, R.J. T., Lavorel, S., Lindner, M., Metzger, M.J., Meyer, J., Mitchell, T.D., Reginster, I., Rounsevell, M., Sabate, S., Sitch, S., Smith, B., Smith, J., Smith, P., Sykes,

M.T., Thonicke, K., Thuiller, W., Tuck, G., Zaehle, S., Zierl, B. (2005). Ecosystem service supply and vulnerability to global change in Europe. *Science*, 310, 1333–1337.

Scott, D.F., Van Wyk, D.B. (1990). The efects of wildfire on soil wettability and hyrdrological behavior of an afforested catchment. *Journal of Hydrology*, 121, 249-256.

Seitlheko, E. (2003). Gully initiation and expansion in Lesotho: a case of the Buasono Area. *South African Geographical Journal*, 8, 175–181.

Shackleton, C.M., Gambiza, J. (2008). Social and ecological trade offs in combating land degradation: the case of invasion by a woody shrub (Euryops floribundus) at Macubeni, South Africa. *Land Degradation and* Development, 19, 454–464.

Silleos, N. G., Alexandridis, T.K., Gitas, I.Z. Perakis, K. (2006). Vegetation indices: Advances made in biomass estimation and vegetation monitoring in the last 30 years. *Geocarto International*, 21(4), 21–28.

Smithen, A.A., Schulze, R.E. (1982). The spatial distribution in Southern Africa of Rainfall Erosivity for use in the Universal Soil Loss Equation. *Water SA*, 8(2), 74-78.

Song, C., Dannenberg, M,P., Hwang, T. (2013). Optical remote sensing of terrestrial ecosystem primary productivity. *Progress in Physical Geography*, 37, 834–54.

Srur, A.A., Villalba, R., Baldi, G. (2011). Variations in *Anarthrophyllum rigidum* radial growth, NDVI and ecosystem productivity in the Patagonian shrubby steppes. *Plant Ecology*, 212, 1841-1854.

Stocking, M.A., Elwell, H.A. (1976). Rainfall Erosivity over Rhodesia. *Transactions of the Institute of British Geographers*, 1(2), 231-245.

Sumner, P.D., Hall, K.J., van Rooy, J.L., Meiklejohn, K.I. (2009). Rock weathering on the eastern mountains of southern Africa: Review and insights from case studies. *Journal of African Earth Sciences*, 55, 236-244.

Syvitski, J.P.M. (2003). Supply and flux of sediment along hydrological pathways: research for the 21st century. *Global and Planetary* Change, 39, 1–11.

Thenkabail, P.S. (2004). Inter-sensor relationships between IKONOS and Landsat-7 ETM+ NDVI data in three ecoregions of Africa. *International Journal of remote Sensing*, 25(2), 389-408.

Trimble SW. (1983). A sediment budget for Coon Creek, Driftless area, Wisconsin, 1853–1977. *American Journal of Science*, 283, 454–474.

Trimble, S.W. Mendel, A.C. (1995). The cow as a geomorphic agent – a critical review. *Geomorphology*, 13, 233-253.

Trollope, W.S.W. (1990). Development of a technique for assessing veld condition in the Kruger National Park using key grass species. *Journal of the Grassland Society of Southern Africa*, 7, 46–51.

USGS Earth Explorer. (2019). *Satellite Sensors*. [Online]. https://earthexplorer.usgs.gov/. [07/09/2019].

Vacca, A., Loddo, S., Ollesch, G., Puddu, R., Serra, G., Tomasi, D., Aru, A. (2000). Measurement of runoff and soil erosion in three areas under different land use in Sardinia (Italy). *Catena*, 40, 69-92.

van der Waal, B. (2015). *Sediment Connectivity in the Upper Thina Catchment , Eastern Cape , South Africa*. Grahamstown: Rhodes University (PhD Dissertation) [pdf].

van Tol, J.J., Akpan, W., Lange, D., Bokuva, C., Kanuka, G., Ngesi, S., Rowntree, K.M., Bradley, G., Maroyi, A. (2014). *Conceptualising long-term monitoring to capture environmental, agricultural and socio-economic impacts of the Mzimvubu Water Project in the Tsitsa River.* Unpublished report for the Water Research Comission. Gezina: Water Research Comission.

van Tol, J., Wilson, A., Gcobisa, K., Siphamandla, N., Dirk, L. (2016). Soil erosion and dam dividends: Science facts and rural fiction around the Ntabelanga dam, Eastern Cape, South Africa. *South African Geographical Journal*. Routledge, 98(1),169–181.

Van Veelen, M., Calmeyer, T., Duncan, N. (2014). Republic of South Africa. Department of Water and Sanitation. *Integrated Water Use license Application for the Mzimvubu Water Project: Technical Report.* ILISO Consulting.

van Zijl, G. M. (2010). *An investigation of the soil properties controlling gully erosion in a sub-catchment in Maphutseng, Lesotho*. Stellenbosch: Stellenbosh University, MSc Dissertation [pdf].

Vetter, S. (2005). Rangelands at equilibrium and non-equilibrium: recent developments in the debate. *Journal of Arid Environments*, 62, 321-341.

Vetter, S., Goqwana, W., Bond, W., Trollope, W. (2006). Effects of land tenure, geology and topography on vegetation and soils of two grassland types in South Africa. *African Journal of Range and Forage* Science, 23, 13-27.

Vetter, S. (2013). Degradation of communal rangelands in South Africa: towards an improved understanding to inform policy. *African Journal of Range and Forage Science*, 30(1–2), 57–63.

Walling, D.E, Owens, P.N., Waterfall, B.D, Leeks, G.J.L., Wass, P.D. (2000). The particle size characteristics of fluvial suspended sediment in the Humber and Tweed catchments, UK. *The Science of the Total Environment*, 251/252, 205–222.

Walling, D.E, Fang, D. (2003). Recent trends in the suspended sediment loads of the world's rivers. *Global and Planetary Change*, 39, 111–126.

Washington-Allen, R.A., Ramsey, R.D., West, N.E., Norton, B.E. (2008). Quantification of the ecological resilience of drylands using digital remote sensing. *Ecology and Society*, 13(1).

Wessels, K.J., Prince, S.D., Frost, P.E., van Zyl, D. (2004). Assessing the effects of human-induced land degradation in the former homelands of northern South Africa with a 1 km AVHRR NDVI time-series. *Remote Sensing of Environment*, 91, 47–67.

Wiegand, K., Saitz, D., Ward, D. (2006). A patch-dynamics approach to savanna dynamics and woody plant encroachment – insights from an arid savanna. *Perspectives in Plant Ecology Evolution and Systematics*, 7, 229-242.

Wilcox, B.P., Wood., M.K., Tromble, J.M. (1988). Factors influencing infiltrability of semiarid slopes. *Journal of Range Management*, 41(3), 197-205.

Wood, P.J., Armitage, P.D. (1997). Biological Effects of Fine Sediment in the Lotic Environment. *Environmental Management*, 21(2), 203-217.

Xie, Y., Sha, Z., Yu, M., Bai, Y., Zhang, L. (2009). A comparison of two models with Landsat data for estimating above ground grassland biomass in Inner Mongolia, China. *Ecological Modelling*, 220, 1810–1818.

Yan-Sui, L., Ye-Cui, H., Liu-Ying, P. (2005). Accurate quantification of grassland cover density in an alpine meadow soil based on remote sensing and GPS. *Pedosphere*, 15(6), 778-783.

Yang, J., Udvardi, M. (2018). Senescence and nitrogen use efficiency in perennial grasses for forage and biofuel production. *Journal of Experimental Botany*, 69 (4), 855-865.

Zaady, E., Yonatan, R., Shachak, M., Perevolotsky, A. (2001). The Effects of Grazing on Abiotic and Biotic Parameters in a Semiarid Ecosystem: A Case Study from the Northern Negev Desert, Israel. *Arid Land Research and Management*, 15, 245-261.

Zambatis, N., PJK Zacharias, P.J.K., Morris, C.D., Derry, J.F. (2006). Re-evaluation of the disc pasture meter calibration for the Kruger National Park, South Africa. *African Journal of Range and Forage Science*, 23(2).

Zhang, X.Y., Friedl, M.A., Schaaf, C.B., Strahler, A.H., Liu, Z. (2005). Monitoring the response of vegetation phenology to precipitation in Africa by coupling MODIS and TRMM instruments. *Journal of Geophysical Research*, 110.

Zhang, J.H., Quine, T.A., Ni, S.J., Ge, F.L. (2006). Stocks and dynamics of SOC in relation to soil redistribution by water and tillage erosion. *Global Change Biology*, 12, 1834–1841.

Zhang, C.L., Wieczorek, K., Xie, M.L. (2010). Swelling experiments on mudstones. *Journal of Rock Mechanics and Geotechnical Engineering*, 2(1), 44-51.

Zhang, X., Liao, C., Li, J., Sun, Q. (2013). Fractional vegetation cover estimation in arid and semi-arid environments using HJ-1 satellite hyperspectral data. *International Journal of Applied Earth Observation and Geoinformation,* 21, 506–512.

Personal communications:

Carole Sephton. (2019). Farmer, Cornlands Farming, Maclear. Personal Communication. 25 June.

Laura Bannatyne. (2018). PhD candidate, Rhodes University, Geography Department. Personal Communication. 25 February.

Laura Bannatyne. (2019). PhD candidate, Rhodes University, Geography Department. Personal Communication. 26 August.

Appendices

Appendix A – Relationships between field variables in both catchments

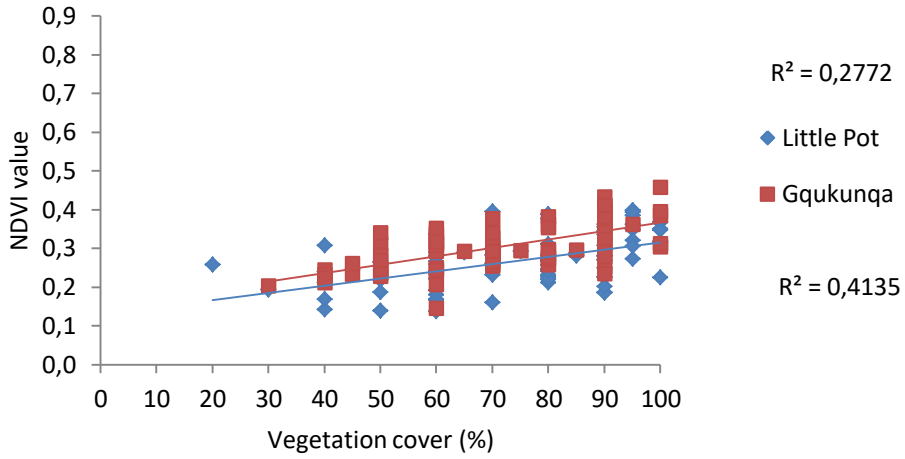

Figure A1: Relationship between NDVI and grassland vegetation cover percentage in the LPRC and GRC in October 2018.

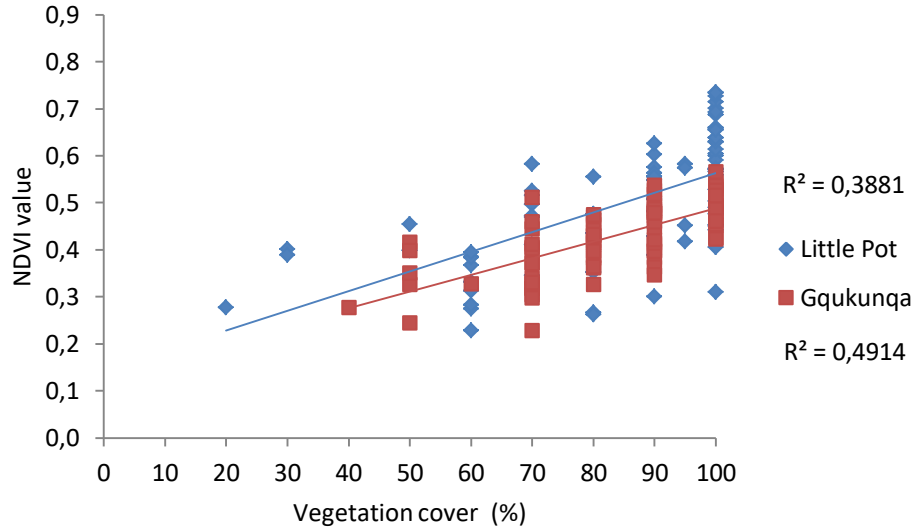

Figure A2: Relationship between NDVI and grassland vegetation cover percentage in the LPRC and GRC in January 2019.

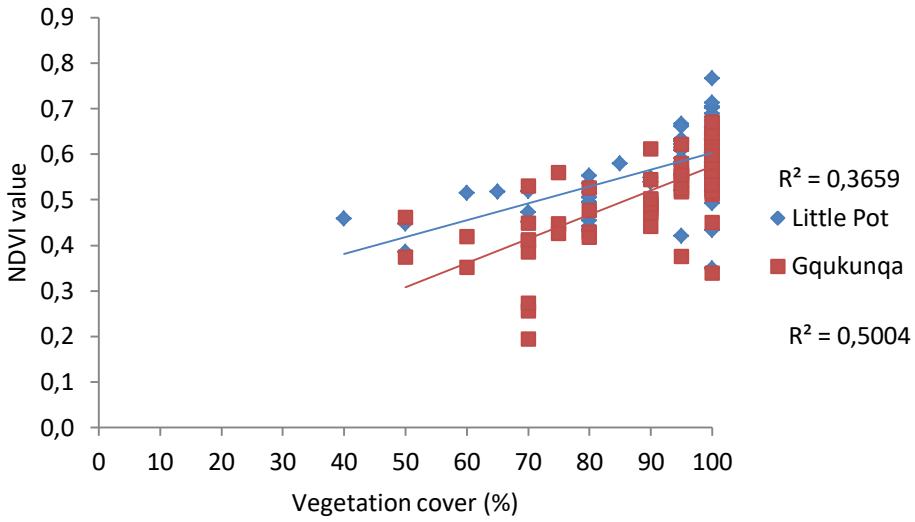

Figure A3: Relationship between NDVI and grassland vegetation cover percentage in the LPRC and GRC in April 2019.

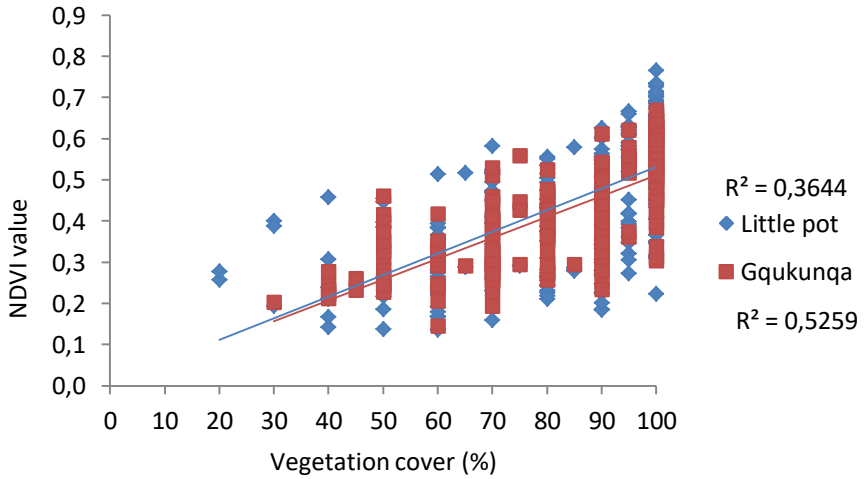

Figure A4: Relationship between NDVI and grassland vegetation cover percentage in the LPRC and GRC throughout the entire wet season of 2018-2019.

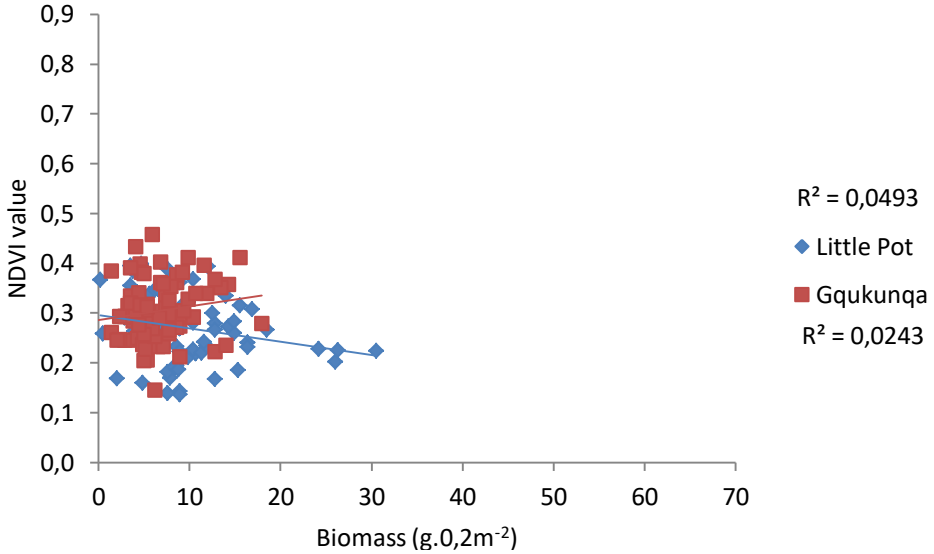

Figure A5: Relationship between NDVI and biomass in the LPRC and GRC in October 2018.

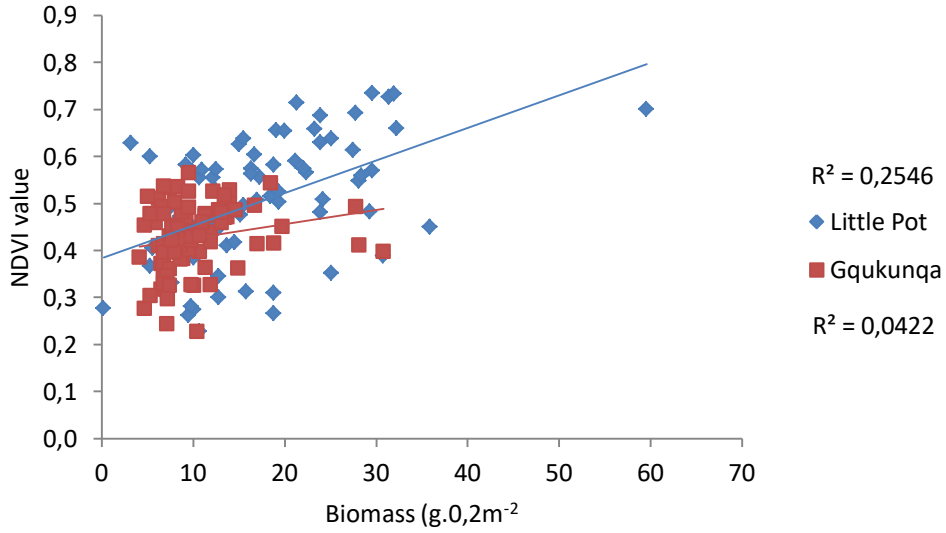

Figure A6: Relationship between NDVI and biomass in the LPRC and GRC in January 2019.

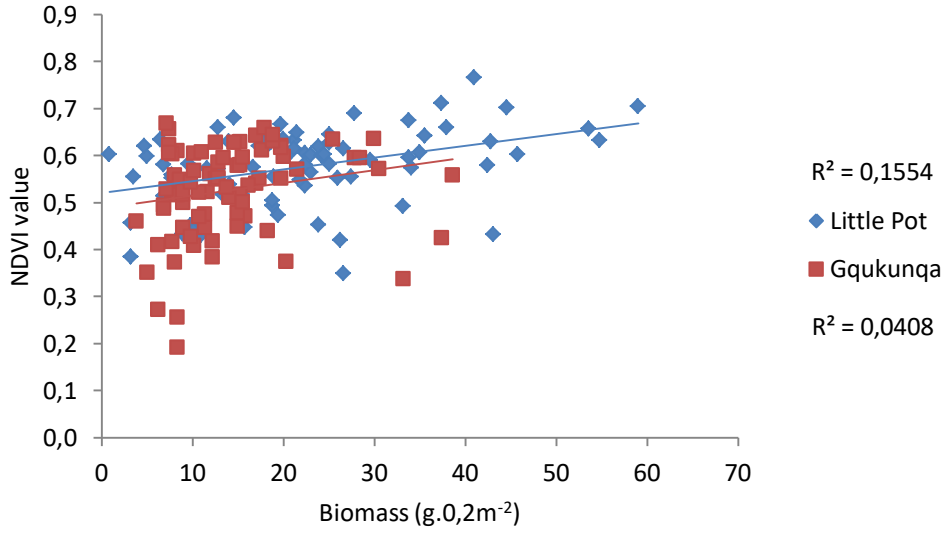

Figure A7: Relationship between NDVI and biomass in the LPRC and GRC in April 2019.

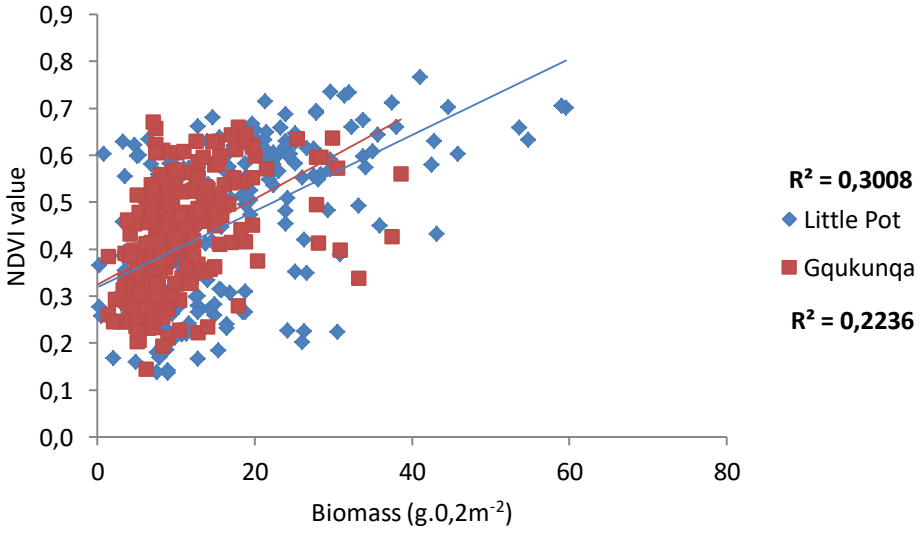

Figure A8: Relationship between NDVI and biomass in the LPRC and GRC throughout the wet season of 2018-2019.

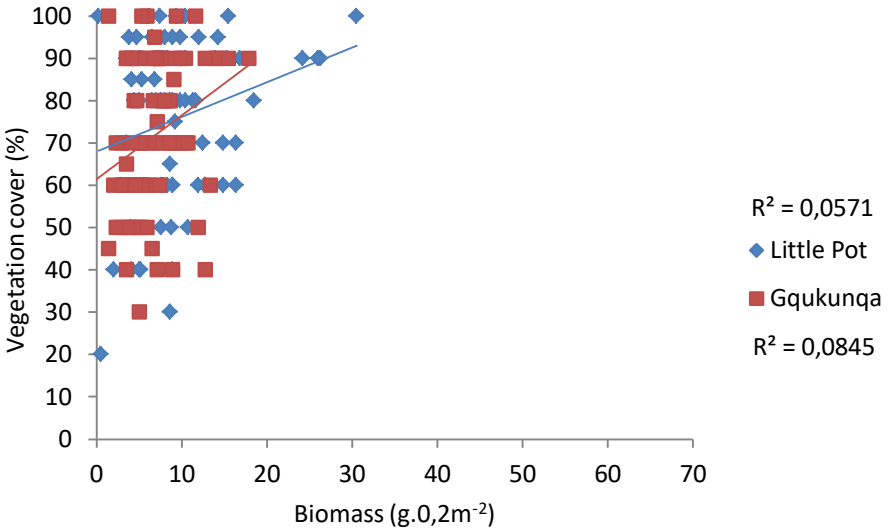

Figure A9: Relationship between vegetation cover and biomass in the LPRC and GRC in October 2018.

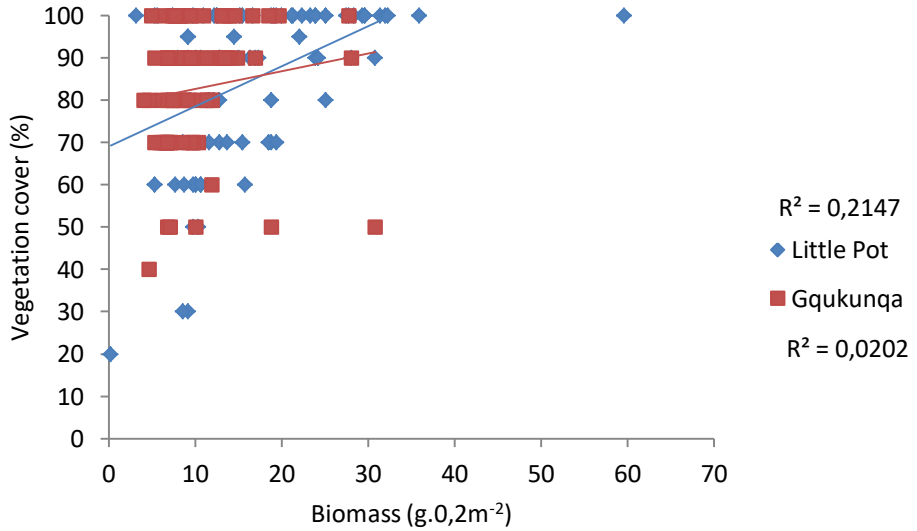

Figure A10: Relationship between vegetation cover and biomass in the LPRC and GRC in January 2019.

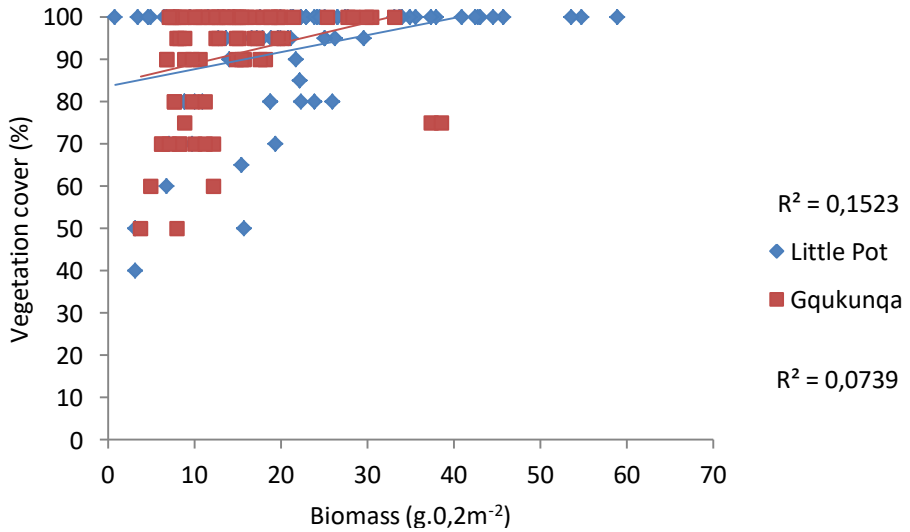

Figure A11: Relationship between vegetation cover and biomass in the LPRC and GRC in April 2019.

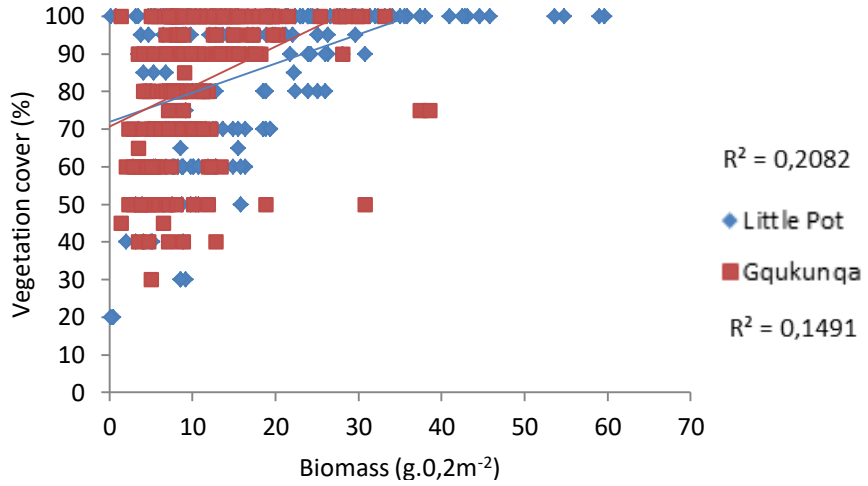

Figure A12: Relationship between vegetation cover and biomass in the LPRC and GRC throughout the wet season of 2018-2019.

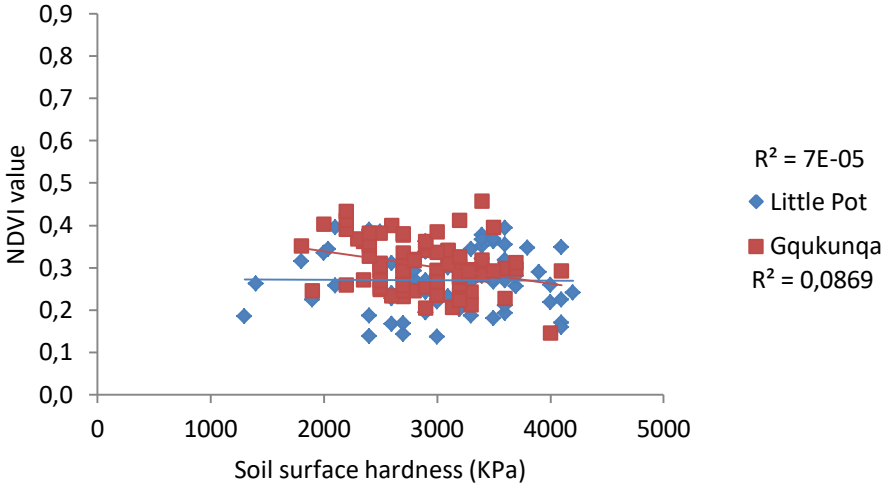

Figure A13: Relationship between soil surface hardness and NDVI in the LPRC and GRC in October 2018.

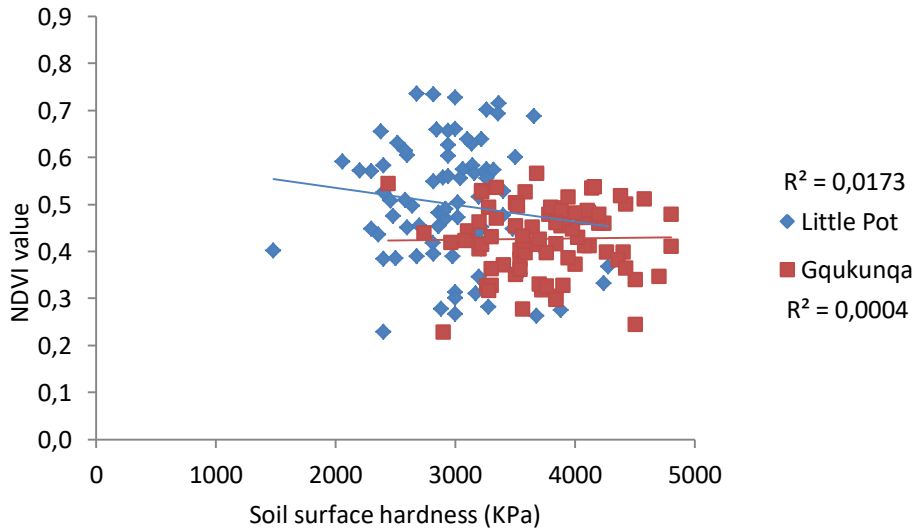

Figure A14: Relationship between soil surface hardness and NDVI in the LPRC and GRC in January 2019.

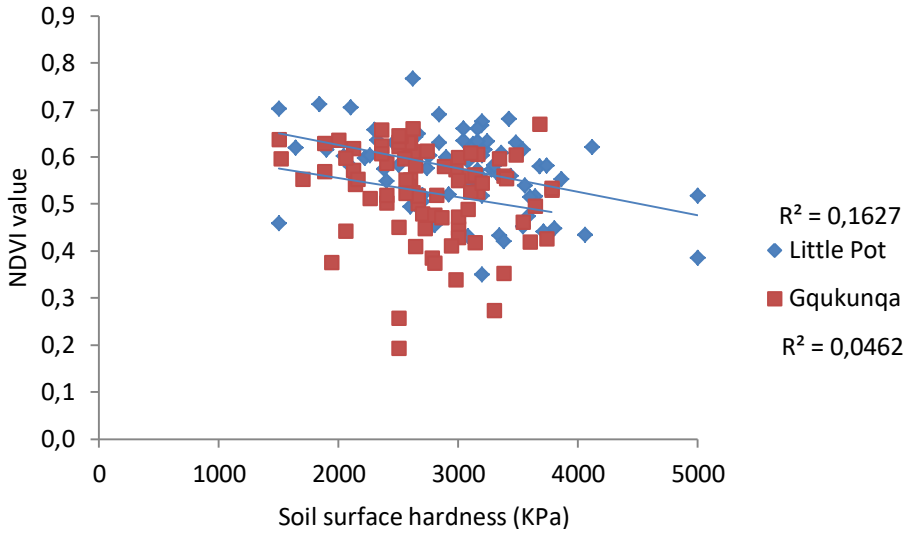

Figure A15: Relationship between soil surface hardness and NDVI in the LPRC and GRC in April 2019.

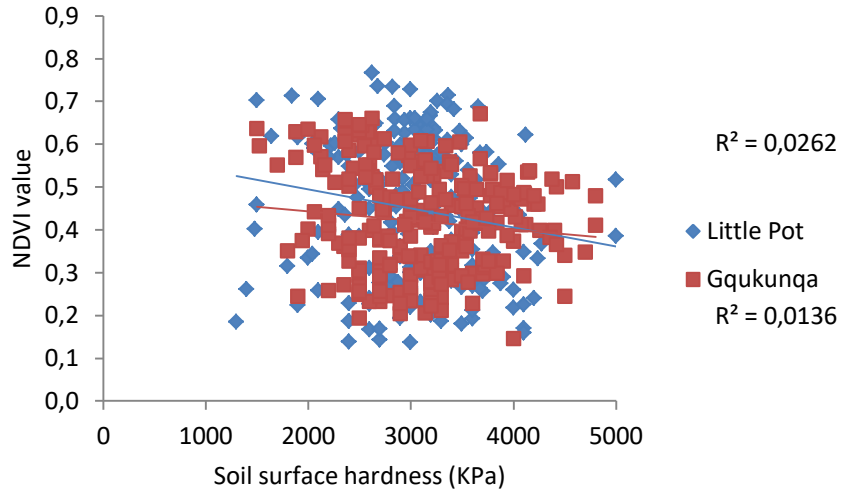

Figure A16: Relationship between soil surface hardness and NDVI in the LPRC and GRC through the wet season of 2018-2019.

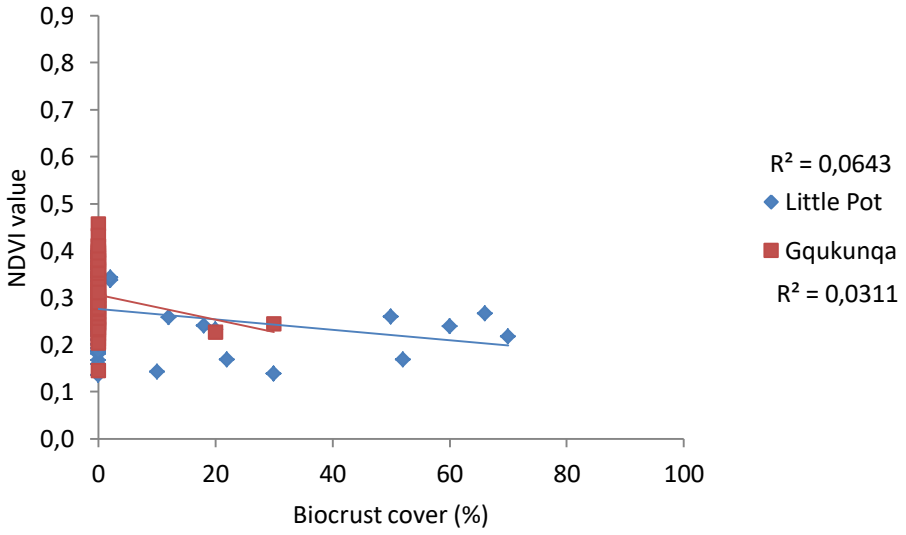

Figure A17: Relationship between biocrust cover and NDVI in the LPRC and GRC in October 2018.

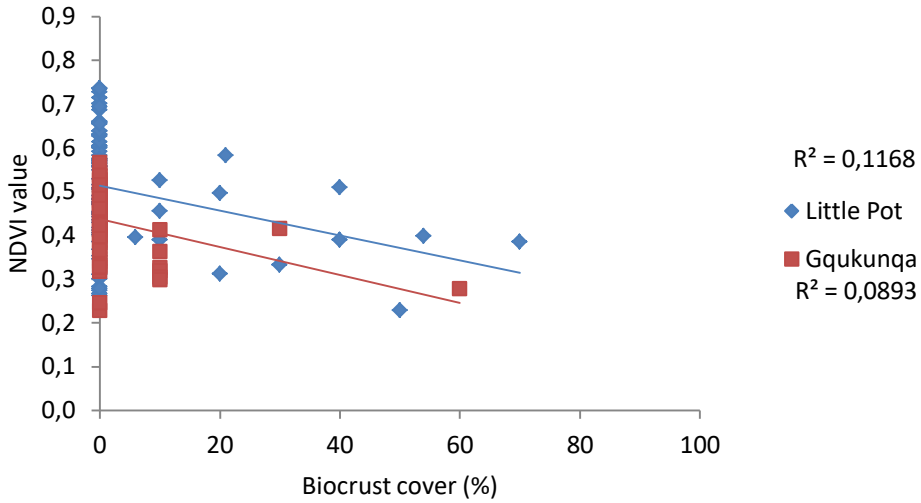

Figure A18: Relationship between biocrust cover and NDVI in the LPRC and GRC in January 2019.

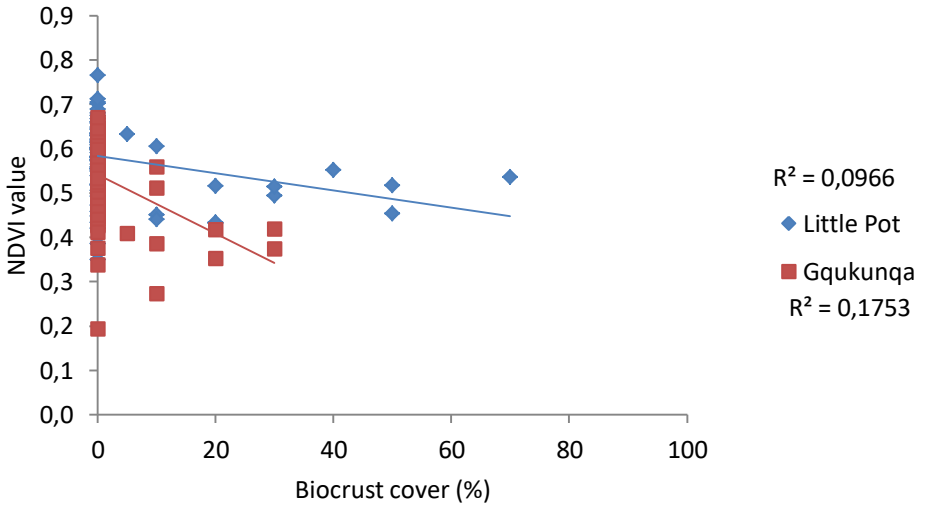

Figure A19: Relationship between biocrust cover and NDVI in the LPRC and GRC in April 2019.

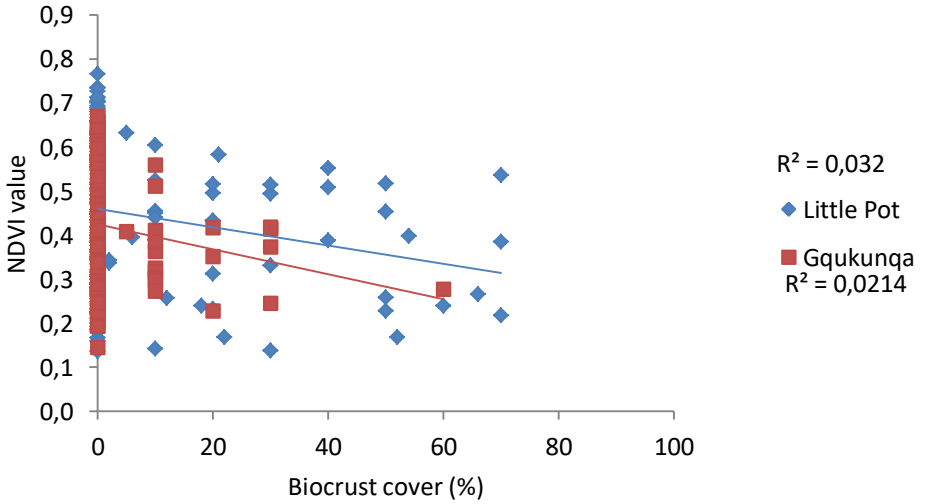

Figure A20: Relationship between biocrust cover and NDVI in the LPRC and GRC throughout the wet season of 2018-2019.

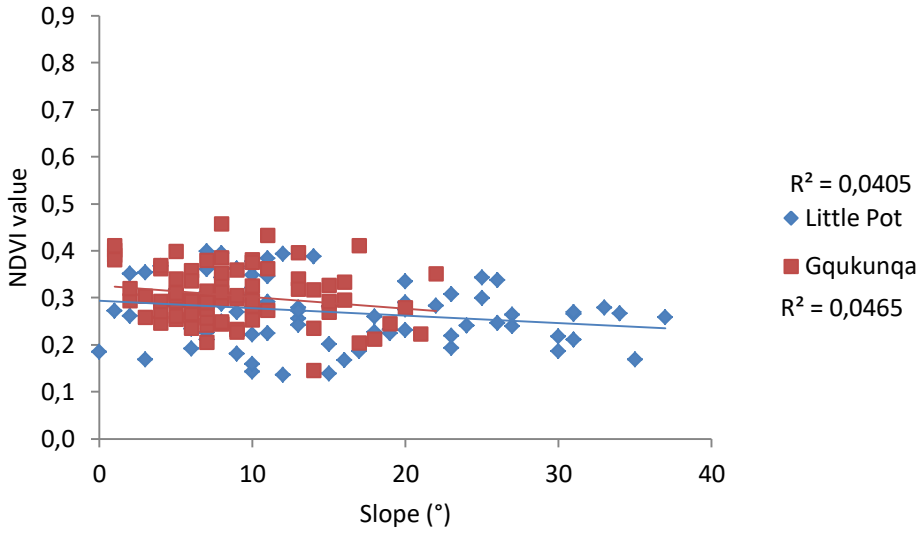

Figure A21: Relationship between slope and NDVI in the LPRC and GRC in October 2018.

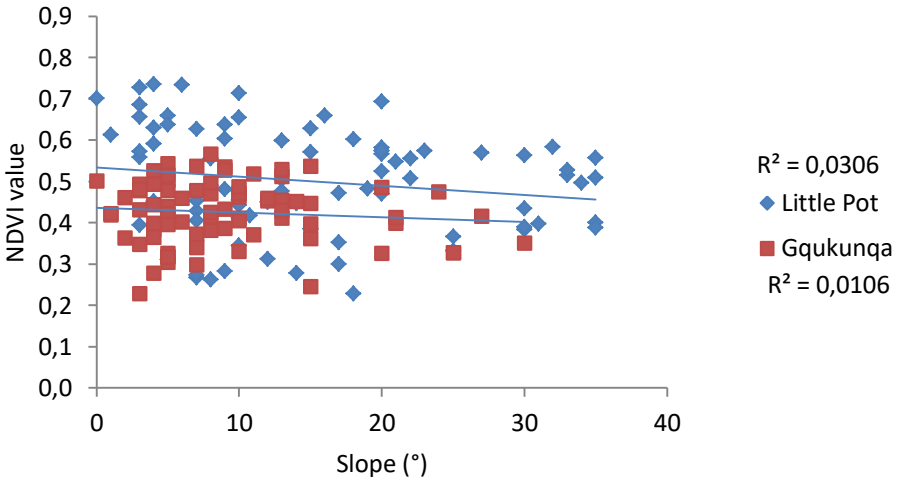

Figure A22: Relationship between slope and NDVI in the LPRC and GRC in January 2019.

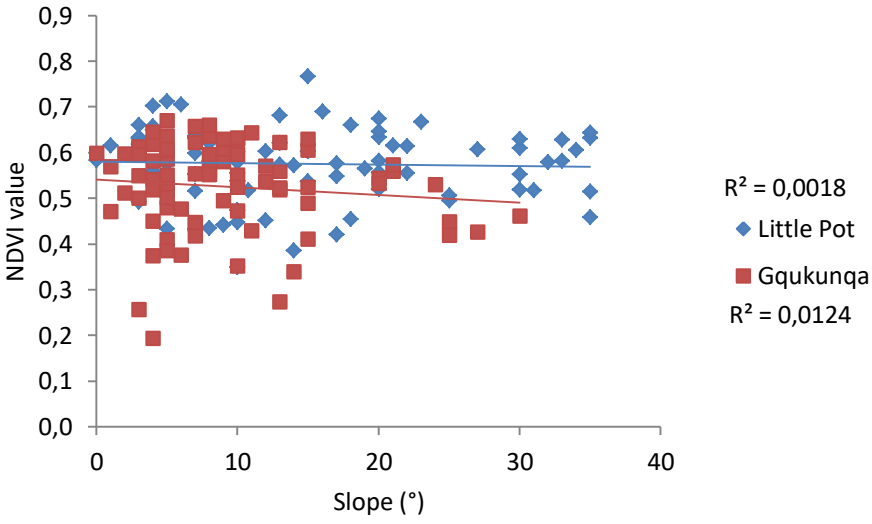

Figure A23: Relationship between slope and NDVI in the LPRC and GRC in April 2019.

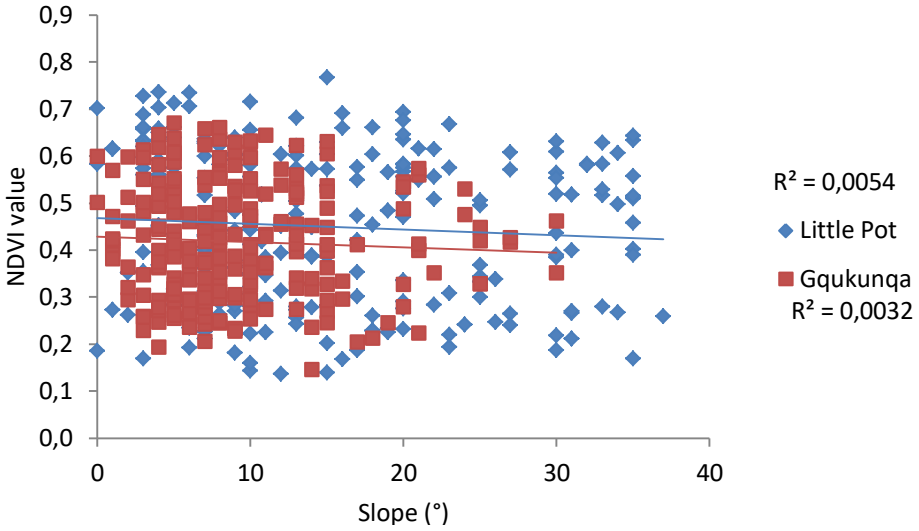

Figure A24: Relationship between slope and NDVI in the LPRC and GRC throughout the wet season of 2018-2019.

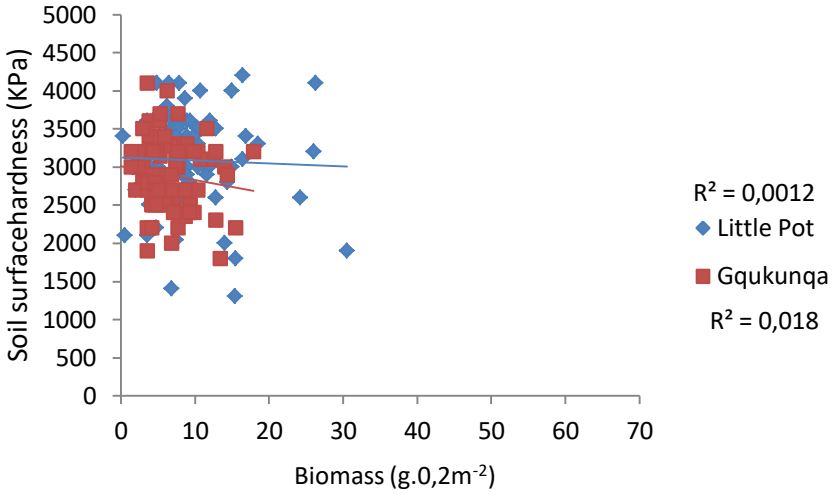

Figure A25: Relationship between soil surface hardness and biomass in the LPRC and GRC in October 2018.

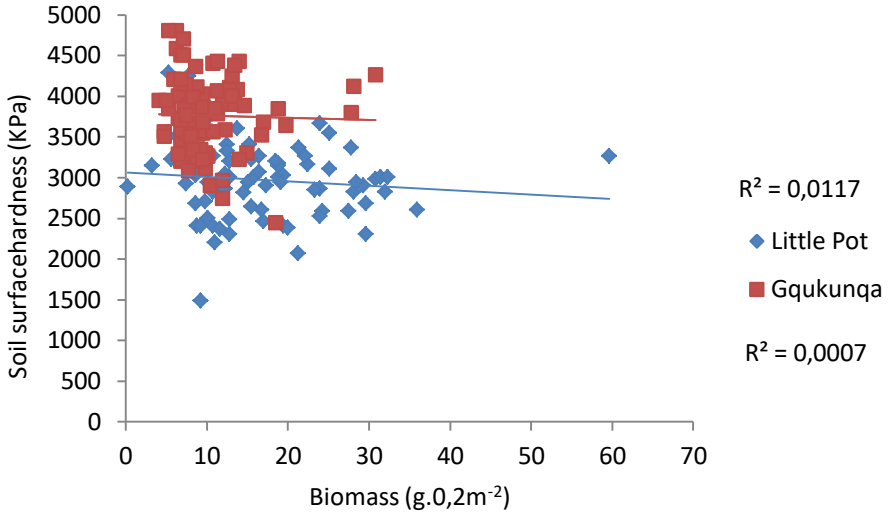

Figure A26: Relationship between soil surface hardness and biomass in the LPRC and GRC in January 2019.

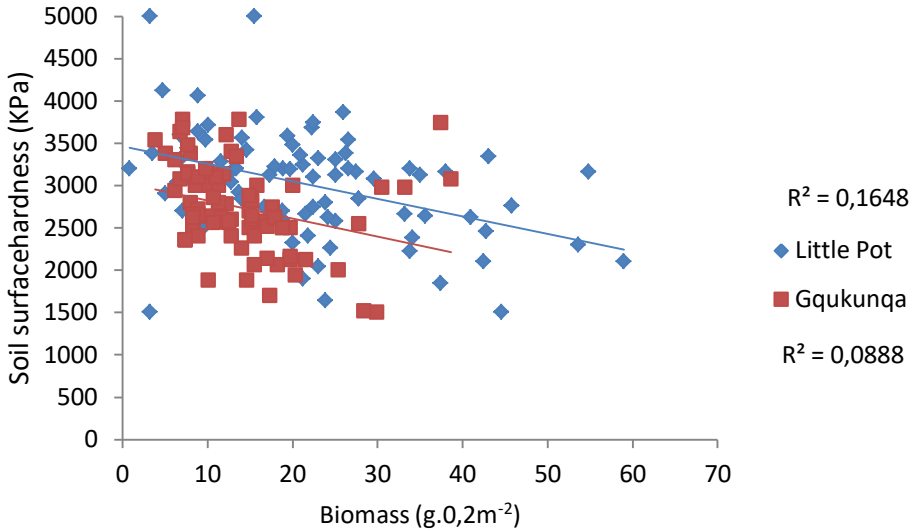

Figure A27: Relationship between soil surface hardness and biomass in the LPRC and GRC in April 2019.

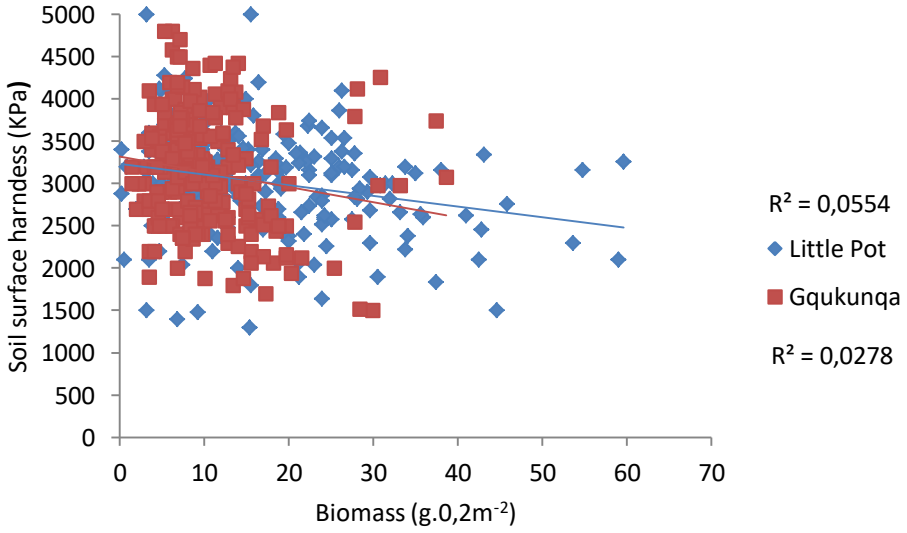

Figure A28: Relationship between soil surface hardness and biomass in the LPRC and GRC throughout the wet season of 2018-2019.

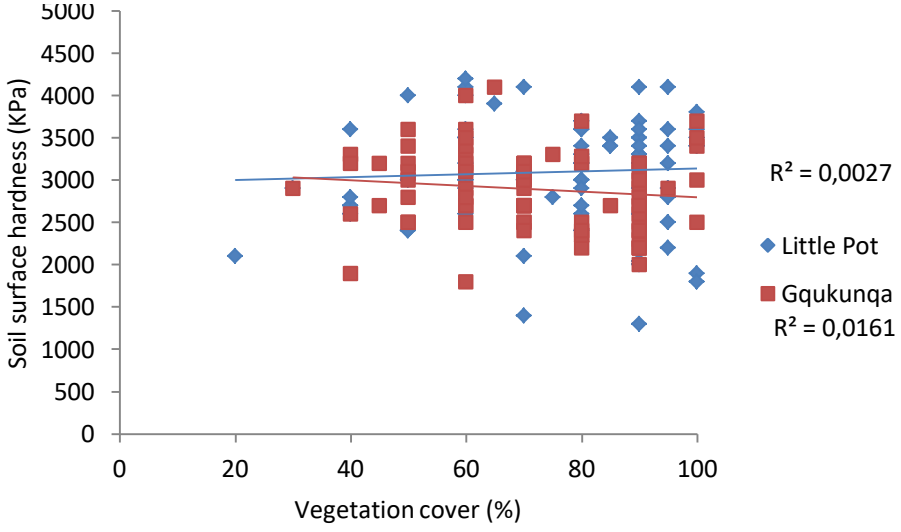

Figure A29: Relationship between soil surface hardness and vegetation cover in the LPRC and GRC in October 2018.

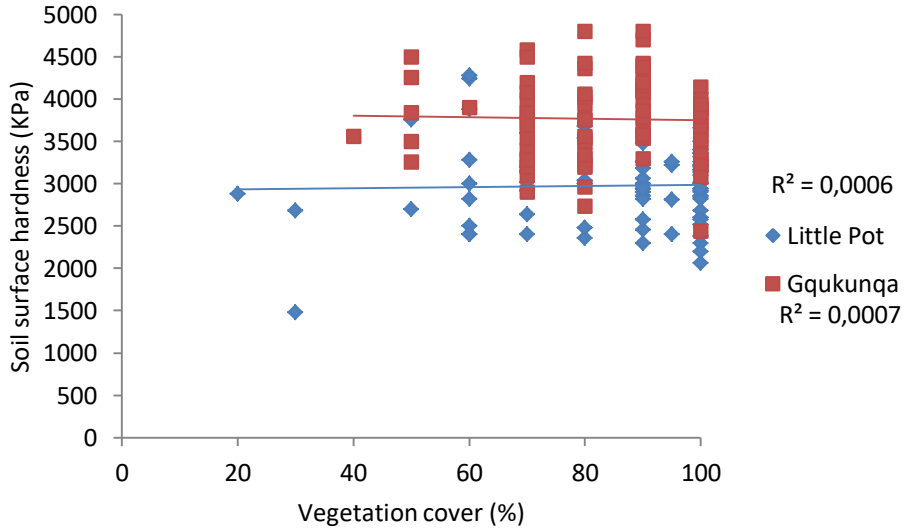

Figure A30: Relationship between soil surface hardness and vegetation cover in the LPRC and GRC in January 2019.

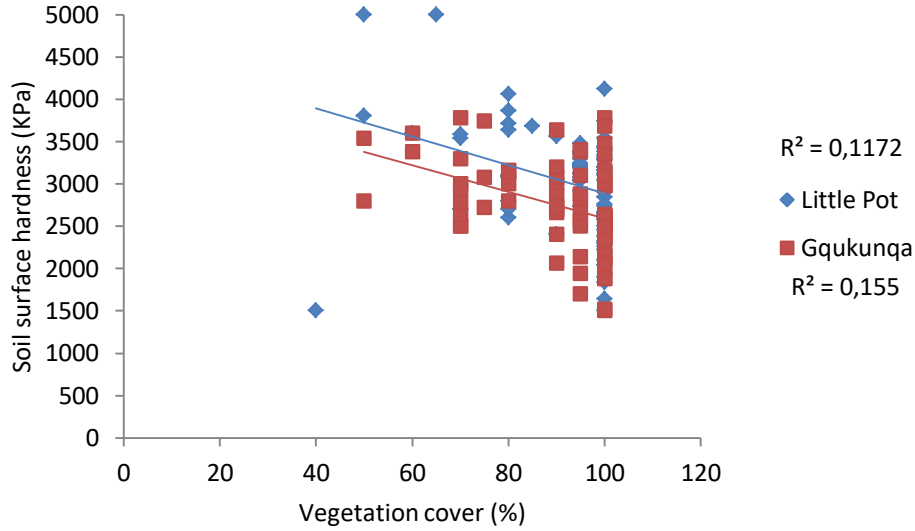

Figure A31: Relationship between soil surface hardness and vegetation cover in the LPRC and GRC in April 2019.

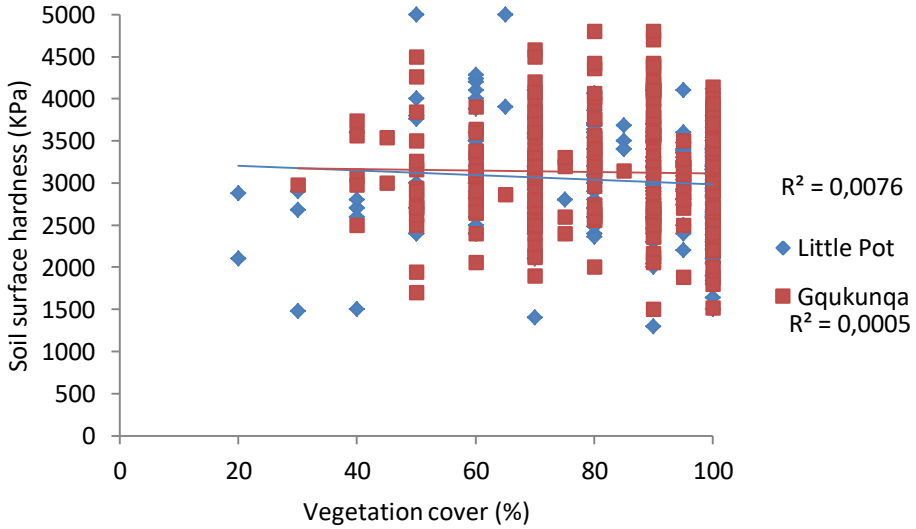

Figure A32: Relationship between soil surface hardness and vegetation cover in the LPRC and GRC throughout the wet season of 2018-2019.

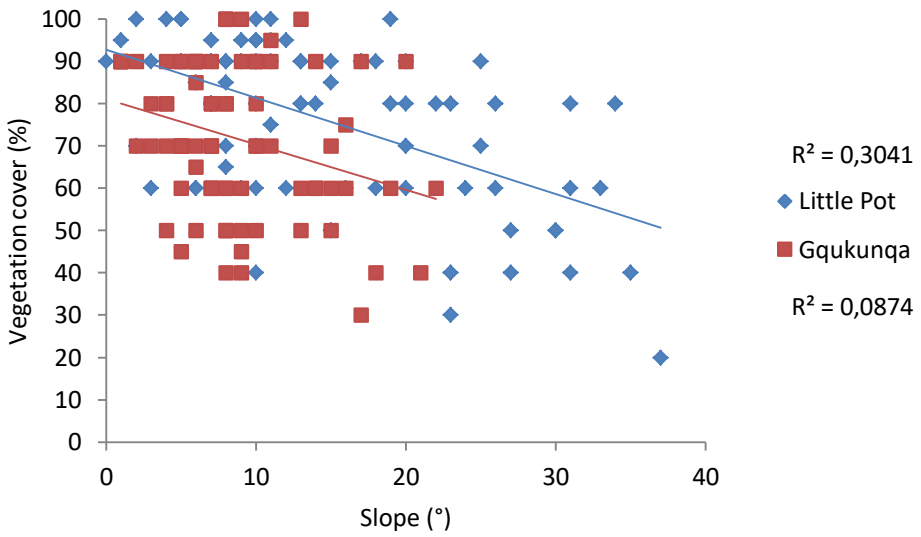

Figure A33: Relationship between vegetation cover and slope in the LPRC and GRC in October 2018.

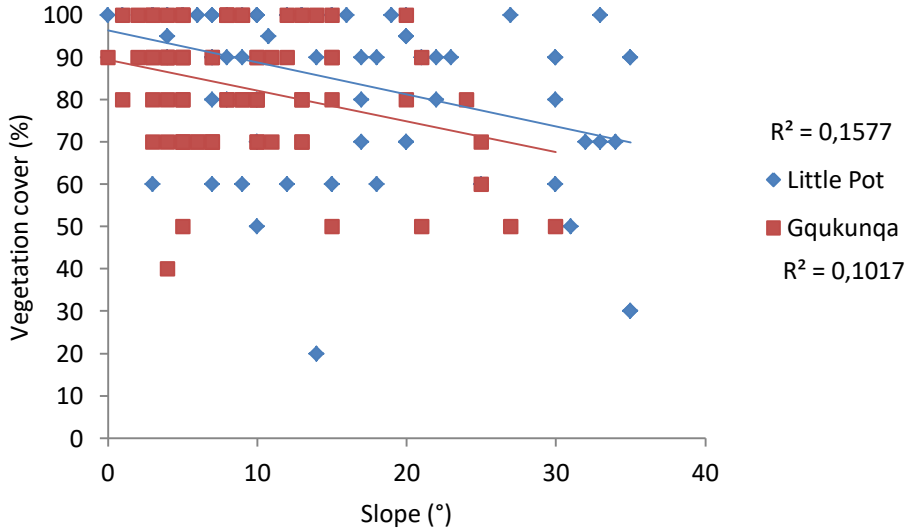

Figure A34: Relationship between vegetation cover and slope in the LPRC and GRC in January 2019.

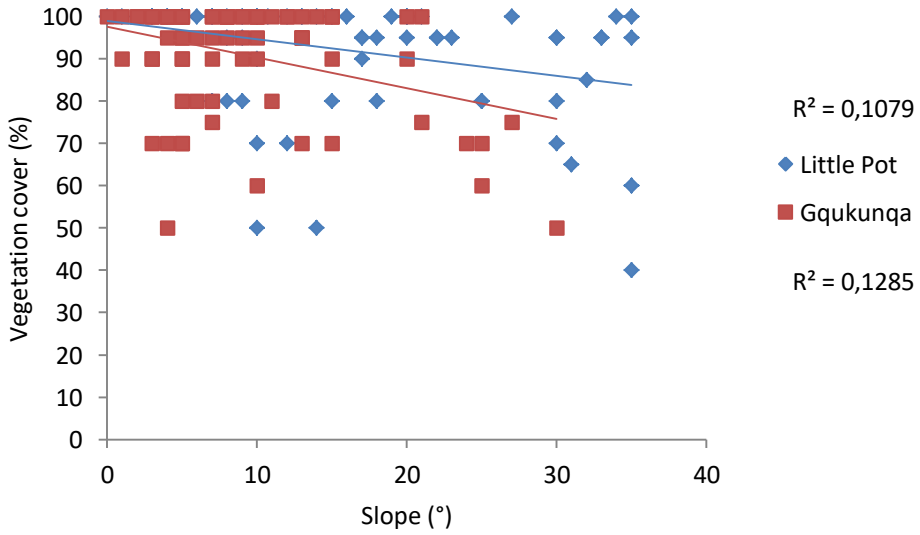

Figure A35: Relationship between vegetation cover and slope in the LPRC and GRC in April 2019.

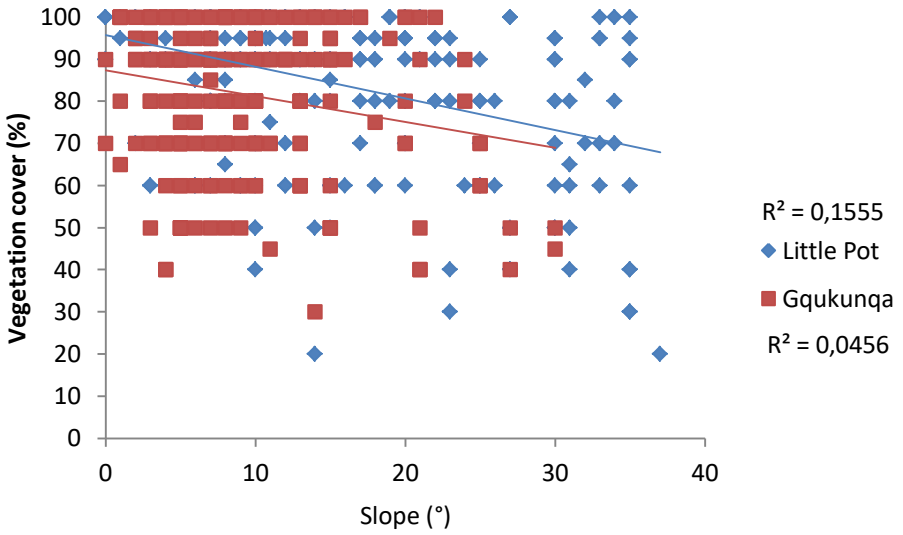

Figure A36: Relationship between vegetation cover and slope in the LPRC and GRC throughout the wet season of 2018-2019.

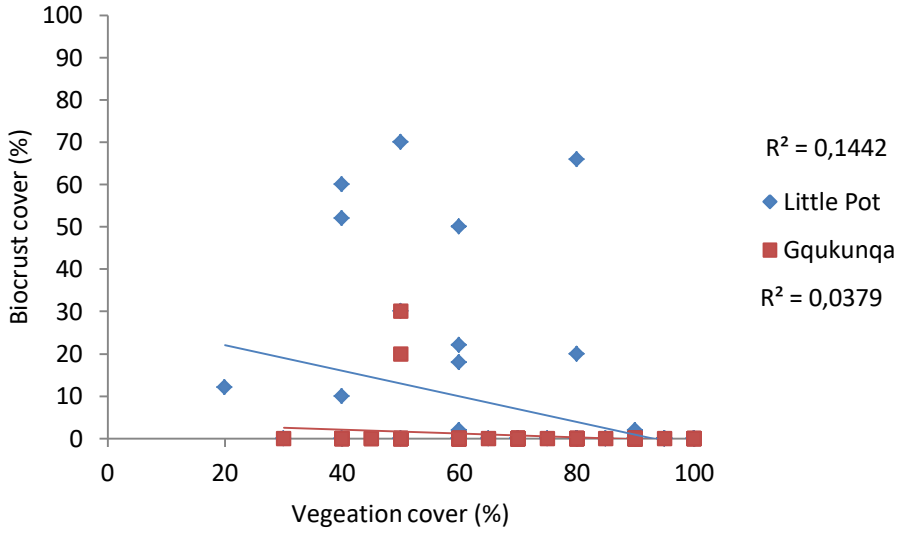

Figure A37: Relationship between vegetation cover and biocrust cover in the LPRC and GRC in October 2018.

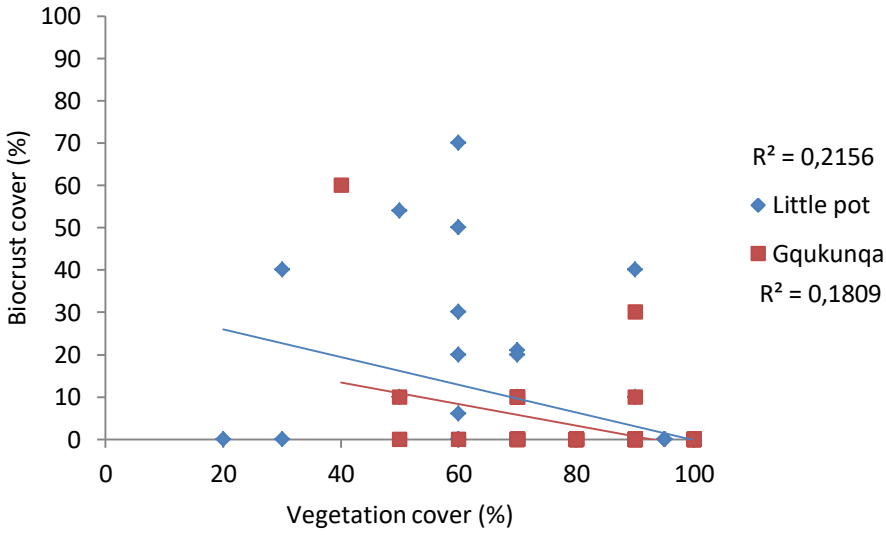

Figure A38: Relationship between vegetation cover and biocrust cover in the LPRC and GRC in January 2019.

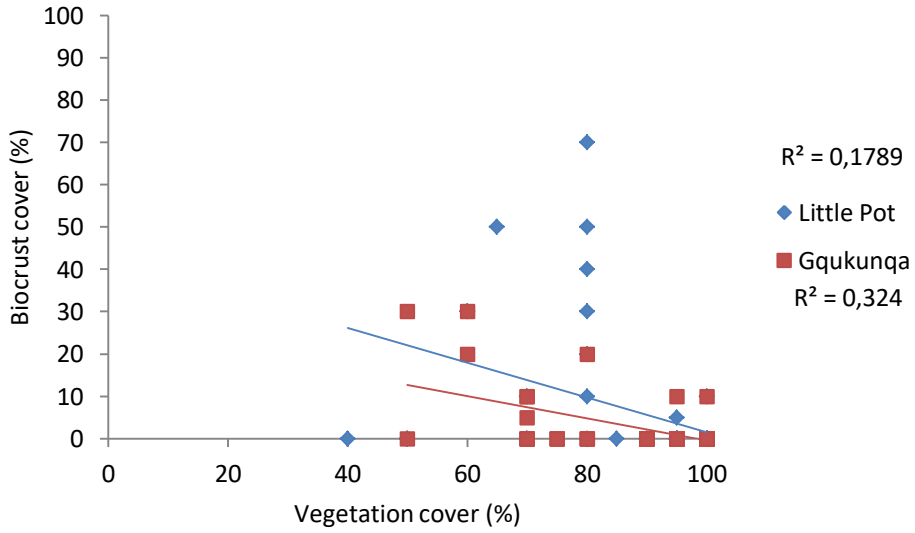

Figure A39: Relationship between vegetation cover and biocrust cover in the LPRC and GRC in April 2019.

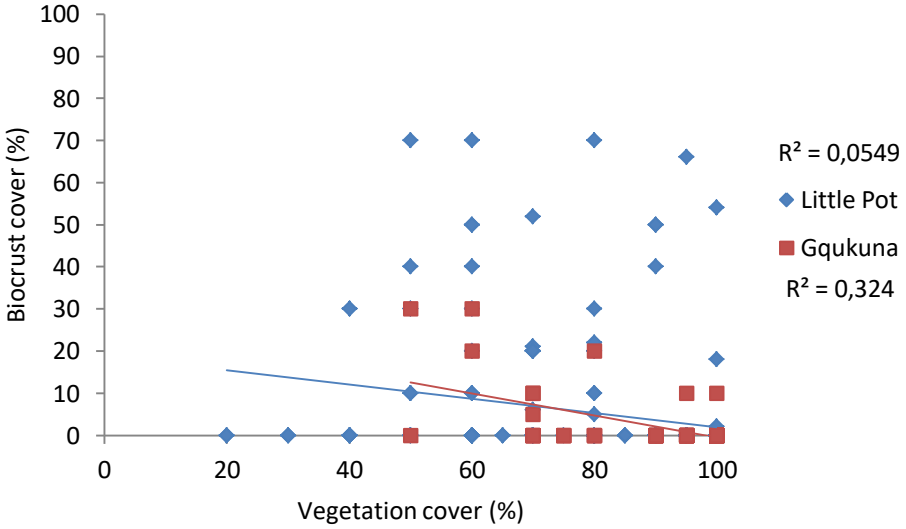

Figure A40: Relationship between vegetation cover and biocrust cover in the LPRC and GRC throughout the wet season of 2018-2019.

Appendix B – Mean monthly NDVI values and sediment event data

Table B1: Average monthly NDVI values for grassland areas in the LPRC.

Month	2015/2016	2016/2017	2017/2018	2018/2019
October	0,33	0,33	0,31	0,26
November	0,42	NoData	0,42	0,34
December	0,49	NoData	NoData	NoData
January	NoData	NoData	0,5	0,5
February	NoData	0,53	0,52	0,5
March	0,58	NoData	0,56	NoData
April	0,49	0,5	0,53	0,55

Table B2: Average monthly NDVI values for grassland areas in the GRC.

Month	2015/2016	2016/2017	2017/2018	2018/2019
October	0,28	0,35	0,31	0,29
November	0,34	NoData	0,42	0,35
December	0,32	NoData	NoData	NoData
January	NoData	NoData	0,49	0,43
February	NoData	0,51	0,52	0,5
March	0,54	NoData	0,56	NoData
April	0,43	0,5	0,54	0,54

Table B3: Sediment event spike 1, LPRC

Date time	Daily rainfall (mm)	Erosive rainfall event ($mm.hr^{-1}$)	Average daily sediment flux ($t.day^{-1}$)
12-Jan-16	0	N/A	16,87
13-Jan-16	1,2	N/A	3,76
14-Jan-16	4	N/A	3,72
15-Jan-16	13,4	N/A	11,78
16-Jan-16	3,4	N/A	NoData
17-Jan-16	0,8	N/A	NoData
18-Jan-16	3,4	N/A	11,34
19-Jan-16	13,4	26,4	**144,31**

Table B4: Sediment event spike 2, LPRC

Date time	Daily rainfall (mm)	Erosive rainfall event ($mm.hr^{-1}$)	Average daily sediment flux (t/day)
17-Jan-16	0,8	N/A	NoData
18-Jan-16	3,4	N/A	11,34
19-Jan-16	13,4	26,4	144,31
20-Jan-16	0	N/A	20,23
21-Jan-16	1,4	N/A	8,51
22-Jan-16	2,4	N/A	7,87
23-Jan-16	2,8	N/A	4,13
24-Jan-16	21,8	N/A	**80,62**

Table B5: Sediment event spike 3, LPRC

Date time	Daily rainfall (mm)	Erosive rainfall event ($mm.hr^{-1}$)	Average daily sediment flux ($t.day^{-1}$)
19-Jan-16	13,4	26,4	144,31
20-Jan-16	0	N/A	20,23
21-Jan-16	1,4	N/A	8,51
22-Jan-16	2,4	N/A	7,87
23-Jan-16	2,8	N/A	4,13
24-Jan-16	21,8	N/A	80,62
25-Jan-16	21,2	28,8	15,83
26-Jan-16	2,4	N/A	**40,34**

Table B6: Sediment event spike 4, LPRC

Date time	Daily rainfall (mm)	Erosive rainfall event ($mm.hr^{-1}$)	Average daily sediment flux ($t.day^{-1}$)
12-Feb-16	0	N/A	0,26
13-Feb-16	4	N/A	NoData
14-Feb-16	0,2	N/A	0,22
15-Feb-16	14,4	79,2	2,09
16-Feb-16	19	N/A	7,31
17-Feb-16	17,4	N/A	9,09
18-Feb-16	5,4	N/A	11,72
19-Feb-16	0,2	N/A	**28,79**

Table B7: Sediment event spike 1, GRC

Date	Daily rainfall (mm)	Erosive rainfall event ($mm.hr^{-1}$)	Average daily sediment flux ($t.day^{-1}$)
01-Mar-16	0	N/A	8,28
02-Mar-16	0,2	N/A	1,04
03-Mar-16	0	N/A	2,28
04-Mar-16	0	N/A	2,49
05-Mar-16	0	N/A	61,41
06-Mar-16	3,2	N/A	NoData
07-Mar-16	15,8	N/A	56,98
08-Mar-16	24,6	N/A	**2863,12**

Table B8: Sediment event spike 2, GRC

Date	Daily rainfall (mm)	Erosive rainfall event ($mm.hr^{-1}$)	Average daily sediment flux ($t.day^{-1}$)
12-Feb-17	18,2	N/A	14,84
13-Feb-17	9,2	N/A	99,91
14-Feb-17	0,2	N/A	410,60
15-Feb-17	2,2	N/A	21,37
16-Feb-17	0	N/A	10,66
17-Feb-17	0	N/A	17,13
18-Feb-17	31,4	45,6	183,68
19-Feb-17	14,6	N/A	**3887,99**

Table B9: Sediment event spike 3, GRC

Date	Daily rainfall (mm)	Erosive rainfall event ($mm.hr^{-1}$)	Average daily sediment flux ($t.day^{-1}$)
25-Jan-18	0,8	N/A	28,02
26-Jan-18	36	72	NoData
27-Jan-18	39,8	74,4	2116,78
28-Jan-18	1,2	N/A	NoData
29-Jan-18	0	N/A	NoData
30-Jan-18	16,4	N/A	NoData
31-Jan-18	34,2	N/A	387,56
01-Feb-18	3	N/A	**6449,65**

Table 10: Sediment event spike 4, GRC

Date	Daily rainfall (mm)	Erosive rainfall event ($mm.hr^{-1}$)	Average daily sediment flux ($t.day^{-1}$)
09-Feb-18	0	N/A	12,62
10-Feb-18	8,6	N/A	129,28
11-Feb-18	5,4	N/A	44,66
12-Feb-18	13	N/A	20,95
13-Feb-18	3,6	N/A	95,675
14-Feb-18	5,6	N/A	45,83
15-Feb-18	3,4	N/A	57,28
16-Feb-18	1	N/A	**5455,82**

Table B11: Sediment event spike 5, GRC

Date	Daily rainfall (mm)	Erosive rainfall event ($mm.hr^{-1}$)	Average daily sediment flux ($t.day^{-1}$)
11-Mar-18	0	N/A	86,55
12-Mar-18	0	N/A	48,34
13-Mar-18	0	N/A	34,20
14-Mar-18	8,8	N/A	25,88
15-Mar-18	12,2	N/A	27,37
16-Mar-18	16,6	N/A	302,05
17-Mar-18	4,2	N/A	577,03
18-Mar-18	4	N/A	**6863,13**

Appendix C – Extra information supporting the PCA

Table C1: Total variance explained by each principal component, in the LPRC.

Component	Variance	Percentage of variance	Cumulative percentage
1	2,423	30,29	30,29
2	1,288	16,10	46,38
3	1,161	14,51	60,90
4	0,989	12,37	73,26
5	0,792	9,90	83,16
6	0,618	7,73	90,89
7	0,437	5,47	96,36
8	0,291	3,64	100,00

Table C2: Coefficients of the linear combinations of each principal component, in the LPRC.

Factor	Component							
	1	2	3	4	5	6	7	8
NDVI	0,49	-0,16	0,35	-0,10	-0,21	-0,10	0,45	-0,58
Vegetation cover	0,54	0,20	0,12	0,09	-0,15	-0,03	0,28	0,74
Biomass	0,45	-0,23	0,33	-0,18	0,15	0,24	-0,73	0,01
Soil surface hardness	-0,22	0,51	0,28	-0,14	-0,67	0,33	-0,17	-0,07
Biocrust	-0,34	-0,21	0,54	-0,08	0,34	0,52	0,36	0,18
Slope	-0,30	-0,45	0,33	-0,26	-0,33	-0,58	-0,09	0,27
Aspect	0,04	0,36	-0,09	-0,86	0,30	-0,14	0,10	0,02
Geology	0,08	-0,50	-0,52	-0,34	-0,37	0,45	0,12	0,10

Table C3: Relationships (Pearson's R) between variables in the Little Pot River catchment.

Pearson's R	NDVI	Vegetation cover	Biomass	Soil surface hardness	Biocrust	Slope	Aspect	Geology
NDVI	-	0,60	0,55	-0,16	-0,18	-0,08	-0,01	0,06
Vegetation cover	0,60	-	0,46	-0,09	-0,40	-0,39	0,03	-0,06
Biomass	0,55	0,46	-	-0,24	-0,09	-0,12	0,04	0,08
Soil surface hardness	-0,16	-0,09	-0,24	-	0,12	0,07	0,11	-0,21
Biocrust	-0,18	-0,40	-0,09	0,12	-	0,33	-0,06	-0,15
Slope	-0,08	-0,39	-0,12	0,07	0,33	-	-0,08	0,06
Aspect	-0,01	0,03	0,04	0,11	-0,06	-0,08	-	0,00
Geology	0,06	-0,06	0,08	-0,21	-0,15	0,06	0,00	-

Table C4: Total variance explained by each principal component, in the GRC.

Component	Variance	Percentage of variance	Cumulative percentage
1	1,810	22,63	22,63
2	1,460	18,25	40,88
3	1,044	13,05	53,94
4	0,997	12,47	66,40
5	0,952	11,90	78,30
6	0,737	9,21	87,51
7	0,562	7,03	94,54
8	0,437	5,46	100,00

Table C5: Coefficients of the linear combinations of each principal component, in the GRC.

Factor	Component							
	1	2	3	4	5	6	7	8
Vegetation cover	0,45	-0,02	0,60	-0,08	0,11	-0,03	0,65	-0,02
Biomass	0,50	0,32	-0,29	0,08	0,25	0,25	-0,08	0,65
NDVI	0,58	0,18	-0,05	0,02	0,19	-0,32	-0,42	-0,56
Soil surface hardness	-0,27	0,32	0,68	-0,12	0,27	0,02	-0,48	0,20
Biocrust	-0,26	-0,14	-0,21	-0,02	0,90	-0,07	0,21	-0,11
Slope	-0,15	0,65	-0,08	0,02	-0,02	0,56	0,23	-0,43
Aspect	0,03	0,06	-0,16	-0,98	-0,04	-0,04	0,02	0,02
Geology	-0,20	0,56	-0,12	0,10	-0,10	-0,71	0,27	0,15

Table C6: Relationships (Pearson's R) between variables in the Gqukunqa River catchment.

Pearson's r	Vegetation cover	NDVI	Biomass	Soil surface hardness	Biocrust	Aspect	Slope	Geology
Vegetation cover	-	0,32	0,20	0,05	-0,17	0,00	-0,13	-0,16
NDVI	0,32	-	0,47	-0,13	-0,14	0,03	-0,06	-0,01
Biomass	0,20	0,47	-	-0,17	-0,09	0,02	0,16	0,01
Soil surface hardness	0,05	-0,13	-0,17	-	0,08	0,00	0,22	0,17
Biocrust	-0,17	-0,14	-0,09	0,08	-	-0,01	-0,05	-0,02
Aspect	0,00	0,03	0,02	0,00	-0,01	-	0,03	0,00
Slope	-0,13	-0,06	0,16	0,22	-0,05	0,03	-	0,31
Geology	-0,16	-0,01	0,01	0,17	-0,02	0,00	0,31	-